8-2016

Determining Mechanisms of Response to Polo-like Kinase 1 Inhibition in Non-Small Cell Lung Cancer

Ruchitha Goonatilake

DETERMINING MECHANISMS OF RESPONSE TO POLO-LIKE KINASE 1 INHIBITION IN NON-SMALL CELL LUNG CANCER

by

Ruchitha Goonatilake, BS

APPROVED:

_____

Faye M. Johnson, MD, Ph.D., Advisory Professor

_____

Khandan Keyomarsi, Ph.D.

_____

Walter N. Hittelman, Ph.D.

_____

Lauren A. Byers, MD.

_____

Jing Wang, Ph.D.

APPROVED:

_____

Dean, The University of Texas

Graduate School of Biomedical Sciences at Houston

DETERMINING MECHANISMS OF RESPONSE TO POLO-LIKE KINASE 1 INHIBITION IN NON-SMALL CELL LUNG CANCER

A

THESIS Presented to the Faculty of
The University of Texas
Health Science Center at Houston
and
The University of Texas
MD Anderson Cancer Center
Graduate School of Biomedical Sciences
in Partial Fulfillment

of the Requirements

for the Degree of

MASTER OF SCIENCE

by

Ruchitha Goonatilake, BS
Houston, Texas

Date of Graduation

August 2016

Dedicated to my family

Acknowledgements:

I would like to express my sincere gratitude to my mentor Dr. Faye Johnson for her kindness, patience, and support while she gave me guidance for the past two years. She was a fantastic mentor and I aspire to be bit like her one day. I am also very grateful for the help I received from all the members of our lab in so many ways: Dr. Tuhina Mazumdar, Dr. Shaohua Peng, Dr. Nene Kalu, Dr. Ratnakar Singh, Dr. Vaishnavi Sambandam, Dr. Ming Zhang, Dr. Yuehong Wang, and Liguang Wang. I am also very grateful to Dr. Uma Giri who has given me a great deal of advice through my time here. I would also like to sincerely thank my committee members Dr. Khandan Keyomarsi, Dr. Walter Hittelman, Dr. Lauren Byers, and Dr. Jing Wang for their excellent advice given during committee meetings. Additionally, I would like to thank the Bioinformatics department who worked very hard to help us find significant results which we studied further in the laboratory. Without them, my life would have been much more difficult. Also, I would like to thank David Peng and Dr. Don Gibbons for their collaboration with regards to the EMT experiments, and Dr. Jonathan Roybal for teaching me to use the fluorescent microscope. Finally, a big thank you to the flow cytometry core for teaching me to run a flow cytometer.

Determining Mechanisms of Response to Polo-like Kinase 1 Inhibition in Non-Small Cell Lung Cancer

Ruchitha Goonatilake, B.S.

Supervisory Professor: Faye M. Johnson, M.D., Ph.D.

Non-small cell lung cancer (NSCLC) is the leading cause of cancer-related death worldwide. The discovery of genetic alterations in some patients (~15%) has made it possible to use targeted therapies without the use of chemotherapy. To identify potential therapeutic targets in NSCLC, we systematically evaluated two cancer cell line databases with sensitivity data for a broad range of drugs. We identified polo-like kinase 1 (Plk1) as the most promising target for further investigation based on a subset of sensitive cell lines and inhibitors that were in advanced clinical development.

To identify potential biomarkers of response and mechanisms of Plk1 inhibitor-induced apoptosis, we performed an integrated analysis of gene and protein expression, gene mutation, and drug sensitivity using three Plk1 inhibitors (volasertib, BI2536, GSK461364) in a large panel of NSCLC cell lines. We observed that the NSCLC cell lines have varying sensitivities to Plk1 inhibition, with a smaller subset demonstrating sensitivity to all three inhibitors. Plk1 inhibition led to increase of cells with 4N DNA content, but only sensitive cell lines underwent substantial apoptosis following Plk1 inhibition. NSCLC lines with a high epithelial-mesenchymal transition gene signature score (i.e., mesenchymal lines) were more sensitive to Plk1 inhibitors than epithelial lines ($p<0.02$). Similarly, proteomic profiling demonstrated that E-cadherin expression was higher in the resistant cell lines ($p<0.01$). Induction of an epithelial phenotype using miR-200 expression increased resistance to Plk1 inhibition, whereas expression of ZEB1 increased sensitivity to Plk1 inhibition. Additionally, treatment of with TGF-β to induce EMT sensitized a resistant cell line and led to increased

apoptosis after Plk1 inhibition, compared to parental cells. *KRAS* mutation and alterations in tight-junction, ErbB, and Rho signaling pathways also correlated with drug response.

We demonstrate that epithelial-mesenchymal transition leads to Plk1 inhibitor sensitivity in a large-scale, integrated analysis of Plk1 inhibitor sensitivity. Our findings have important clinical implications for mesenchymal NSCLC, as a significant subset of this disease associated with resistance to currently approved targeted therapies.

TABLE OF CONTENTS:

LIST OF FIGURES:

LIST OF TABLES:

Chapter 1: Introduction

Lung Cancer

Lung cancer is the deadliest cause of cancer in the world, with estimates approximating more than 200,000 deaths in the United States alone for 2015 (1). Lung cancer is usually split into two main categories: non-small cell lung cancer (NSCLC) and small cell lung cancer (SCLC). NSCLC makes up approximately 85% of all lung cancer cases whereas SCLC makes up 15% (1) Most of the lung cancer cases are attributed to tobacco use. However, there are a host of other factors which may contribute, including environmental causes, such as exposure to secondhand smoke, air pollution, inherited factors, , and other substances (2-4). Lung cancer is not frequently found in people under 35, and the incidence of lung cancer rises exponentially afterwards (5). Although there have been great advances in terms of early detection and treatment, most new cases are usually found at late stages and are resistant to therapy (6). The five-year survival rate for all stages of lung cancer is 54% for localized disease, but decreases to 4% in cases of distant metastasis (1, 7).

Non-small cell lung cancer

NSCLC is made up of three major histologies: squamous cell carcinoma (SCC), large cell carcinoma, and adenocarcinoma. There are several other histologies which occur much less frequently. Adenocarcinoma accounts for approximately 50% of NSCLC, and usually originates in the more peripheral regions of the lungs (8). Although adenocarcinoma is associated with tobacco use, it is more common in the non-smoking population than other subtypes (9). Another major histology of NSCLC is the squamous cell carcinoma which originates from the proximal airway. SCC accounts for

approximately 35% of NSCLC, and 11% are accounted for by large cell carcinoma, originating from the bronchi located more towards the center of the lungs (8).

Common genetic aberrations in NSCLC

The development of tumors is not a single step process; on the contrary, it is a complex process which occurs due to the accumulation of several genetic alterations over a period of time (10). These accumulating alterations allow for cancer cells to have advantages in growth and survival compared to normal cells. Genetic aberrations have been characterized in NSCLC which contribute to various advantages in proliferation, survival, migration, invasion, and resistance to programmed cell death - all hallmarks of cancer (11). The most frequent aberrations in adenocarcinoma include mutations in Kirsten rat sarcoma viral oncogene homolog (*KRAS*), epidermal growth factor receptor (*EGFR),* met proto-oncogene (*MET*), *LKB1* (serine/threonine kinase 11), and *TP53* (12). *EGFR* gene amplification is seen in around 15% of patients while *MET* amplification is seen in approximately 20% of adenocarcinoma patients (12). In the squamous cell carcinoma, mutations which frequently occur also include *MET, TP53*, *LKB1*, and *KRAS*. *EGFR* and *MET* amplification are seen in 30% and 21% of SCCs and *EGFR* mutations are rare (12). Other aberrations which have been found in NSCLC at lower frequencies include *BRAF* mutations, *HER2* mutations, *TITF-1* amplification, and *ALK* translocations (13).

Treatment of NSCLC

Patients diagnosed with early stages of disease usually undergo surgery and adjuvant chemotherapy may allow for more beneficial results with resected tumors (4).

Patients with locally advanced disease are treated with chemotherapy and radiation in conjunction, either with or without surgery (14). Patients with metastatic disease are usually treated with palliative chemotherapy (14). Chemotherapy usually is made up of platinum based compounds which are combined with other cytotoxic agents such as taxanes or pemetrexed (8).

Treatments targeting a specific oncogenic driver molecule based on genetic alterations have recently been developed for NSCLC. An example of these targeted therapies are the EGFR tyrosine kinase inhibitors, which have resulted in significant improvements in response rates and progression-free survival for subsets of patients with these genetic alterations (15). Another example is the development of anaplastic lymphoma kinase (ALK) inhibitors for NSCLC patients with EML4-ALK translocations. ALK and EGFR inhibitors are currently approved for use in NSCLC patients with metastatic cancer (16). Despite these promising results, some patients do not respond to the inhibitors and nearly all who initially respond develop resistance (15).

Hallmarks of cancer

Cancer development is a complex process in which cancer cells must overcome many obstacles to thrive. Their genomes are changed at several stages through mutations, amplification, deletion and other mechanisms. Douglas Hanahan and Robert Weinberg proposed that the diversity of cancer genotypes is a result of eight essential physiological alterations: evading apoptosis, self-sufficiency in growth signals, insensitivity to anti-growth signals, sustained angiogenesis, limitless replicative potential, tissue invasion & metastasis, abnormal metabolic pathways, and evading the immune system (10). These hallmarks are novel capabilities that cells acquire during

tumorigenesis, that enable them to overcome anticancer mechanisms which have been programmed into cells.

In addition to breaking through the physiological barriers through acquisition of these hallmarks, cancer is viewed as a disease of the cell cycle (17). This is due to the fact that cells undergo disruptions which can affect the cell cycle machinery which leads to the increased or inappropriate proliferation, a major hallmark of cancer. These defects can target the cell cycle itself or upstream signaling which has consequences in the cell cycle.

Phases of the cell cycle

The eukaryotic process of cell division known as mitosis has been well studied (18). Eukaryotic cells follow a program to divide and proliferate called the cell cycle; this process can be divided into three phases: interphase, mitotic (M) phase, and cytokinesis. In interphase, the cell grows, duplicates its DNA content, and obtains the necessary nutrients for the ensuing division. In the M phase, the cell divides into two daughter cells. This process is finalized in the cytokinesis. To make sure cells divide correctly, there are control mechanisms termed the cell cycle checkpoints.

Nonproliferating cells are thought to be in the G0 phase. Here, the cells are able to remain quiescent for a long interval of time. Senescent cells enter this phase permanently in response to DNA damage or degradation (19). Interphase of the cell cycle consists of three subphases, Gap 1 (G1), S, and Gap 2 (G2). Interphase consists of about 90% of the total time necessary for the cell cycle process (20). The G1 phase is the interval between the M phase of the previous cycle to S phase of the subsequent cycle. Here, the cells need to acquire the necessary nutrients to be able to sustain

themselves during the cell cycle. The ensuing S phase begins as the DNA replication starts; it is completed once all the chromosomes have replicated resulting in two sister chromatids. After the S phase is properly completed, the G2 phase of interphase occurs. The G2 phase is often characterized by quick cell growth and the synthesis of various proteins essential for cell division (21).

After the G2 phase, the relatively short M phase begins. In the M phase, the cell separates its chromosomes into two separate nuclei. Chromosomes condense and are pulled apart by cellular machinery to opposite parts of the cell. The nuclear envelope forms around the chromosomes, and begins forming the two identical daughter cells. The M phase consists of four stages: prophase, prometaphase/metaphase, anaphase, and telophase. Prophase is the beginning of mitosis, where the nuclear envelope breaks down, and condensed chromosomes start to appear, consisting of two sister chromatids which have been produced during the S phase. Additionally, the duplicated centrosomes move towards the opposite sides of the nucleus and will be the two poles of the mitotic spindle. In prometaphase the microtubules of the spindle attach to the kinetochores of the chromosomes. The kinetochores of the sister chromatids are located on both sides of each chromosome, so the microtubules from the two sides of the spindle will be able to attach. During metaphase the condensed chromosomes then align at the equatorial plate of the dividing cell known as the metaphase plate. In anaphase the sister chromatids break apart and move towards the opposite sides of the mitotic spindle. The last step is telophase, where the nuclei form again and the chromosomes decondense. The process is then followed by cytokinesis, a process in

which the nuclei, organelles and other features are equally distributed to the two identical daughter cells which will be in interphase (21).

Many checkpoints exist so that damaged or incomplete DNA is not taken up by the daughter cells. The main checkpoints that exist in the cell cycle are the G1/S, G2/M, and M checkpoints. The G1/S checkpoint is the rate-limiting and most important step in the cell cycle; it is known as the restriction point (21). The stages of the cell cycle are regulated by several proteins discussed in the next section.

Cyclins, CDKs, and Mitotic Entry

Two kinds of regulatory proteins are in charge of the cell's progress in the cell cycle: these are the cyclins and the cyclin-dependent kinases (CDKs). Together the two components form heterodimers where the cyclins are the regulatory subunit and the CDK is the catalytic subunit (17). Cyclins do not have catalytic activity on their own, whereas CDKs are inactive without the cyclin subunit. When the cyclin binds to the CDK, they phosphorylate downstream signaling and either activate or inactivate downstream targets to control the progression to different phases of the cycle. Eukaryotic cells have nine CDKs, of which five have direct involvement in the cell cycle(17). In mammals, CDK1 and its binding cyclin partners A2 and B are enough to drive the cell cycle. Cyclin-CDK complexes involved in earlier cell-cycle phases are needed to activate complexes in later phases. Each phase of the cell cycle is governed by the complexes of different cyclins and CDKs as shown in Table 1.

Phase	Cyclin	CDK
G0	C	CDK3
G1	D, E	CDK4, CDK2, CDK6
S	A, E	CDK2
G2	A	CDK2, CDK1
M	B	CDK1

Table 1. Cyclin-CDK complexes involved in the phases of the cell cycle.

The entry into mitosis is regulated by the CDK1-cyclin B complex (22). Normal cells usually have low cyclin B expression when the S phase begins and the levels increase at the end of G2. Cyclin B levels are regulated by several transcription factors, including p53, p21, and c-Myc. These transcription factors allow for the accumulation of CDK1-cyclin B complex. Near the end of the G2 phase, the complex is inactivated due to inhibitory phosphorylation of CDK1 by Wee1 (Tyr15) and Myt1 (Thr14 and Tyr15). Cdc25 phosphatases dephosphorylate these sites to activate the CDK1-cyclin complex (17). Inhibition of the Wee1 and Myt1 kinases induce mitotic entry of cells which have been arrested in the S phase (23, 24).

Plk family

In addition to the cyclin-CDK complexes, polo-like kinases play a major role in cell cycle progression and control. The founding member of the family is the *polo* gene that was first discovered and characterized in *drosophila* mutants with spindle pole defects (25). After these findings, Plks have been characterized in eukaryotic cells. The Plk family consists of five known members: Plk1, 2, 3, 4, and 5.

All Plk family members have the same basic structure, consisting of a serine/threonine kinase domain at the amino terminus, and a regulatory portion, consisting of the polo boxes in the carboxyl terminus as seen in Figure 3 (25, 26). The Plk family members have either one (Plk5) or 2 (Plk1,2,3) or 3 (Plk4) polo-boxes.

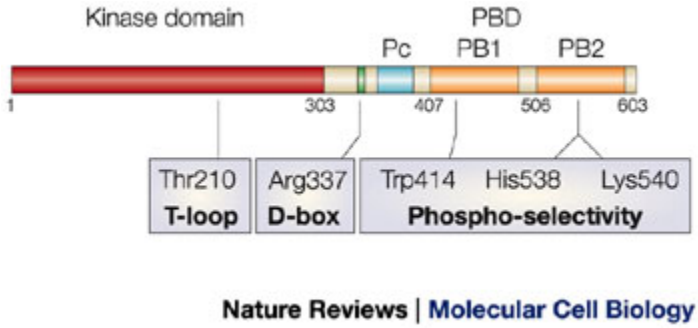

Figure 1. Structure of Plk. The structure of Plks consist of the kinase domain and the polo-box domain, containing one or more polo boxes, connected by a linker. Reprinted by permission from Macmillan Publishers Ltd: Nature Reviews: Molecular Cell Biology, Barr FA, Sillje HH, Nigg EA. Polo-like kinases and the orchestration of cell division. Nature reviews Molecular cell biology. 2004;5(6):429-40. 2004. (25)

The kinase domain is evolutionarily conserved among all members of the Plk family. The unique feature of the Plk family is the complex of polo boxes, called the polo box domain (PBD). The PBD binds to a serine or threonine site that has been

phosphorylated by another kinase or by a Plk itself – a process called priming. Additionally, the PBD can bind to non-phosphorylated peptides such as Map205 (27).

Of the Plk family members Plk1 is the best characterized member, whereas the functions of Plk2, 3, and 4 are not as well understood. In humans, Plk1 has been primarily linked to the regulation of different events, mostly with the proper entry into mitosis, the spindle assembly, and cytokinesis. Plk1 has also functions in the DNA damage checkpoints (28). Plk2 is known as a tumor suppressor which functions in centriole duplication and progression in G1-S of the cell cycle (29). Plk3 is known to regulate the cell cycle, responses to various stresses, and disassembly of the Golgi apparatus (30). Additionally Plk3 has tumor suppressor functions as well. Plk4 is also known to function in centriole duplication and has regulatory roles in mitosis (31). Recently, Plk5 has also been found which has lower catalytic activity, but has significant functions in neurons (32).

A systematic evaluation of two screening databases, the Cancer Cell Line Encyclopedia (CCLE), and Genomics of Drug Sensitivity to Cancer (GDSC) led to the identification of Plk1 as a promising target for further investigation (33, 34). Plk1 emerged as the top candidate based on specific criteria: inhibition of the target must be highly effective in a subset of NSCLC cell lines, the target should not extensively studied in NSCLC, and the target must have inhibitors in development for potential translational studies. Studies in non-selected, refractory NSCLC patients showed 4% derived a significant benefit from Plk1 inhibitors (35). However, it is unclear why a small subset of patients respond to Plk1 inhibitors. We sought to further investigate the effect of Plk1 inhibition on NSCLC cell lines.

Plk1 regulation

The activities of Plks are regulated by localization, phosphorylation and relative abundance. For example, during prophase and metaphase, Plk1 is localizes to the centrosomes and kinetochores, where it functions in the maturation of the centrosomes and the spindle assembly checkpoint (36). Regulation primarily occurs through the phosphorylation of target proteins involved in these pathways. The polo box domain is crucial for Plk1 localization and activity, as mutations in residues have demonstrated inability for Plk1 to localize to the spindle poles (32).

Plk1 is expressed from G2 to the end of mitosis when it is rapidly degraded. Plk1 has a short half-life, and is expressed from G2 to the end of mitosis when it is rapidly degraded during anaphase. The degradation of Plk1 is triggered by APC/C (26).

Plk1 transcription is repressed during G1 and activated in G2 (26). RB and E2F transcription factors repress Plk1 transcription. The DREAM complex and FOXM1 promote *Plk1* transcription (26).

The kinase activity of Plk1 is observed mainly in the G2-M transition and peaks during the M phase (25). Post-translational modification (phosphorylation) is reported to be a major regulatory mechanism for Plk1. Phosphorylation of Plk1 results in its activation. The activation of Plk1 has been proposed to work through priming phosphorylation of binding partners by the CDK1-cyclin B complex which allows for the binding of the PBD thereby uncoupling it from the kinase domain (37). It has been reported in human cells that Plk1 activation occurs a few hours before entry into the

mitotic phase (27). Phosphorylation of Ser128 (hinge region) and Thr210 (T loop) are required for activity. Aurora A and its co-factor Bora phosphorylate Plk1at Thr210 (26). This phosphorylation is a crucial step for Plk1 to start mitotic entry and in promoting mitosis after G2 checkpoint arrest.

Plk1 and mitotic entry

One of the main functions of Plk1 is to facilitate mitotic entry. Mitotic entry is regulated by the levels of the active CDK1-cyclin B complex. In G2, there is increased activity of the cyclin B promoter and more stabilization of cyclin B mRNA levels as compared to other phases of the cell cycle, leading to higher levels of protein (38). Cyclin B is able to bind to the inactive CDK1, but the complex is initially inactive due to phosphorylation by Wee1 and Myt1 (Fig. 4).

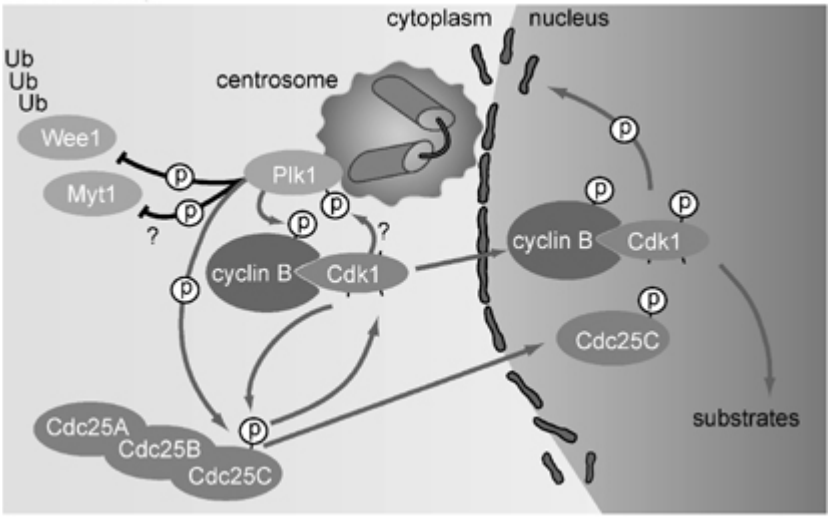

Figure 2. Role of Plk1 in Mitotic Entry. Plk1 facilitates mitotic entry by acting on several substrates including cyclin B, Wee1, Myt1, and Cdc25. Reprinted by permission from Macmillan Publishers Ltd: Oncogene, van Vugt MA, Medema RH. Getting in and out of mitosis with Polo-like kinase-1. Oncogene. 2005;24(17):2844-59. 2005.(39)

CDK1 is phosphorylated by the Wee1 and Myt1 kinases on the ATP binding site of Tyr15 and by Myt1 on Thr14. This phosphorylation prevents ATP from binding and the transfer of the phosphate group for the kinase activity (39). Additionally, the complex is regulated by the localization within the cell. For entry into mitosis, dephosphorylation of the sites on the CDK1-cyclin B complex is crucial for complex activation. The dephosphorylation is done by the members of the Cdc25 family of phosphatases (a, b, and c). Plk1 regulates the activity of the Wee1 and Myt1 kinases along with the Cdc25c phosphatase. Plk1 phosphorylates Myt1 and Wee1, primarily to inhibit them and also marks Wee1 for degradation (39). Plk1 activates Cdc25c, promoting the activity of the CDK1-cyclin B complex.

Plk1 and DNA damage response

Additionally, Plk1 plays a role in the DNA damage response. When DNA damage occurs, cells are unable to proceed in mitosis until the DNA is repaired– a process termed the G2 DNA damage checkpoint (28). Inactivation of Plk1 is a key mediator of this G2 arrest. Before entry into mitosis, Plk1 is phosphorylated by Aurora A kinase together with Bora, at the Thr210 site, activating it. Bora is able to open up the closed formation of Plk1 and Aurora A is able to phosphorylate Plk1 for activation during the mitotic entry. In response to the DNA damage, two kinases : ATM (ataxia talangectasia mutated) and ATR (ATM and RAD3-related) are activated. ATM and ATR phosphorylate Bora at Thr 501, causing it to be recognized by the E3 ubiquitin ligase for degradation (28). Once degraded, however, Bora cannot facilitate the activation of Plk1 (28). As Plk1 is not able to be activated, CDK1 is unable to be activated, resulting in a G2 arrest.

When DNA damage occurs in cells at the G2 phase, they avoid production of abnormal chromosomes by not going into mitosis. Following DNA repair, Plk1 is again activated, allowing for the mitotic entry and recovery of cell division.

Plk1 and the spindle assembly checkpoint (SAC)

The SAC is a process which ensures that the kinetochores of the chromosomes are properly attached to spindle microtubules for proper cell division. It prevents the start of anaphase until all kinetochores are attached properly to the microtubules coming from the poles from the opposite sides of the parental cell (40). Plk1 functions to relieve the inhibitory signal of the spindle checkpoint. During meta- and anaphase, Plk1 is localized to the chromatids, where it is required for stable attachment of kinetochores to the microtubules of the spindle apparatus (36). Plk1 depleted cells which are also co-depleted of surviving are not able to arrest, suggesting that Plk1 is crucial to producing the tension on the kinetochores to start the spindle checkpoint signaling (41).

Additionally, Plk1 is known to phosphorylate the translationally controlled tumor protein (TCTP) at Ser46 (42). TCTP is a highly expressed protein which is known to have a function in a variety of cellular processes, one of which is stabilization of microtubules (43). It is known to localize with other factors towards the spindle during its assembly (44). Checkpoint proteins, including Mad and Bub and Mps1 kinase negatively regulate the activity of the Anaphase-Promoting Complex (APC) by inactivating Cdc20. Once the kinetochores and microtubules are properly attached, these signals will deteriorate and the APC will activate. The degradation of securin, which normally binds and inhibits the protease, separase, is an important step in

promoting anaphase (45). Separase, which is now active, then cleaves the Scc1 (sister-chromatid cohesion-1) subunit of the cohesin complex, which results in the loss of sister-chromatid cohesion. The chromatids now are able to separate in the anaphase stage. The Cdc20 form of APC also targets cyclin B for degradation, leading to the inactivation of CDK1 (36).

Plk1 in cancer

Plk1 was first reported to be associated with neoplastic growth based on studies showing increased levels of Plk1 expression are increased in cancer. Plk1 is overexpressed in different types of cancers including NSCLC, melanoma, colon, and prostate cancers (46). While the expression of Plk1 is below the limit of detection in most adult tissues, organs with an increased population of proliferative cells, such as the thymus, spleen and testes, express detectable Plk1 at low concentrations (46). Plk1 overexpression leads to oncogenesis by causing chromosomal instability and other aberrations in mitosis caused by checkpoint defects. Plk1 overexpression has also been reported to transform NIH 3T3 cells in vitro and in vivo (47).

Plk1 inhibitors in cancer

Given its apparent role in neoplasias, several inhibitors of Plk1 activity have been developed. In cancer cells, the silencing of Plk1 expression using RNA interference or small molecule inhibitors results in various biological effects, including G2/M accumulation, mitotic catastrophe, apoptosis, and senescence (48-50). Knockdown of

Plk1 using siRNA in primary human cells reduces the rate of cell division but did not increase apoptosis significantly (51, 52).

Small molecule inhibitors of Plk1 inhibitors have been developed as therapeutic strategies for cancer. These Plk1 inhibitors are ATP competitive inhibitors that bind to the ATP binding site of Plk1 and prevent its enzymatic activity. The Plk1 inhibitors currently most advanced in clinical development are: BI2536, BI6727 (volasertib), and GSK461364. All three are ATP-competitive kinase inhibitors. BI2536 and volasertib (both from Boehringer Ingelheim) are dihydropteridinone derivatives. In cell culture assays, BI2536 inhibits the proliferation of a variety of human cancer cell lines with IC_{50} values ranging from 2 to 25 nM. Following treatment with BI2536, cancer cells are arrested in pro-metaphase, stain positive for phospho-histone H3 indicating chromatin condensation . These cells have also been reported to aberrant numbers of mitotic spindles with unfocused poles, and have misaligned chromosomes on the mitotic spindles . In addition to mitotic arrest, these treated cells undergo apoptosis as seen by poly-(ADP-ribose) polymerase (PARP) cleavage, flow cytometry and TUNEL assays (53).

However the effects on cancer cell lines are not uniform and some lines are resistant to the effects of Plk1 inhibition or knock-down (48). Due to these varying responses to treatment options, it is important to establish biomarkers of response to different therapies. Currently, there are no established predictive biomarkers of response for Plk1 inhibitors. Some potential biomarkers include p53 and KRAS. Tumors with both p53 deficiency and high Plk1 expression may be more sensitive to Plk1 inhibitors, although some controversial data exist (31). p53 deficient cells have been

reported to have decreased cell growth in comparison to p53 wild type cells after treatment with small-molecule inhibitors of Plk1 (54).

On the other hand, in Plk1 expression may be essential for the proliferation of KRAS mutant cancers because .However, detailed studies investigating the effects of Plk1 inhibitors in KRAS mutant cancers have not been reported. In stably oncogenic KRAS-G13D mutant colorectal cancer cells, cell death was increased by Plk1 depletion using shRNA or treatment with the Plk1 inhibitor, BI2536 (52). KRAS mutant cells treated with BI2536 accumulated in G2/M, suggesting that KRAS-mutant cells depend more on Plk1 for mitotic progression than cells with wild type KRAS, and that KRAS mutant tumors may respond well to drugs which inhibit Plk1.

BI2536 has been studied in Phase I and II clinical trials; however, it has not shown sufficient levels of antitumor activity for further clinical development in solid tumors. In single agent clinical trials of BI2536 in refractory solid tumors, a fraction of patients respond: 14% urothelial (55), 4.2 % in NSCLC, 5% in advanced solid tumors (55, 56). This has been caused, in large part, to poor pharmacokinetic properties, and off target effects that result in the inhibition of Plk3, a tumor suppressor (57). In contrast, volasertib has advanced from clinical trials and recently has been given “breakthrough status” by the FDA after significant benefit was observed in treating acute myeloid leukemia in combination with cytarabine (58). The results of a Phase I clinical trial for GSK461364 have also been recently published (59).

Non-ATP competitive Plk1 inhibitors have been in development, primarily targeting the polo box domain (60). The focus of these non-competitive inhibitors is on minimizing the binding of phosphopeptides to the PBD, thus preventing the

conformational change that opens up the kinase domain for further activation. These inhibitors have not been extensively studied to date.

Plk1 inhibitors in NSCLC

Plk1 inhibitors have not been extensively studied in NSCLC. NSCLC patients with higher levels of Plk1 expression have worse prognosis (60). Studies in non-selected, refractory NSCLC patients showed 4% of these patients had a significant benefit from Plk1 inhibitors (35). The three Plk1 inhibitors which are most relevant clinically are volasertib, GSK461364, and BI2536. Volasertib was found to have antitumor activity against H460 NSCLC cell line in vitro and in mice (61). GSK461364 had antitumor activity against 2 of 3 NSCLC cell lines in mice (61). In 3 NSCLC cell lines, BI2536 led to prolonged spindle assembly checkpoint and subsequent mitotic catastrophe (62). BI2536 has been combined with pemetrexed in NSCLC and 2 of 33 patients had a partial response (61). Additionally, siRNA targeting Plk1 led to cell cycle arrest and apoptosis of NSCLC cell line in vitro and decreased tumor growth in vivo (63). It has been shown that Plk1 inactivation has antitumor activity in a small subset of NSCLC cells. The observed effects of Plk1 inhibition in a subset NSCLC may be linked to the epithelial or mesenchymal phenotypes often observed in NSCLC cell lines (64).

Epithelial to Mesenchymal Transition (EMT)

EMT is a process which was first characterized in embryonic development (65). EMT allows an epithelial cell to lose its polarity, cell adhesion, and causes it to become migratory and invasive, hence, becoming a mesenchymal cell. A mesenchymal cell has

several properties, including that it is more mobile, invasive, and can evade programmed cell death (66).

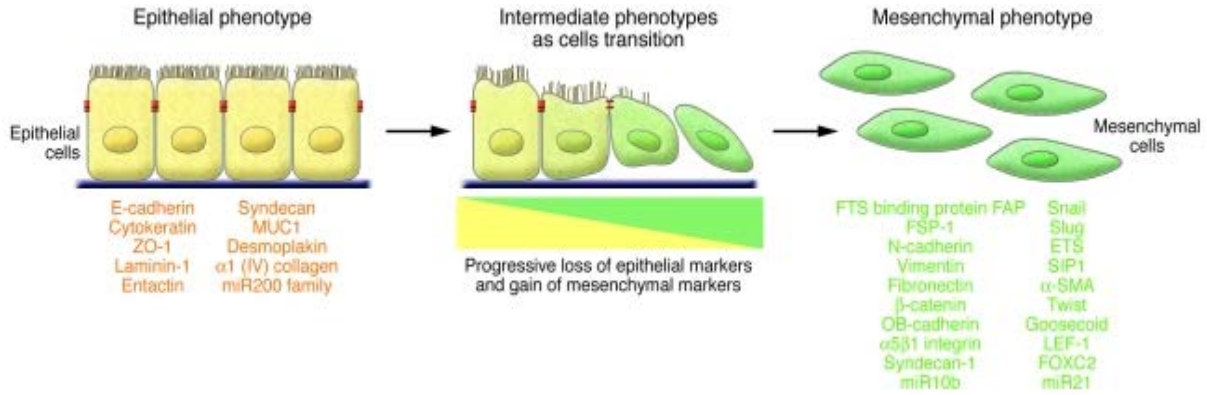

Figure 3. Epithelial to mesenchymal transition EMT is the transition of a polarized epithelial cell into a mobile mesenchymal cell. Several factors play a role in this transition. Reprinted by permission from AMERICAN SOCIETY FOR CLINICAL INVESTIGATION: Journal of Clinical Investigation, Kalluri R, Weinberg RA. The basics of epithelial-mesenchymal transition. The Journal of Clinical Investigation. 2009;119(6):1420-8. 2009. (67)

EMT and its reverse process, the mesenchymal to epithelial transition (MET) are very important in several developmental processes including gastrulation, neural crest formation, and myogenesis (68). It is also extremely important in wound healing, and plays a role in metastasis of cancer. The loss of the protein E-cadherin is a crucial event of EMT (67). Several transcription factors including Snail and ZEB1 inhibit E-cadherin by binding to its promoter and inhibiting its transcription. The miR-200 family of micro RNAs are known to directly target mRNA of repressors of E-cadherin, such as ZEB1 (69). Other transcription factors can repress tight-junction related proteins including claudins and desmosomes which also enhances EMT (67).

Additionally, signaling pathways including TGF- β, FGF, EGF, HGF, Wnt and β-catenin and Notch have been known to facilitate EMT transitions (70). RAS and MAPK

pathways have been shown to activate the transcription factors Snail and Slug (71). TGF-β is a significant inhibitor of epithelial cell proliferation and primary cell tumorigenesis. It can also serve as a positive regulator of tumor progression and metastasis (72). In vitro studies have demonstrated that TGF-β can induce an EMT in certain types of cancer cells by way of Smad-protein mediated signaling (73). Through ligand binding with the TGF- β receptors, Smad family proteins are activated and form a complex which translocates into the nucleus of cells to transcriptionally regulate target genes (74). This signaling can activate transcription factors which promote EMT. TGF- β signaling induces expression of micro RNAs which repress epithelial proteins. Additionally, TGF- β can induce pathways which are not related to Smad signaling which still contribute to EMT. These include activation of the PI3K-AKT pathway signaling, as well as regulation of Rho-GTPases which are involved in cell junction destruction (74).

EMT and cancer

EMT is known to play roles in both development and in cancer. The primary difference between the two is that in normal cells, these events are highly regulated, both spatially and temporally, where in cancer cells, such processes are not strictly regulated and can bypass certain events and checkpoints (75). During tumorigenesis (Figure 4), EMT helps cancer cells become more motile and invasive (67). The transformation to malignancy is associated with signaling pathways which promote EMT.

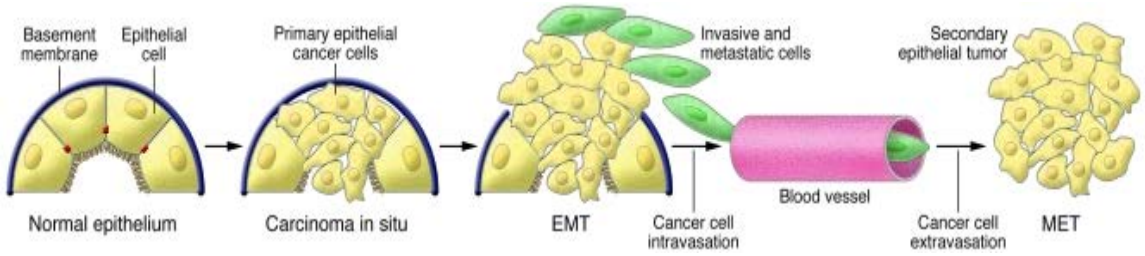

Figure 4. Epithelial to mesenchymal transition in cancer Cancer cells undergoing EMT have to go through several stages to invade and establish in a secondary site. Reprinted by permission from AMERICAN SOCIETY FOR CLINICAL INVESTIGATION: Journal of Clinical Investigation, Kalluri R, Weinberg RA. The basics of epithelial-mesenchymal transition. The Journal of clinical investigation. 2009;119(6):1420-8. 2009. (67).

The growth of neoplastic cells after transformation is quite slow, and for the tumor to grow to a certain size, it needs to vascularize (76). Invasion of the stromal cells of the host is important for the tumor to replenish the nutrients and other factors needed to survive (76). Epithelial to mesenchymal transitions facilitate this process, as the primary cells are more invasive and motile and are able to break through the basement membrane and are able to enter the bloodstream (67). As the cells are able to enter the bloodstream, they are able to adhere to other cells, eventually escape, and establish a secondary tumor at a distant site.

EMT and cell cycle

Few studies have linked the important features of cancer, EMT and the cell cycle. These reports suggest that upregulation of some Rho GTPases can increase the invasive capabilities of cancer cells. These Rho GTPases, known to have functions in deteriorating cell junctions and cytoskeletal changes, have been reported to downregulate cyclin A2, which binds to CDK2 and CDK1, important in S phase and G2/M phase progression, respectively (77). Additionally, TGF-β, a known inducer of

EMT is known to induce survivin, which stabilizes Aurora B. Aurora B is a kinase which plays an important role during the cell cycle by activating Plk1 (78).

The link between EMT and Plk1 has not been explored and needs to be elucidated further in NSCLC. Based on gene and protein expression in NSCLC cell lines in our study, EMT related genes and proteins were significantly correlated with response to Plk1 inhibition. In this thesis, we examine the responses of NSCLC cell lines to Plk1 inhibition. We then proceed to look at the biological effects of Plk1 inhibition on NSCLC cell lines. Finally, we assess the relationship of gene and protein expression to Plk1 inhibitor sensitivity to find predictive biomarkers of response to Plk1 inhibition.

Chapter 2: Materials and Methods

This chapter is based upon our submitted manuscript entitled “Epithelial-Mesenchymal Transition Predicts Polo-Like Kinase 1 Inhibitor-Mediated Apoptosis in Non-Small Cell Lung Cancer” which is currently under review.

Antibodies and reagents

The following antibodies were used: anti- Plk1 (Invitrogen); phosphorylated Myt1 (Thr495) and Myt1 (Thermo Scientific); phosphorylated CDK1 (Tyr15), FOXM1, PARP, cleaved PARP, phosphorylated translational controlled tumor protein (TCTP) (Ser46), Cyclin B, E-cadherin, TCTP, vimentin, β-catenin, and ZEB1 (Cell Signaling Technology); and β-actin (Sigma). The Plk1 inhibitors BI2536, volasertib, and GSK461364 and P-glycoprotein inhibitor PSC-833 were purchased from Selleck Chemicals (Houston, TX) and prepared as 10 mM stock solutions in dimethyl sulfoxide. We used predesigned sets of 4 independent siRNA sequences of the target genes PLK1 and CDH1 (siGENOME SMARTpool, Dharmacon, Thermo Scientific, Pittsburgh PA). The human TGF-β1 was purchased from Cell Signaling Technology.

Cell culture and characterization

Sixty three human NSCLC cell lines were authenticated with DNA fingerprinting, routinely tested for *Mycoplasma* spp., and maintained as previously described (79). The cell line Cal-12T was purchased from DSMZ. The cell lines' mutational profiles for 264 genes (Supplemental Table 1) were obtained from the catalog COSMIC (version 67) and the Cancer Cell line Encyclopedia. Baseline mRNA (48,804 probe sets) and protein (193 proteins and phosphoproteins) expression levels were determined using Illumina and reverse phase protein arrays, respectively, as previously described (80, 81).

Cell viability assays

Fifty NSCLC cell lines were incubated with dimethyl sulfoxide (vehicle control), BI2536, or volasertib for 120 h at nine distinct concentrations, with the maximum dose being the peak concentration of each drug in humans (C_{max}): 1.6 μM for BI2536 and 1.2 μM for volasertib. Cell viability was measured using the MTT assay as previously described (82). For GSK461364, 63 NSCLC cell lines were incubated with dimethyl sulfoxide or GSK461364 for 72 h at seven distinct concentrations, with the maximum dose being the C_{max} (1 μM). CellTiter-Glo luminescent cell viability assay (Promega) was performed per the manufacturer's specifications. For both assays, six replicates were tested each concentration, and each test was completed at least twice on different days.

For colony formation assays, cells were treated for 24 h with dimethyl sulfoxide or volasertib and then incubated in drug-free medium for 14 to 21 days. Plates were stained with crystal violet, and total colony area per well was estimated using ImageJ software as previously described (79, 83).

Calculation of the drugs' effects on viability

IC50 and IC70 values were estimated from the best-fit dose-response model selected by calculating residual standard error using the R packages Dose Finding and drc (84). For many cell lines, the dose-response curve plateaued at or near the IC50, so we used IC70 values to distinguish sensitive and resistant cell lines. Cell lines with IC70 values greater than the Cmax were considered resistant; cell lines with IC_{70} values less or equal to the Cmax were classified as sensitive.

Statistical analysis

IC50 and IC70 values were estimated from the best-fit dose-response model selected by calculating residual standard error using the R packages Dose Finding and drc (84). Gene expression data were available for 43 of the 50 cell lines treated with BI2536 and volasertib and 50 of the 63 lines treated with GSK461364. Forty-one cell lines had gene expression and drug sensitivity data for all 3 drugs. Reverse phase protein array (RPPA) data were obtained as previously described and available for 44 lines tested with BI2536 and volasertib and 45 lines tested with GSK461364 (80, 81). For the cell lines that were consistently sensitive or resistant to all 3 drugs (universal group), gene expression data were available for 10 sensitive and 11 resistant lines, and protein expression data were available for 10 sensitive and 13 resistant lines.

To compare gene and protein expression patterns between resistant and sensitive lines, two-sample t-tests were performed on a gene-by-gene or protein-by-protein basis. To adjust for multiple testing, we applied the beta-uniform mixture model to modelling P values in order to select an appropriate false discovery rate cutoff (85). For correlations between drug sensitivity and gene mutations, we performed Fisher exact test. Additionally, associations between drug sensitivity and epithelial-mesenchymal transition (EMT) scores (80) were evaluated using two-sample t-tests.

To evaluate pre-established signatures for KRAS dependency (64) and chromosomal instability (86), we applied a two-way hierarchical clustering technique to the dataset in order to produce heat maps (80). We tested correlation between the sensitivities of three drugs using the chi-square test. For assessment of association between each

pair of drugs, we performed the Fisher exact test. All statistical analyses were performed using R software (87).

Pathway analysis was performed with the Ingenuity Pathway Analysis tool (http://www.ingenuity.com/) using gene sets as described in the Results section.

Cell cycle analysis and apoptosis assays

For cell cycle analysis, cells were harvested, fixed, incorporated with bromodeoxyuridine (BrdU) and stained with 7-aminoactinomycin D (7AAD) (BrdU Flow kit; BD Biosciences). DNA content was analyzed with a cytofluorimeter, a fluorescence-activated cell sorter (FACScan; Becton Dickinson), and the ModFit software program (Verity Software House) (79). To measure apoptosis, we used TUNEL (terminal deoxynucleotidyl transferase dUTP nick end labeling) staining (APO-BrdU kit; BD Biosciences) and quantitated bromodeoxyuridine incorporation by fluorescence-activated cell sorting (BrdU Flow kits; BD Biosciences) according to the manufacturers' protocols.

Western blotting

For Western blots, sub-confluent cells were lysed on ice, and the lysates were centrifuged at 20,000g for 5 min at 4°C as described previously (79). Whole-cell lysates containing 30 to 50 μg of proteins were separated by sodium dodecyl sulfate-polyacrylamide gel electrophoresis, immunoblotted with the indicated primary antibodies, and detected with horseradish peroxidase-conjugated secondary antibody (Bio-Rad Laboratories) and an enhanced chemiluminescence reagent (Amersham Biosciences).

Transient Transfection

Cultured cells were plated in six-well plates 24 hours prior to transfection. On the following day, cells were transfected RNA iMax. siRNA was mixed with the reagent in serum free media. Liposomal complexes were formed in the serum free media and incubated at the room temperature for five minutes. The mixture was then added to the indicated wells and incubated for the indicated time points.

Inducible miR-200 Transfections

A modified doxycycline-inducible pTRIPz-RFP vector expressing miR-200a, miR-200b, or both (miR-200ab) was generously provided by Dr. Gregory Goodall at the University of Adelaide. H157 NSCLC cells were transduced by Lipofectamine LTX or lentiviral delivery of pTRIPz–miR-200, ZEB1B or a control vector. Lentiviruses were produced by cotransfecting HEK-293 cells with 1.5 µg of the viral packaging vector psPAX2, 0.5 µg of the viral envelope vector pMD2.G, and 2 µg of pTRIPz–miR-200 or the control vector using Lipofectamine LTX. HEK-293 cell medium was changed 24 h after transfection, and the cells were incubated at 37^{o}C for 48 h to allow for virus production. After 48 h, HEK-293 media containing virus particles were transferred onto H157 NSCLC cell culture plates and incubated at 37^{o}C for 48 h. After transduction, fresh RPMI 1640 medium with 10% FBS was added to the H157 cell culture plates, and the cells were allowed to recover for 24 h. Cells were selected using 3 µg/mL puromycin, and 2 µg/mL doxycycline was used for induction of miR-200 and RFP. Induced RFP expression was used to visually verify successfully infected

cells. H1299 cells expressing miR-200 were sorted using flow cytometry for RFP positivity to obtain the transfected cell population.

H1299 cells were transfected with 4 µg of pTRIPz–miR-200 or the control vector using Lipofectamine LTX. After 24 h of transfection, cells were selected using 3 µg/mL puromycin in RPMI 1640 with 10% FBS. Expression of miR-200 and RFP was induced with 2 µg/mL doxycycline. H1299 cells expressing miR-200 were sorted using flow cytometry for RFP positivity to obtain the transfected cell population.

Immunofluorescence Microscopy

Cells were plated on MilliCell EZ-Slides (Millipore). After 24 hours, the cells were treated with vehicle or volasertib for the time points indicated. Following treatment, cells were rinsed with PBS, fixed with 4% paraformaldehyde. After washing, the samples were blocked in 1% BSA, and primary antibody was added. Slides were kept overnight in 4°C. Afterwards, the cells were washed, and were incubated with the secondary antibody for one hour, protected from light. After washing, mounting media with DAPI was added along with coverslips. Slides were visualized using a fluorescence microscope.

H&E staining

Cells were plated on MilliCell EZ-Slides (Millipore). After 24 hours, the cells were treated with vehicle or volasertib for the time points indicated. Following treatment, the cells were washed with PBS, fixed with 4% paraformaldehyde. Then cells were stained with hematoxylin for one minute, washed with tap water for bluing. Following this, cells were

dehydrated with increasing concentrations of ethanol. Cells were then stained with eosin for one minute, and excess eosin was removed by ethanol washing. Following this, slides were air-dried and mounted with DPX.

ELISA Plk1 activity assay

A Plk1 ELISA assay from MBL Technologies was used to assess Plk1 activity after treatment with volasertib. Briefly, subconfluent cells were pre-treated with the inhibitor for the indicated time points, harvested, lysed, and used immediately afterward for the assay. The concentration of the protein was quantified using the Bradford method and added to the ELISA plate coated with the substrate. After incubation to bind the substrate, there was incubation with the kinase buffer, followed by incubation with the primary anti-phospho-threonine antibody. This was followed by incubation with the HRP-linked secondary antibody, which was then detected after incubation with HRP substrate, and the optical density was measured at a wavelength of 450nm.

Doubling Time (DAPI)

Cells were seeded in a 384 well plate at different densities ((125 cells/well, 250 cells/well, 500 cells/well, 1000 cells/well and 2000 cells/well). After one day, the cells were fixed in 1% paraformaldehyde for 10 minutes. Following fixation, DAPI was added to the cells and cells were counted using an INCELL analyzer. This was repeated at 48, 72, and 96 hour time points. The averages and standard deviations are calculated, and the doubling time was calculated using the following equation: 3*(LOG(2)/LOG(96h Std Dev. /48h Std Dev.)).

Kaplan Meier Plotter

For Kaplan Meier analysis, we used Kaplan Meier Plot software analysis from www.kmplot.com (88). We used the latest 2015 version of the database generated from 1926 lung cancer patients. In our analysis, we included adenocarcinomas and squamous carcinomas, with stage III/IV disease; we did not restrict based on gender, and smoking status.

Chapter 3. Results

This chapter is based upon our submitted manuscript entitled “Epithelial-Mesenchymal Transition Predicts Polo-Like Kinase 1 Inhibitor-Mediated Apoptosis in Non-Small Cell Lung Cancer” which is currently under review.

Plk1 overexpression correlates with poor survival in lung patients

To enforce Plk1 as a target for further study, we determined the correlation of Plk1 mRNA expression and progression free survival in 2435 lung cancer patients. Using the Kaplan Meier Plotter, we utilized microarray data which had been published from the caArray project, Gene Expression Omnibus (GEO), and The Cancer Genome Atlas (TCGA) (88). Patients were not differentiated based on smoking history or gender. There was a significant relationship (p = 4.8e-15) between high Plk1 mRNA expression and lower survival (Fig. 5). To determine the cutoff for the gene, the percentile of expression between the lower and upper quartiles were computed, and the best predictive threshold was used as the cutoff through univariate Cox regression (88).

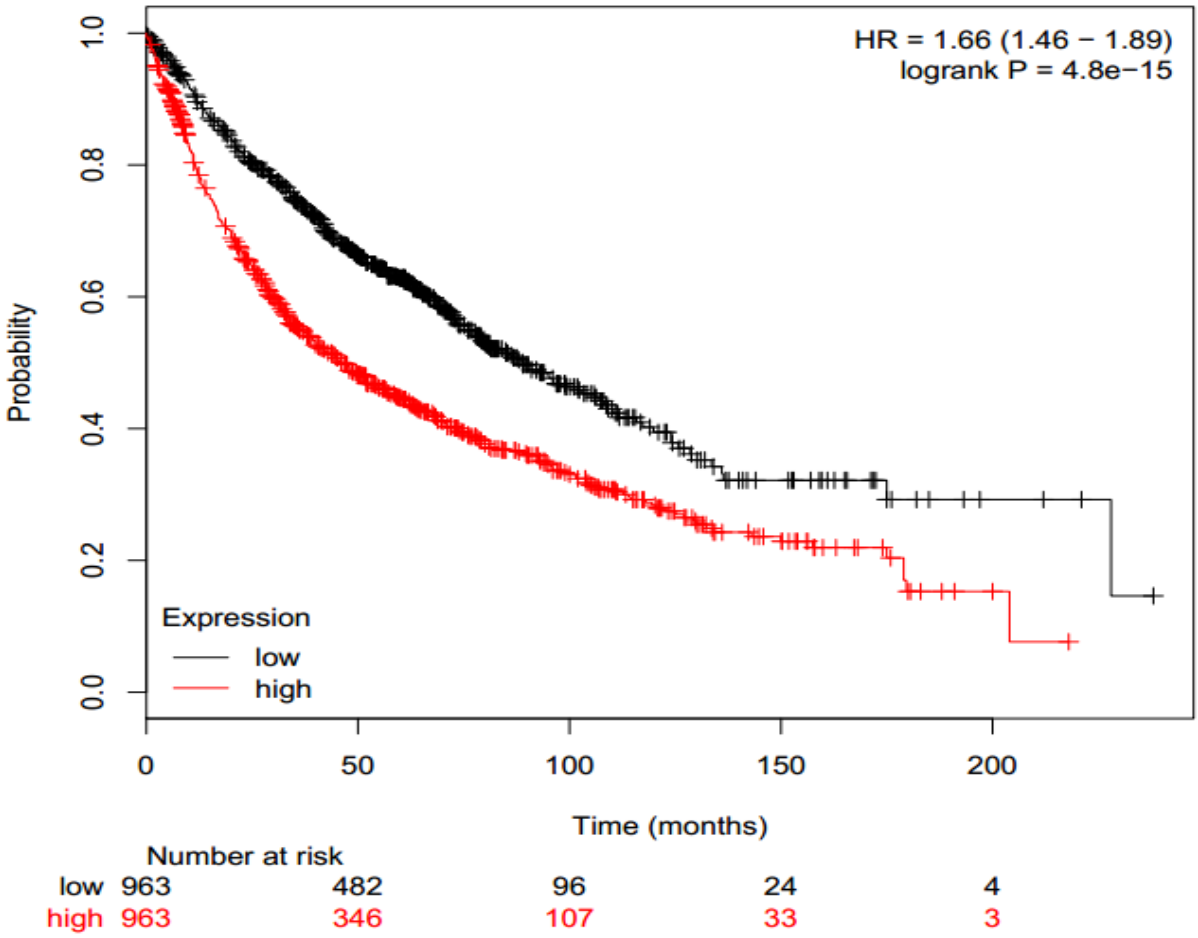

Figure 5. High *Plk1* mRNA expression correlates with lower progression free survival in lung cancer patient samples. Kaplan Meier curve showing the *Plk1* mRNA expression and progression free survival generated from www.kmplot.com. (n = 2435 patients).

NSCLC cell lines have diverse sensitivities to Plk1 inhibitors

The Genomics of Drug Sensitivity in Cancer contains drug sensitivity data on 14 NSCLC cell lines treated with 2 Plk1 inhibitors (Fig.6a) (89). To enhance future clinical translation, we used the three most clinically advanced Plk1 inhibitors, BI2536, BI6727 (Volasertib), and GSK461364. We tested 50 NSCLC cell lines for sensitivity to BI2536 (Cmax 1.6 μM) and volasertib (Cmax 1.2 μM) using MTT viability assays. To validate our findings, we also separately tested 63 NSCLC lines with GSK461364 (Cmax 1.0 μM) using CellTiter Glo assays (GSK461364 was tested by Drs. Uma Giri and Shaohua Peng, in collaboration with Dr. John Heymach's lab). Dose response curves were generated for these data and distinct groups were observed (Fig. 6b). Cell lines' sensitivity to the drugs varied widely. In many cell lines, the dose response curves plateaued near the IC50. To better distinguish the sensitive and resistant cell lines, we used the IC70 values. Those cell lines which had IC70 values which were lower than the Cmax for the drug were considered sensitive and those which did not reach the IC70 value prior to the Cmax were considered resistant which resulted in a dichotomous population.

A

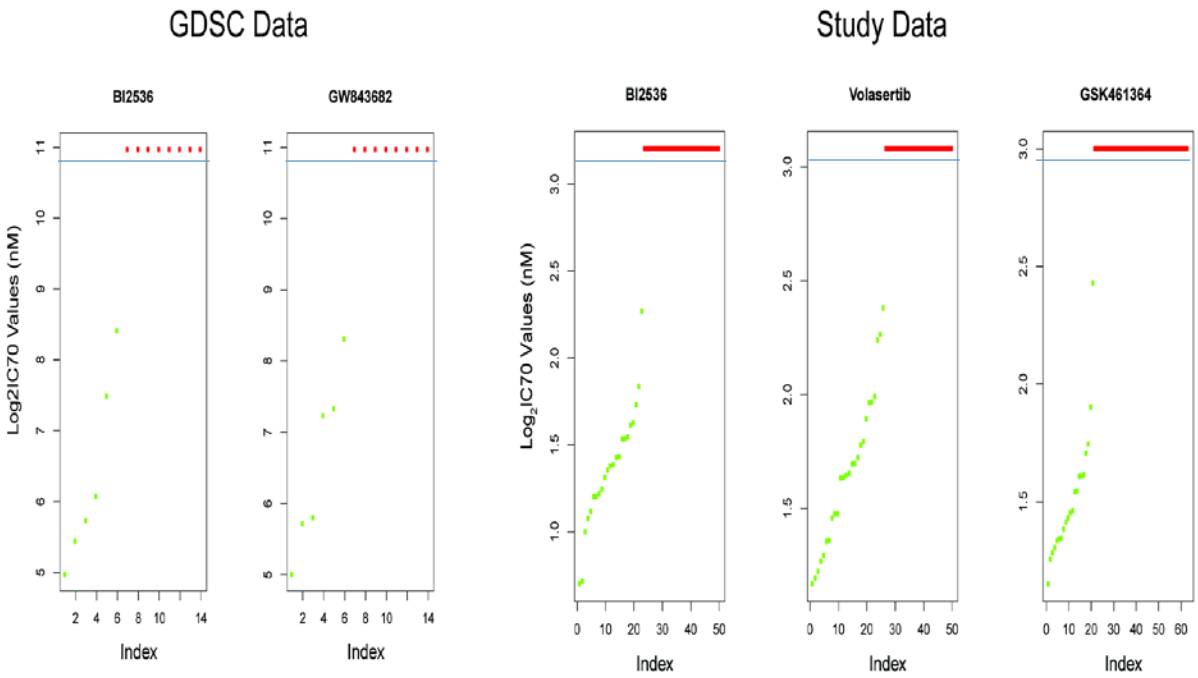
GDSC Data
Study Data
BI2536
GW843682
BI2536
Volasertib
GSK461364
Log2IC70 Values (nM)
Log2IC70 Values (nM)
Index
Index
Index
Index
Index

B

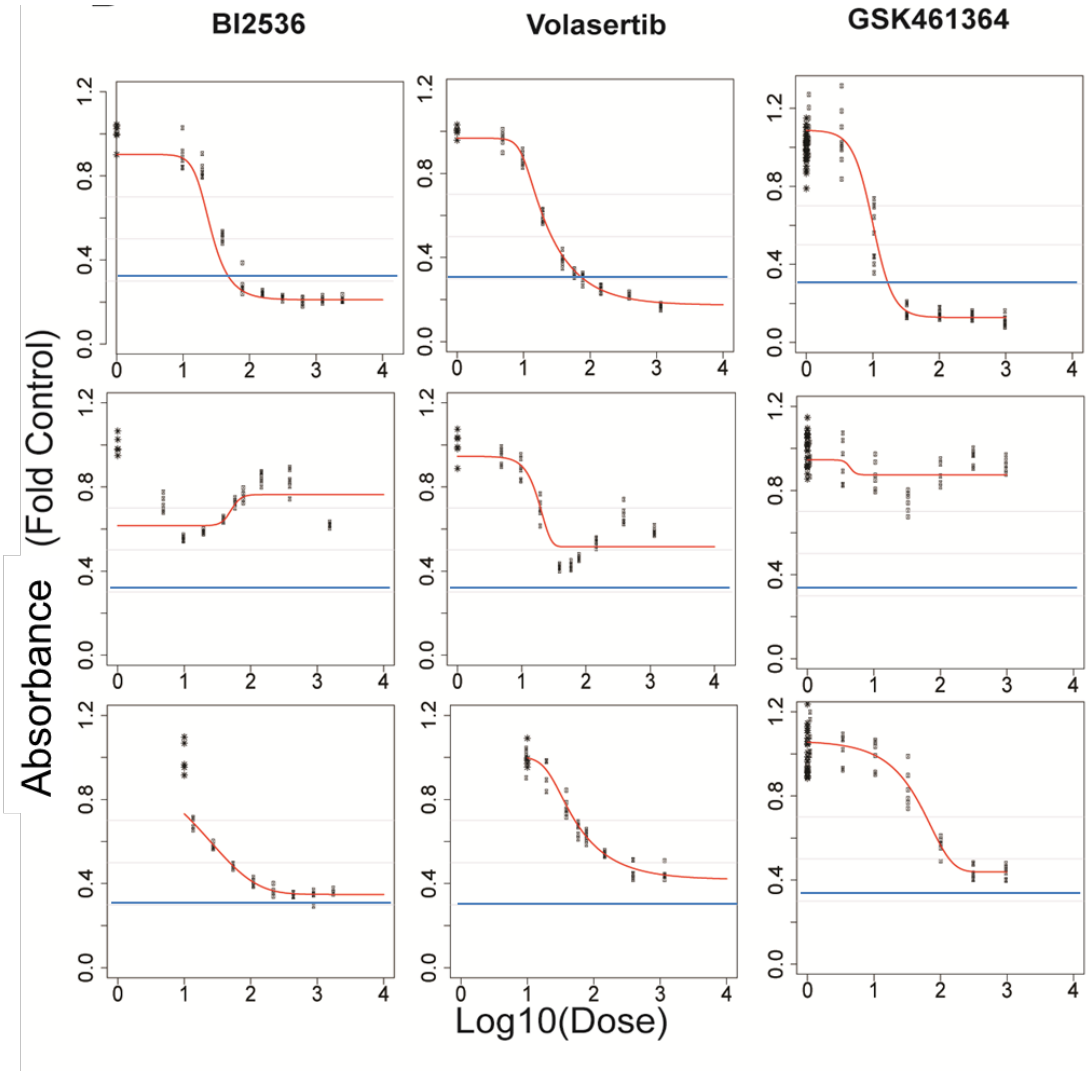

Figure 6. NSCLC cell lines have diverse sensitivities to Plk1 inhibition. (A) Drug sensitivity for two Plk1 inhibitors in 14 NSCLC cell lines was obtained from the GDSC online database (left). Each data point indicates the IC_{75} values for one individual cell line. NSCLC cell lines were treated with BI2536, volasertib, or GSK461364 for 72-120 h, and viability was estimated using MTT or CellTiter-Glo assay. Each data point indicates the IC_{70} for one individual cell line. The horizontal blue line on each chart represents the Cmax value for each drug, which was used as the cutoff for sensitivity. (B) Replicate data were graphed for each concentration, and the best dose-response model was selected by the residual standard error (RSE) method (84). The horizontal blue line on each dose response curve represents the IC70. The GSK461364 compound was screened by Drs. Uma Giri and Shaohua Peng in collaboration with Dr. John Heymach's laboratory. Dose response curves were generated in collaboration with the Bioinformatics Department, including Drs. Pan Tong, Suk-Young Yoo, and Jing Wang.

We then examined the correlation between the sensitivities drug to drug. Sensitivities to the three drugs were correlated at a p-value of 1.4e-06 (chi-square test). When drug sensitivities were compared pair-wise by the Fisher exact test, the correlation between BI2536 and volasertib ($p = 1.1e-06$), was stronger than that the correlation between GSK461364 and volasertib ($p = 0.186$) or between GSK461364 and BI2536 ($p = 0.020$). This result was expected given these drugs' structural and chemical similarities. To ensure that the observed sensitivity differences were not due to technical differences between the MTT and CellTiter-Glo viability assays, we tested the universal lines for sensitivity to all three drugs using identical conditions. Although the IC70 values were not absolutely identical between the two assays, all the universal cell lines remained in the same category (sensitive or resistant) regardless of the assay used (Table 2).

Cell line	IC_{70}					
	Volasertib		GSK461364		BI2536	
	MTT 120h	Cell Titer Glo 72h	MTT 120h	Cell Titer Glo 72h	MTT 120h	Cell Titer Glo 72h
CALU-6	18.5	61.9	58.8	21.9	10.0	16.2
H1703	43.2	66.3	118.2	28.9	13.1	25.4
H1155	22.8	31.9	53.6	18.0	16.6	18.8
H2087	52.8	65.9	350.1	26.9	20.6	25.3
H460	98.1	291.2	187.9	28.3	24.3	184.0
H838	60.0	490.8	484.6	41.0	26.8	121.1
H1299	49.4	162	60.1	268.4	34.4	16
H1355	16.7	129	53.6	35.0	35.0	33.9
H1792	78.2	97.6	114.4	22.1	53.6	45.0
H1944	183.2	346.2	522.1	34.7	185.3	303.8
H1650	>1200	>1200	>1000	>1000	>1600	>1600
H1975	>1200	>1200	>1000	>1000	>1600	>1600
H1993	>1200	>1200	>1000	>1000	>1600	>1600
H2009	>1200	>1200	>1200	>1000	>1600	>1600
H2126	>1200	>1200	>1000	>1000	>1600	>1600
H2170	>1200	>1200	>1000	>1000	>1600	>1600
H322	>1200	>1200	>1000	>1000	>1600	>1600
H358	>1200	>1200	>1000	>1000	>1600	>1600
H520	>1200	>1200	>1000	>1000	>1600	>1600
HCC15	>1200	>1200	>1200	>1000	>1600	>1600
HCC2302	>1200	>1200	>1200	>1000	>1600	>1600
HCC366	>1200	>1200	>1000	>1000	>1600	>1600
HCC4006	>1200	>1200	>1000	>1000	>1600	>1600

Table 2. MTT and CellTiter-Glo assays confirmed universal sensitive and universal resistant cell lines to three Plk1 inhibitors. After screening all cell lines we assayed the cell lines which were either sensitive to all three inhibitors (universally sensitive) or resistant to all three inhibitors (universally resistant) using both MTT and Cell TiterGlo assays. The IC70 values obtained are shown above. IC70 values were generated with the help of the Bioinformatics Department, including Drs. Pan Tong, Suk-Young Yoo, and Jing Wang.

BI2536, volasertib, and GSK461364 inhibit Plk1 targets in NSCLC cell lines

To determine if BI2536, volasertib, and GSK461364 are indeed inhibiting Plk1 in the NSCLC cell lines, we used two universally sensitive cell lines, H1792 and Calu-6, and two universally resistant cell lines, H322 and H358, to study the effects of Plk1 inhibition on known Plk1 targets. We examined the phosphorylation of Myt1 kinase at the inhibitory phosphorylation site of Thr495 for H1792 and H322 and phosphorylation of TCTP at Ser46 for all four cell lines, which are both known phosphorylation targets of Plk1 at different concentrations and time points. We examined the dose dependent response to determine the relevant dose needed to inhibit Plk1 in the cell lines (Fig. 7a), which we determined to be 50nM. We were able to see target inhibition persist up to 120 hours, which mirrored the maximum time interval we exposed the cell lines to the drugs in the viability assays (Fig. 7b). As we expected, inhibition of Plk1 led to a decrease in phosphorylation of Myt1 in the NSCLC cell lines. We additionally observed that although TCTP phosphorylation after treatment, the decrease was much lower in the two resistant lines tested. We observed an increase in the levels of phospho-CDK1 at Tyr15, indicating an inactive CDK1 after Plk1 inhibition using volasertib. Additionally, we were able to see stabilization of levels of cyclin B after Plk1 inhibition (Fig 7c).

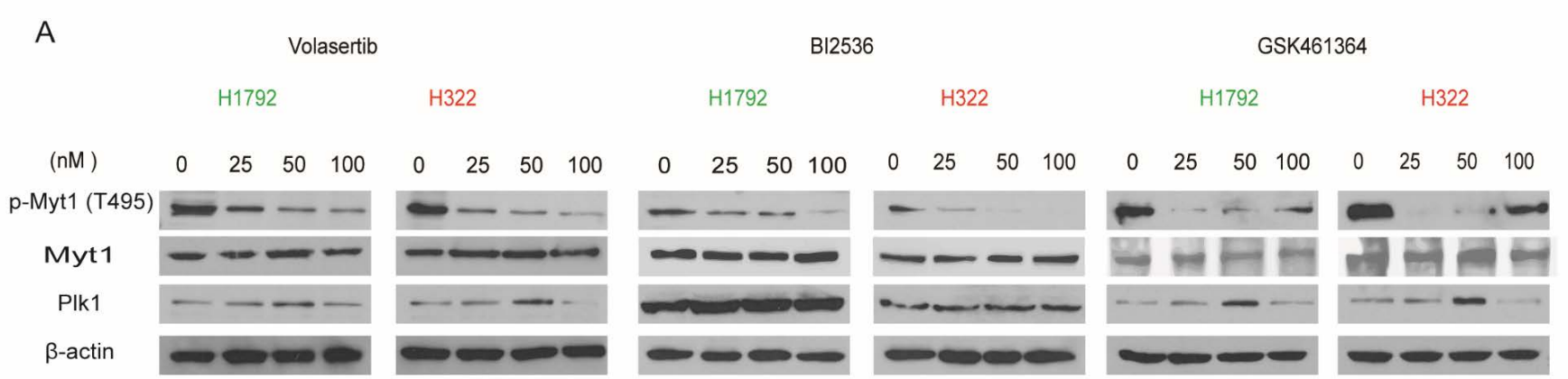
A
Volasertib
BI2536
GSK461364
H1792
H322
H1792
H322
H1792
H322
(nM)
0 25 50 100 0 25 50 100 0 25 50 100 0 25 50 100 0 25 50 100 0 25 50 100
p-Myt1 (T495)
Myt1
Plk1
β-actin

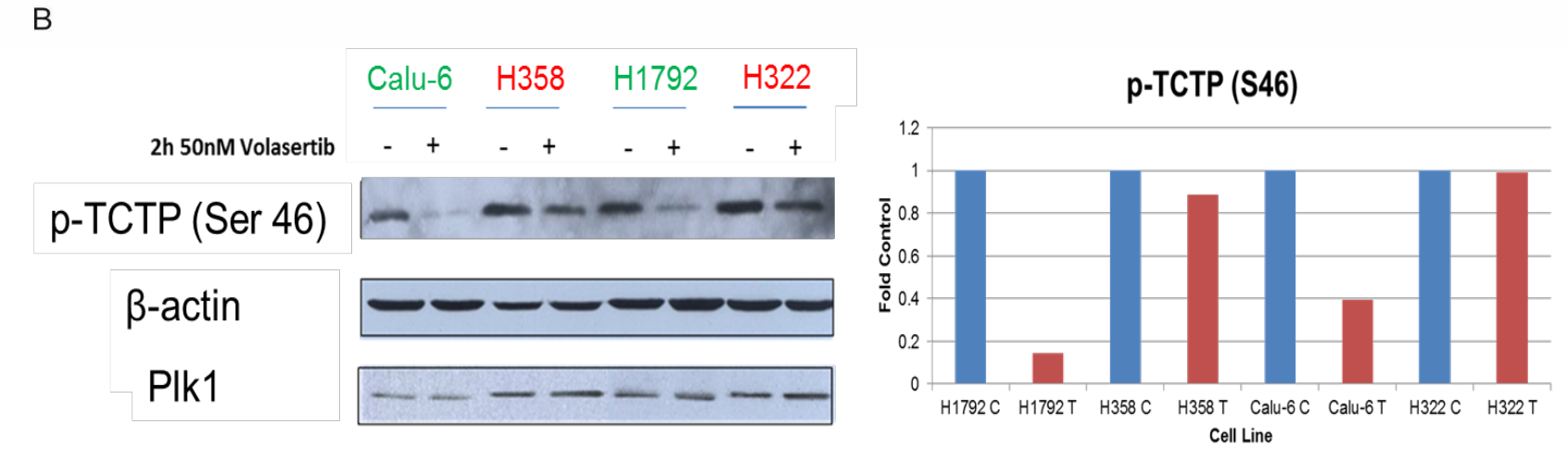
B
Calu-6
H358
H1792
H322
2h 50nM Volasertib
- + - + - + - +
p-TCTP (Ser 46)
β-actin
Plk1
p-TCTP (S46)
Fold Control
1.2
1
0.8
0.6
0.4
0.2
0
H1792 C
H1792 T
H358 C
H358 T
Calu-6 C
Calu-6 T
H322 C
H322 T
Cell Line

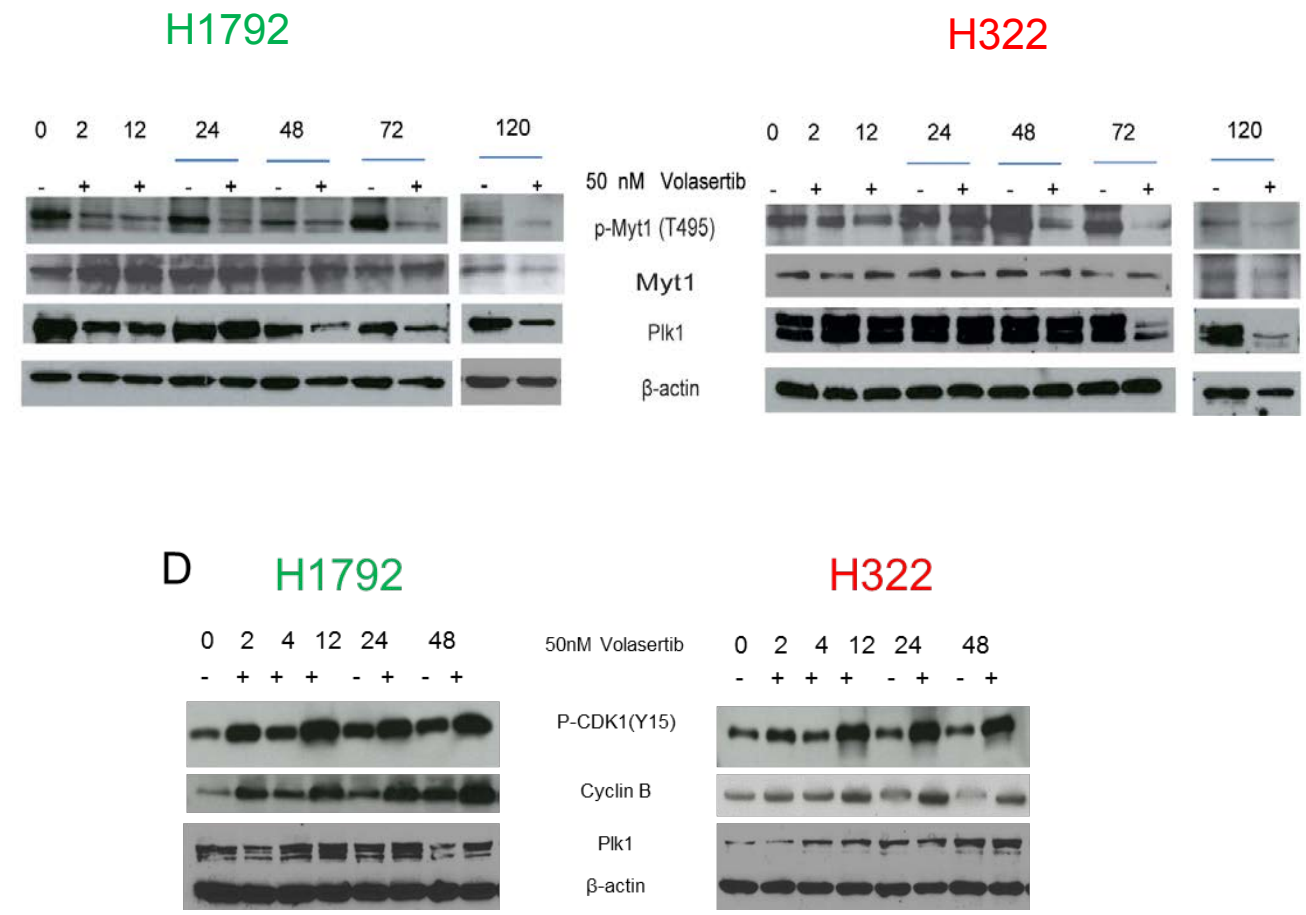

Figure 7. Inhibition of Plk1 substrates after treatment with Plk1 inhibitors. NSCLC cell lines were incubated with dimethyl sulfoxide (vehicle control), BI2536, volasertib, or GSK461364 using the indicated concentrations for 2 h (A, B) or at 50 nM for the indicated periods (in hours) (D). Cells were then lysed and subjected to Western blotting (A-D) with the indicated primary antibodies and (B) p-TCTP band density was quantitated.

We noticed in the dose response western blots that there was incomplete target inhibition at higher doses, in regards to GSK461364. To test whether the drug was being actively pumped out by the cells, we also examined ATP binding cassette (ABC) protein expression that has been reported to be possible resistance mechanism for Plk1

inhibition (90). We observed that GSK461364 induced ABCC1 and ABCG2 expression at high concentrations (Fig. 8).

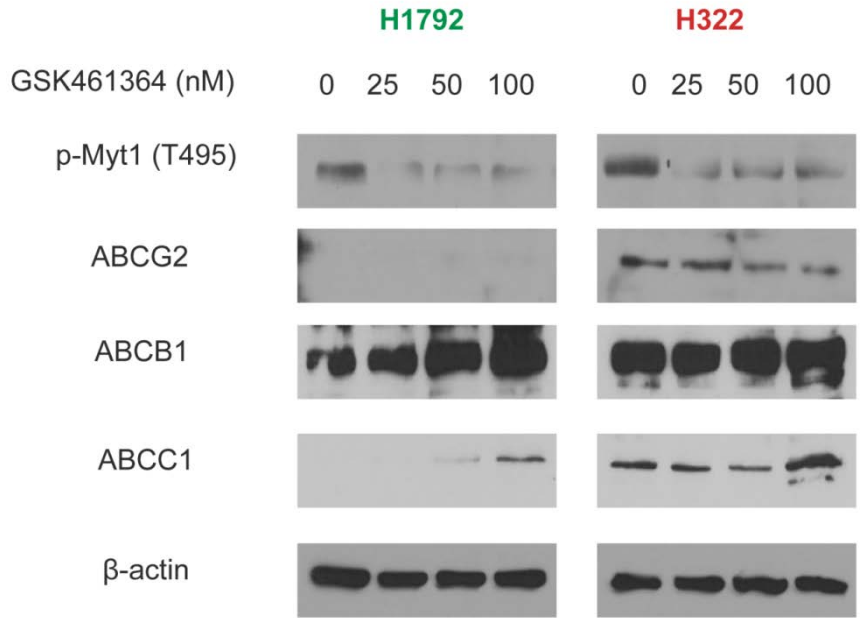

Figure 8. Plk1 inhibition with GSK461364 led to increase in ABCB1 and ABCC1 protein expression. Cells were incubated for 4 hours with 50nM GSK461364, lysed, and protein expression was analyzed through Western blot.

Plk1 inhibition leads to lower Plk1 kinase activity in NSCLC cell lines

To more directly test if Plk1 inhibitors were inhibiting Plk1 function, we assayed for Plk1 enzyme activity using an ELISA based assay that measures the phosphorylation of protein-X, a substrate of Plk1. Plk1 activity was decreased up to 80% with concentrations of 50 nM and 1 μM volasertib in extracted cell lysates to which inhibitor was added directly to the lysates (Fig 9a). NSCLC cell lines were incubated with 50nM volasertib for 24 and 48h time points. In intact cells, we observe a lower inhibition efficiency at short time points, and incomplete inhibition in resistant cell lines

(Fig. 9b). However, in experiments in which volasertib was added to the intact cells, volasertib was not added to the lysates incubated with the Plk1 substrate.

A

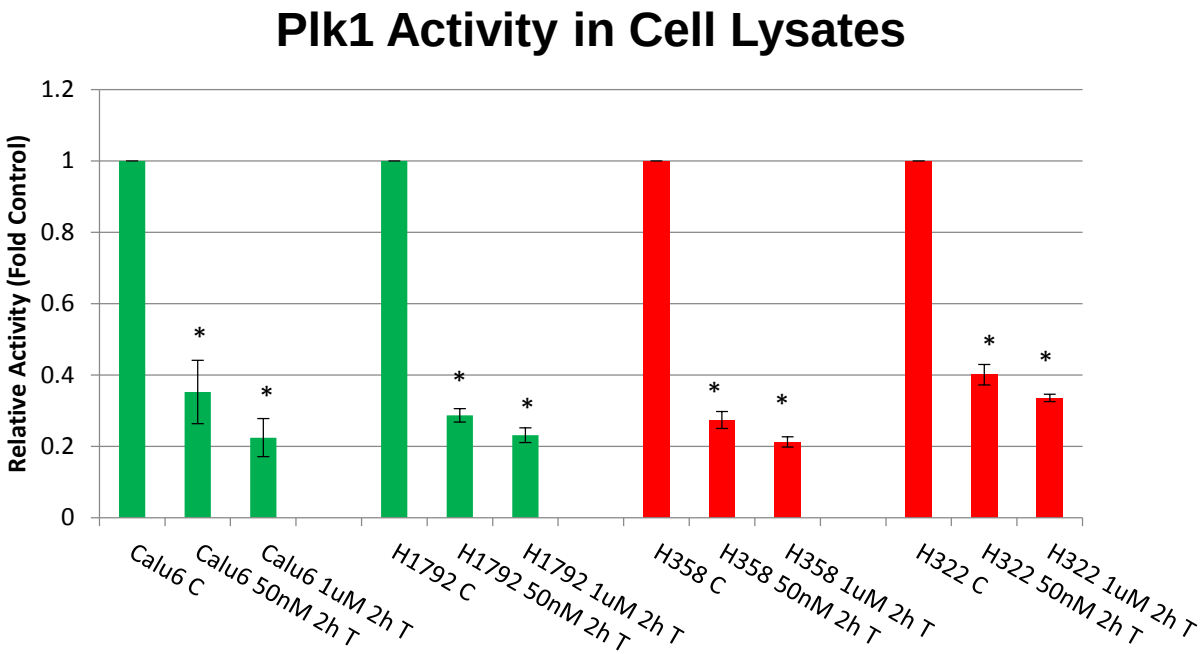

B

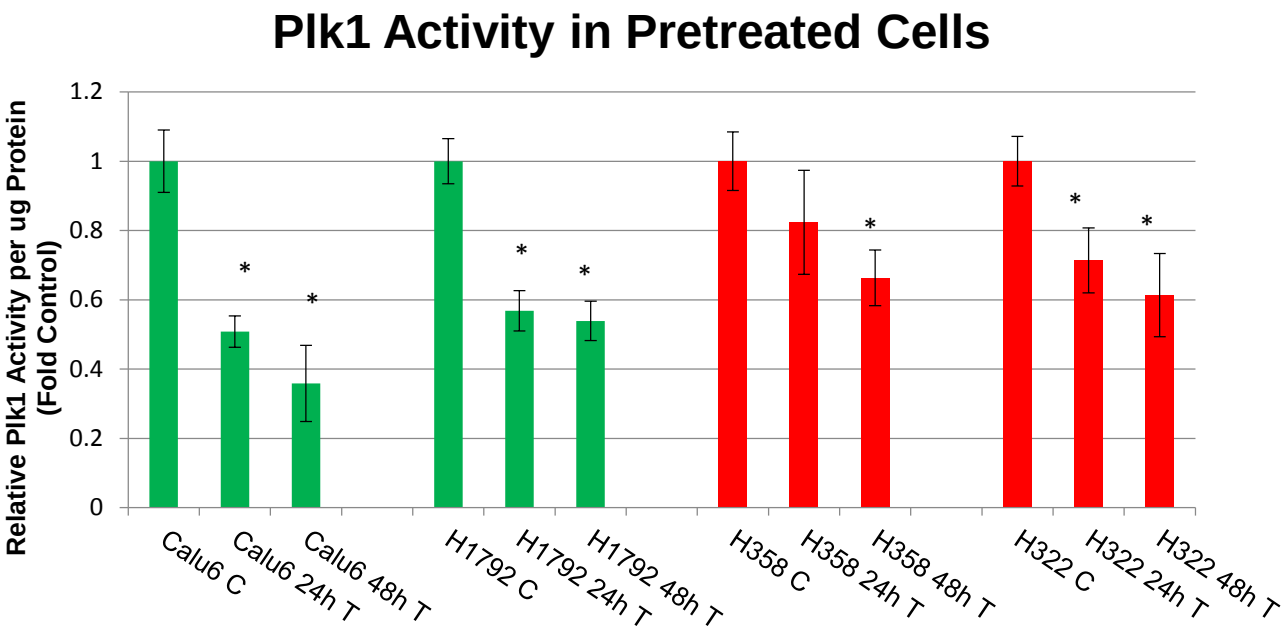

Figure 9. Plk1 activity assay demonstrates inhibition of Plk1 kinase activity in 2h treated lysed cell extracts, and at 24 and 48h time points in pretreated cells. Plk1 activity was assayed using an ELISA kit. Cells were either treated after lysis for four hours (A) or after treatment (B) with volasertib for the indicated time points. (C is vehicle control, T is treated with 50nM volasertib)**.** Asterisks represent significant differences ($p < 0.05$) for the treated samples compared to the controls.

Plk1 inhibition leads to inhibition of colony formation in sensitive cell lines

In the cell line screening, the cells were incubated for the complete time period with the drug. To measure if the effects of Plk1 inhibition in NSCLC cell lines were irreversible, we incubated two sensitive and two resistant NSCLC cell lines with 50 nM volasertib for 24 hours and measured colony formation 14-21 days later. Mirroring our results from the viability assays, the sensitive cell lines H1792 and Calu-6 had irreversible cell growth and inhibition of colony formation compared to the resistant cell lines H322 and H358 (Fig. 10a). As another marker for cell proliferation, we also looked at the effects of Plk1 inhibition on average colony size. Similarly to what is observed in

the total area, the average colony area decreases in sensitive and resistant NSCLC cell lines. Sensitive NSCLC cell lines have significantly greater reduction of average colony area at low concentrations (Fig 10b).

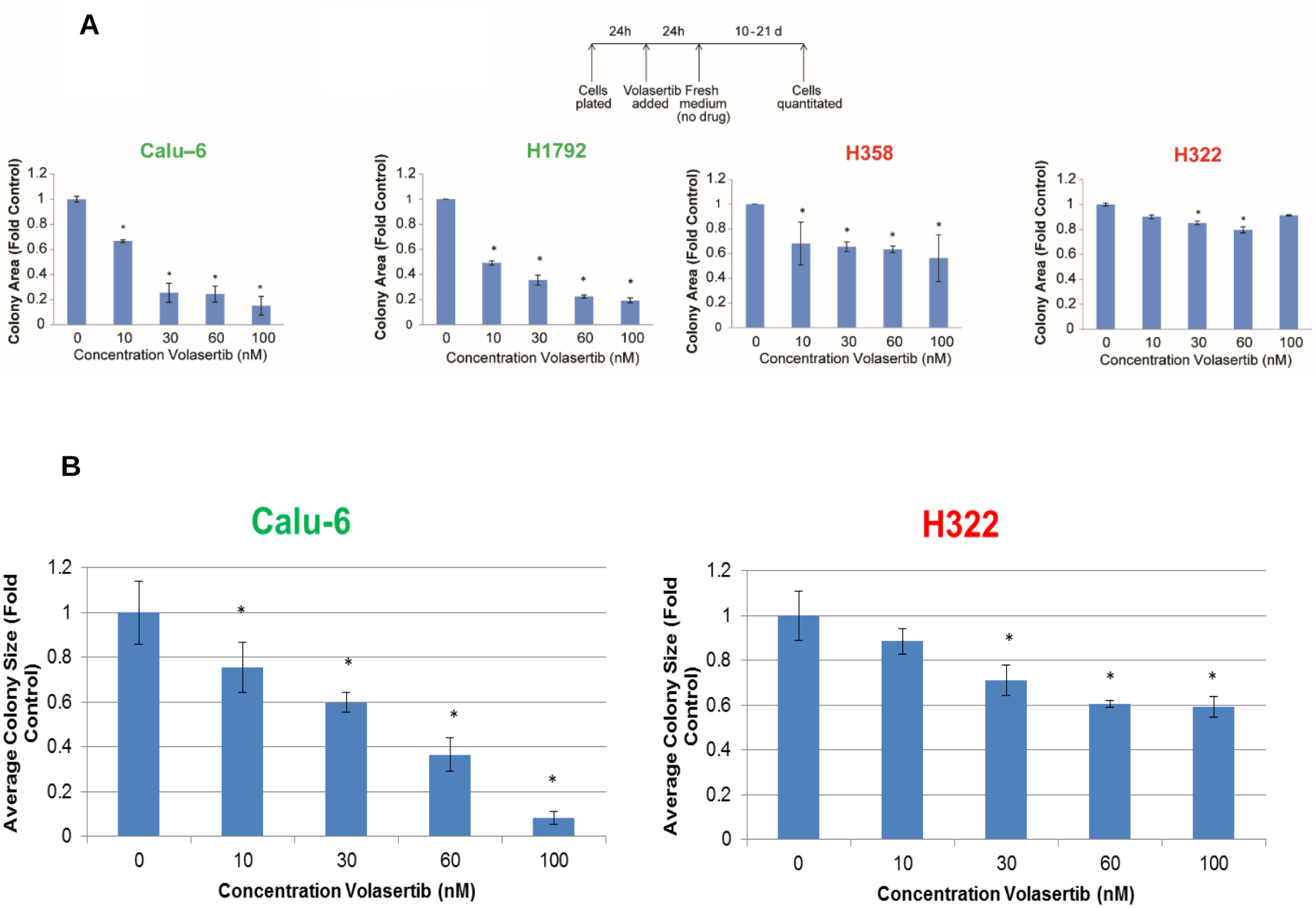
A
24h
24h
10-21 d
Cells plated
Volasertib added
Fresh medium (no drug)
Cells quantitated
Calu–6
H1792
H358
H322
Colony Area (Fold Control)
Concentration Volasertib (nM)
0
10
30
60
100
B
Calu-6
H322
Average Colony Size (Fold Control)
Concentration Volasertib (nM)

C

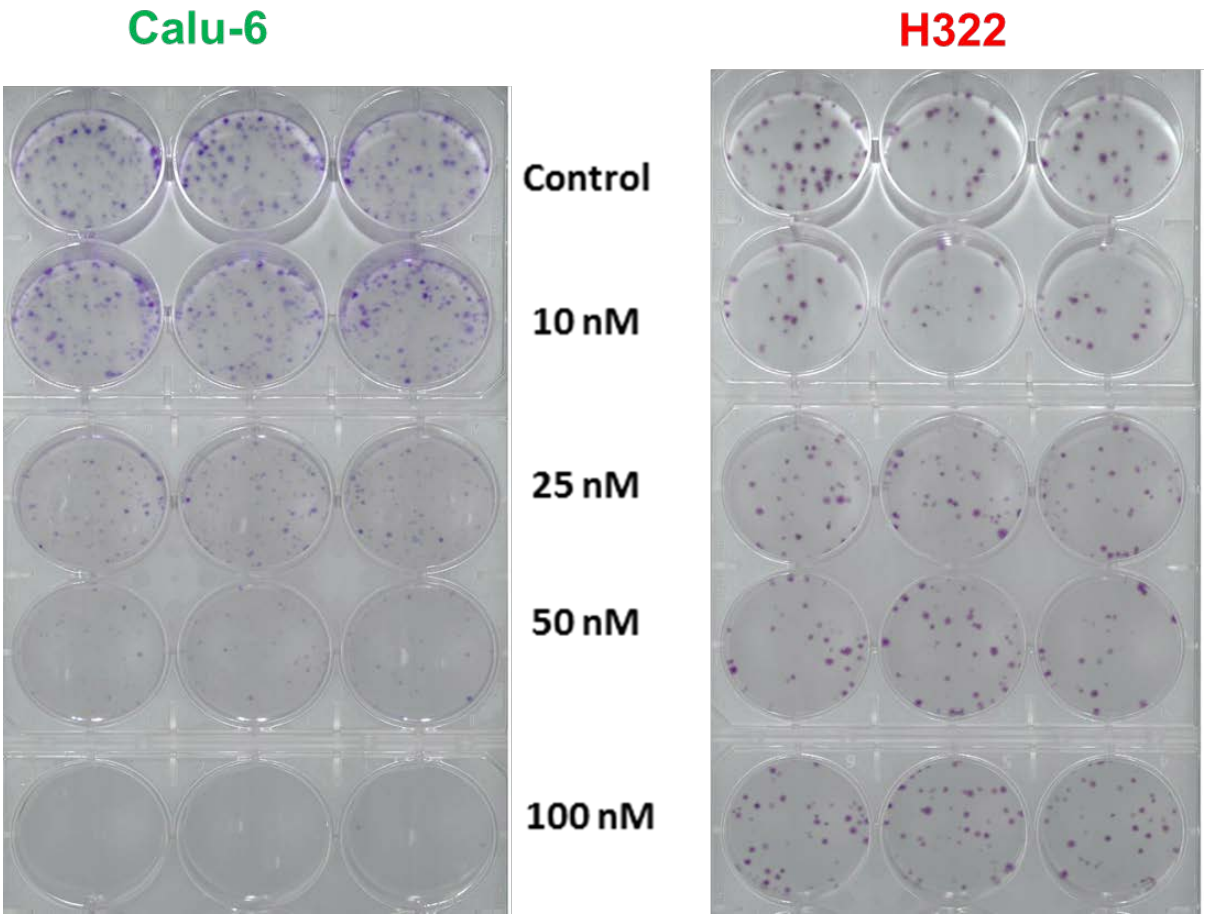

Figure 10. Sensitive cell lines show greater colony formation inhibition compared to resistant cell lines after 24h pulse treatment of volasertib. After 24h pulse treatment, there was a reduction in the cell colonies growing in the assay wells (given here as colony area in A) in the sensitive cell lines. As an additional measure of colony growth, average colony area was quantitated (B) for a sensitive cell line (Calu-6) and a resistant cell line (H322). There was significant ($p < 0.05$) decrease in average colony size compared to controls for Calu-6 at lower concentrations of the inhibitor compared to H322. (C) A representative scanned image of a sensitive cell line and a resistant cell line. *, $P \leq 0.05$ compared to control or as indicated.

Plk1 inhibition increases cells with 4N DNA content in NSCLC cell lines

The effect of Plk1 inhibition in the cell cycle has been widely reported and known to cause prometaphase arrest (31, 53, 61, 91). We observed an accumulation of cells with 4N DNA content as well as an increase in cells with greater than 4N DNA content (Fig.11a-b). Additionally, there was a significantly increased sub G0 population of cells in the sensitive cell lines compared to the resistant cell lines. To confirm the finding of more polyploid cells after treatment, we used DAPI staining using immunofluorescence to locate multiple nuclei within single cells (Fig. 12a). Similar results were seen using brightfield microscopy after H&E staining (12b). In addition, we observed increased nuclear chromatin condensation in the sensitive cells after treatment with volasertib (12b), a marker of apoptosis (92). We found that there was an increase in polyploid cells post treatment with Plk1 inhibitor volasertib in resistant NSCLC cell lines.

A

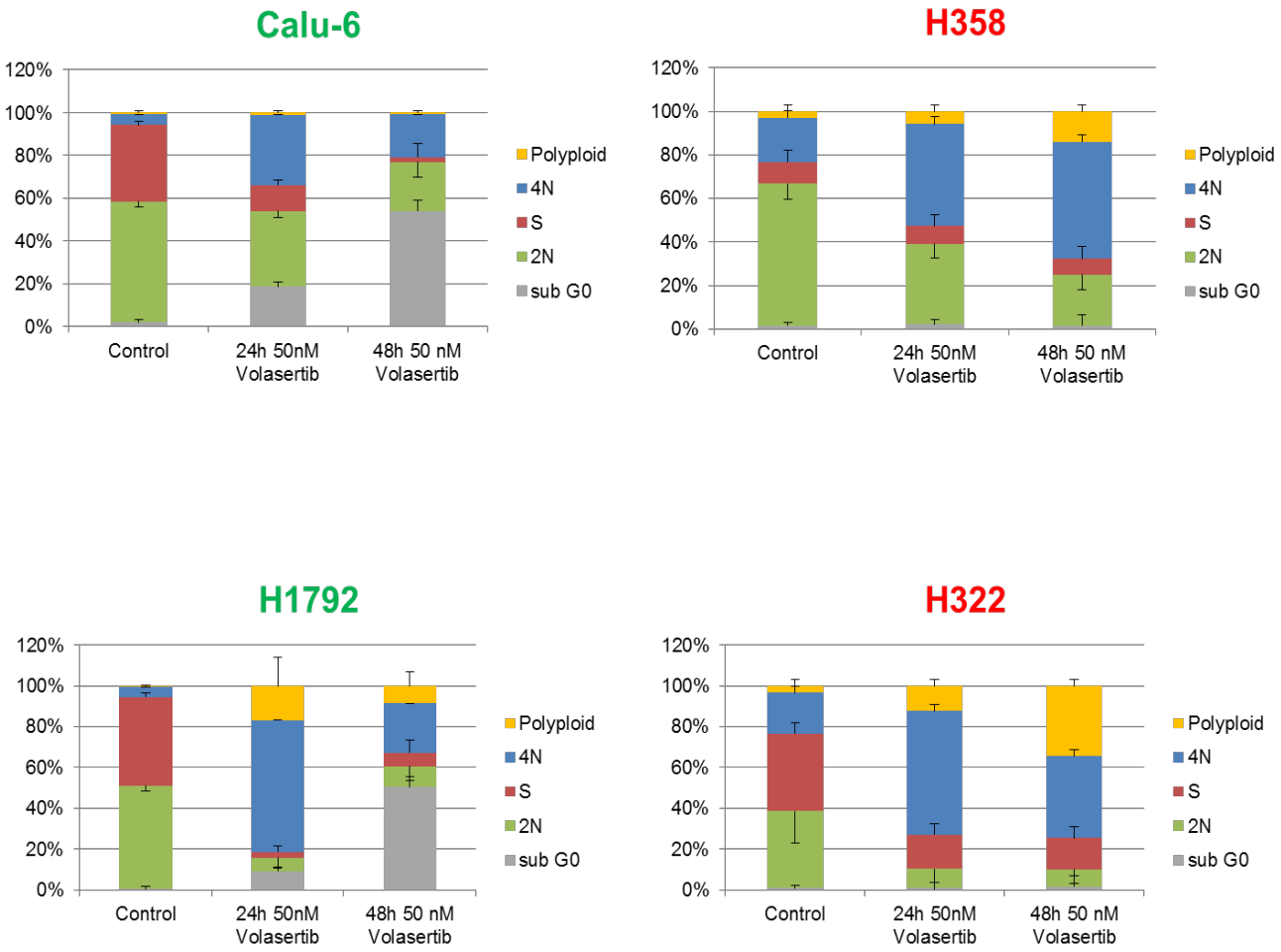
Calu-6
H358
H1792
H322
120%
100%
80%
60%
40%
20%
0%
Control
24h 50nM Volasertib
48h 50 nM Volasertib
Polyploid
4N
S
2N
sub G0

B

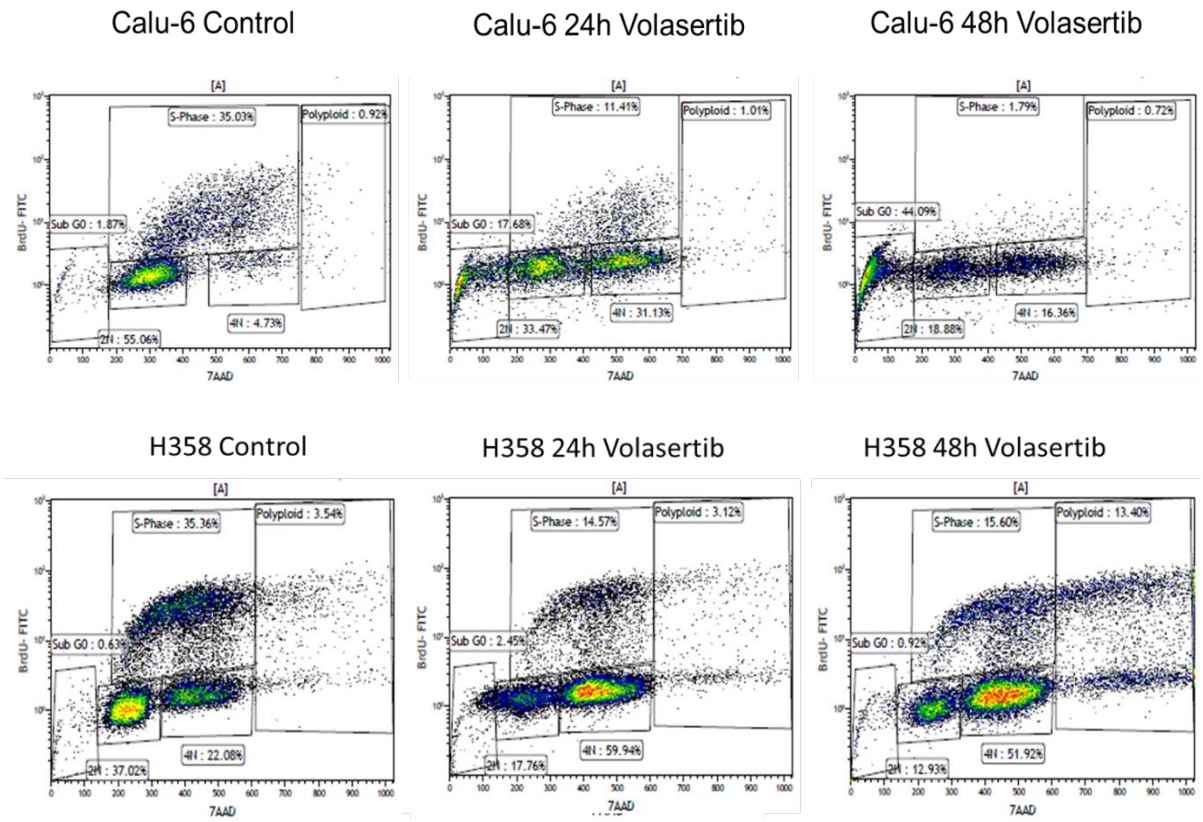

Figure 11. Plk1 inhibition causes an accumulation of cells with 4N DNA content in sensitive and resistant cell lines. After Plk1 inhibition, there was an accumulation of cells with 4N DNA content after 24 and 48 hours for all cell lines. Sensitive cells had an increased sub-G0 population after treatment, and resistant cells had increased number of cells with >4N DNA content (A). A representative profile with gating is given for the resistant cell line H358 and sensitive cell line Calu-6 (B).

A.

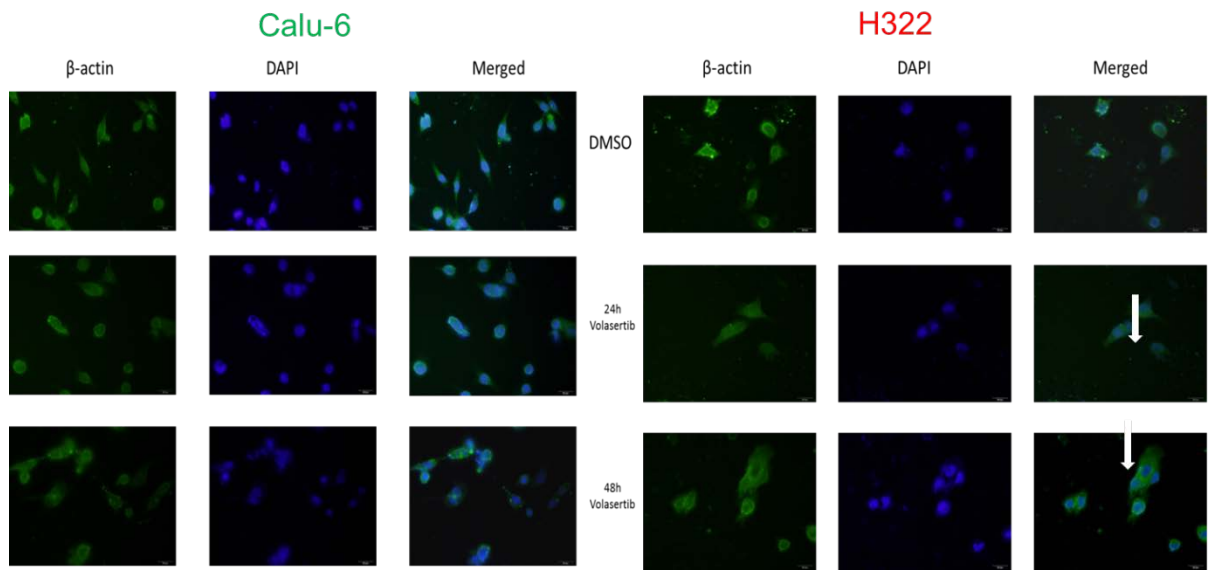
Calu-6
H322
β-actin
DAPI
Merged
β-actin
DAPI
Merged
DMSO
24h Volasertib
48h Volasertib

B.

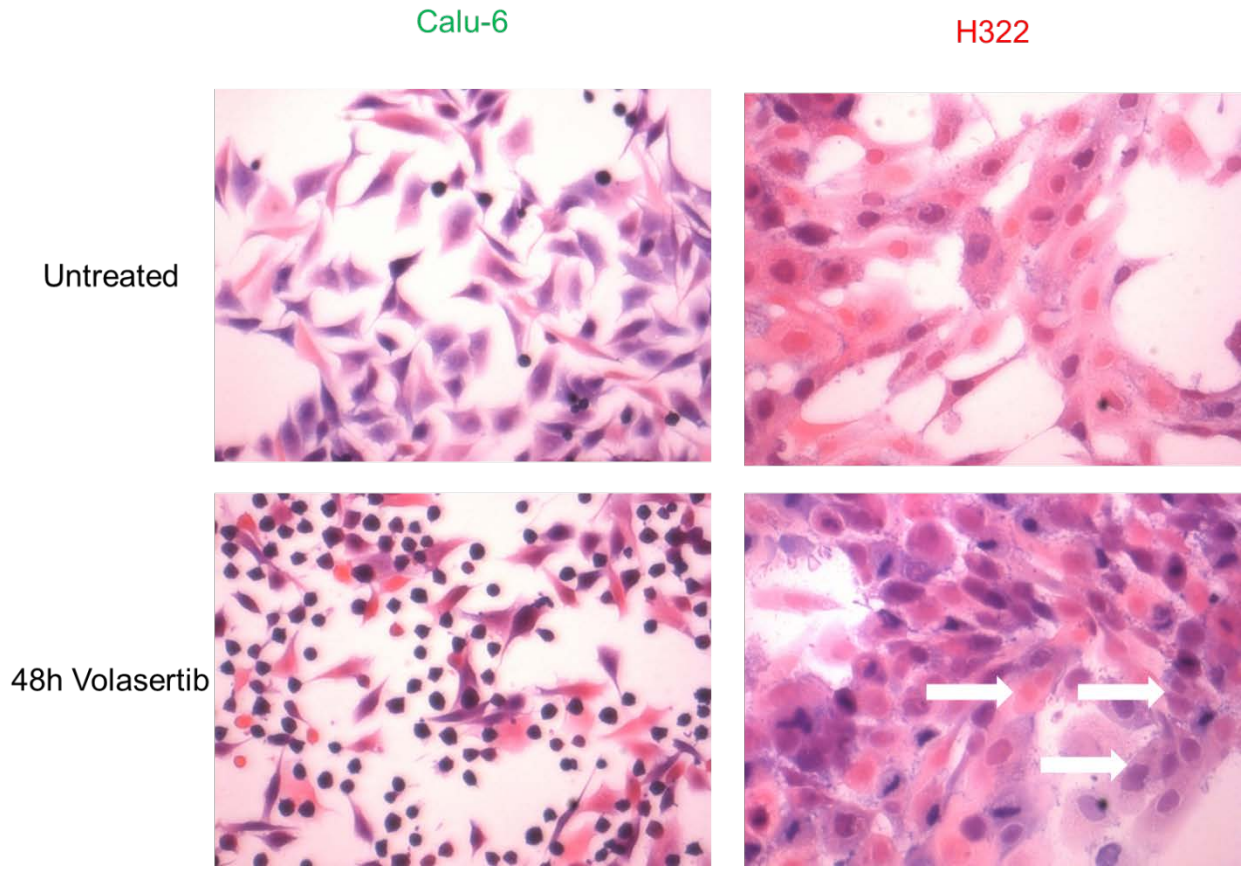
Calu-6
H322
Untreated
48h Volasertib

C.

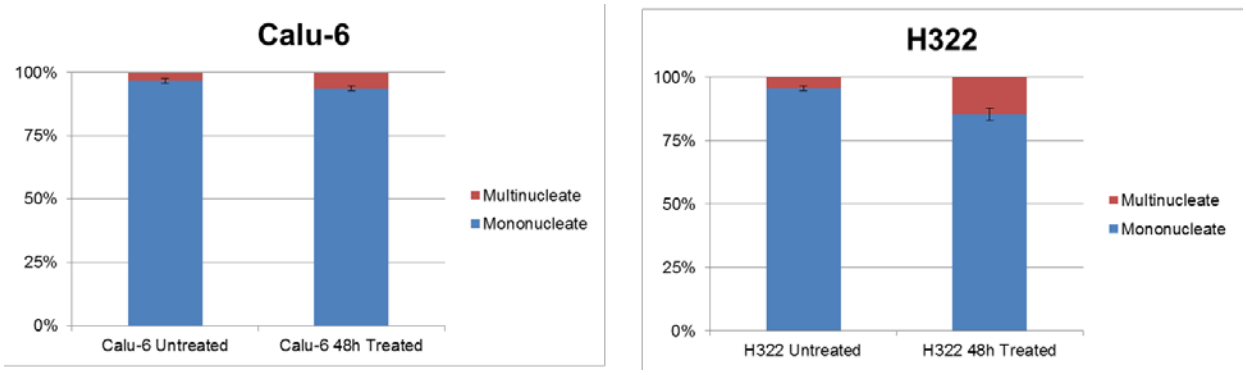

Figure 12. Plk1 inhibition increases the number of polyploid cells in resistant NSCLC cell lines. The cells were visualized using immunofluorescence microscopy (A) and brightfield microscopy (B) after treatment and staining. After quantitation (C), we observed an increase in the number of cells with more than one nucleus in the resistant cell line.

Plk1 inhibition leads to apoptosis in NSCLC cell lines

We also measured cell apoptosis in the two sensitive and two resistant lines. From the TUNEL assay, we were able to see that the sensitive NSCLC cell lines H1792 and Calu-6 underwent significantly more apoptosis after 72 hour incubation with volasertib (Fig 13a). In comparison, the resistant H358 and H322 cell lines underwent less apoptosis compared to the sensitive cell lines. The results were validated using another marker of apoptosis, western blotting for cleaved PARP. Here we found an increase in cleaved PARP after treatment to Plk1 inhibitor volasertib in the two sensitive cell lines (Fig. 13b-c).

A.

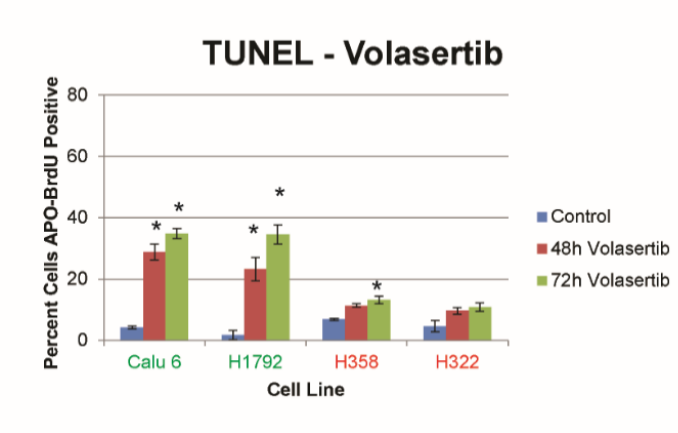

B

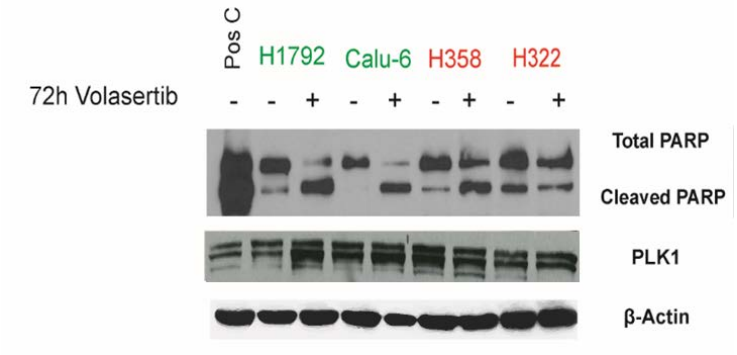

C

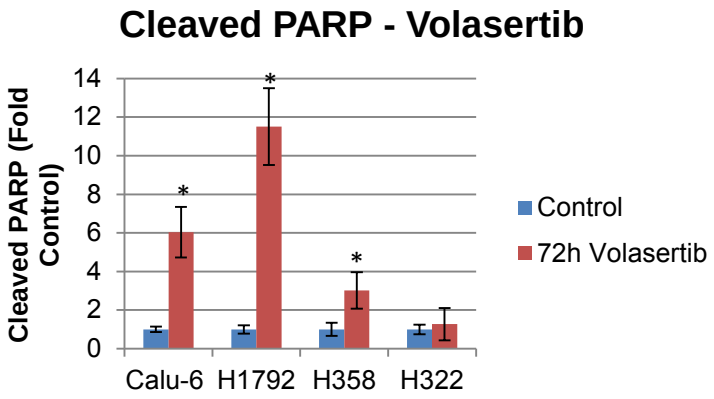

Figure 13. Plk1 inhibition causes significant apoptosis in sensitive cell lines but not resistant cell lines. After 72h treatment with volasertib, sensitive cell lines underwent significantly more TUNEL staining (A) and PARP cleavage (B) compared to resistant cell lines ($p<0.05$). (C) Cleaved PARP bands were quantified using densitometry and adjusted for loading with β-actin. *, $P \leq 0.05$ compared to control or as indicated.

Plk1 knockdown leads to cell cycle arrest and increased apoptosis in NSCLC cell lines

To address the question of specificity of the inhibitors, we used Plk1 specific siRNA to knockdown Plk1 and study the effects on the cell cycle. We found that Plk1 knockdown after 24 and 48 hours caused an accumulation of cells with 4N DNA content in the NSCLC cell lines, as well as an increased sub G0 population in sensitive cell lines (Fig. 14). Additionally, we observed that there was an increase in the number of cells undergoing apoptosis after 72 hours of the Plk1 knockdown. PARP cleavage and TUNEL positive cells was also increased in sensitive cell lines compared to the resistant cells tested after Plk1 knockdown (Fig. 15).

A

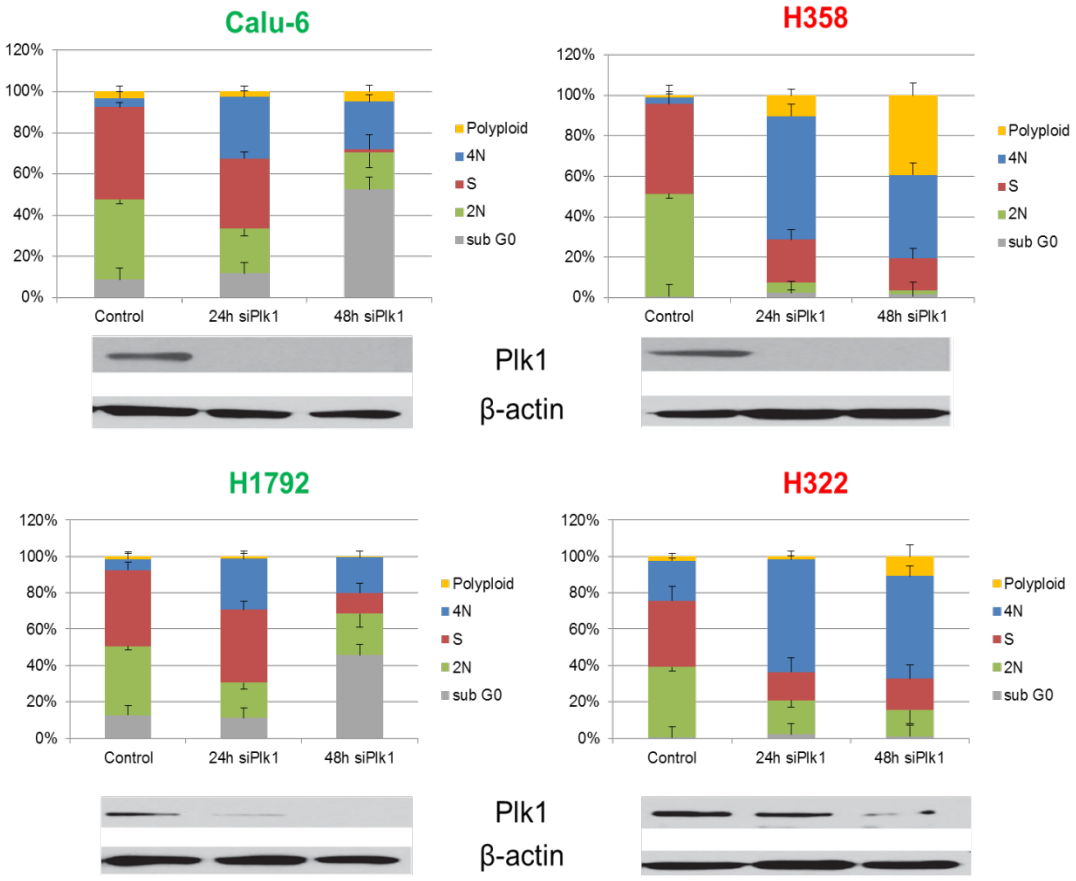
Calu-6
H358
H1792
H322
120%
100%
80%
60%
40%
20%
0%
Control
24h siPlk1
48h siPlk1
Polyploid
4N
S
2N
sub G0
Plk1
β-actin

B

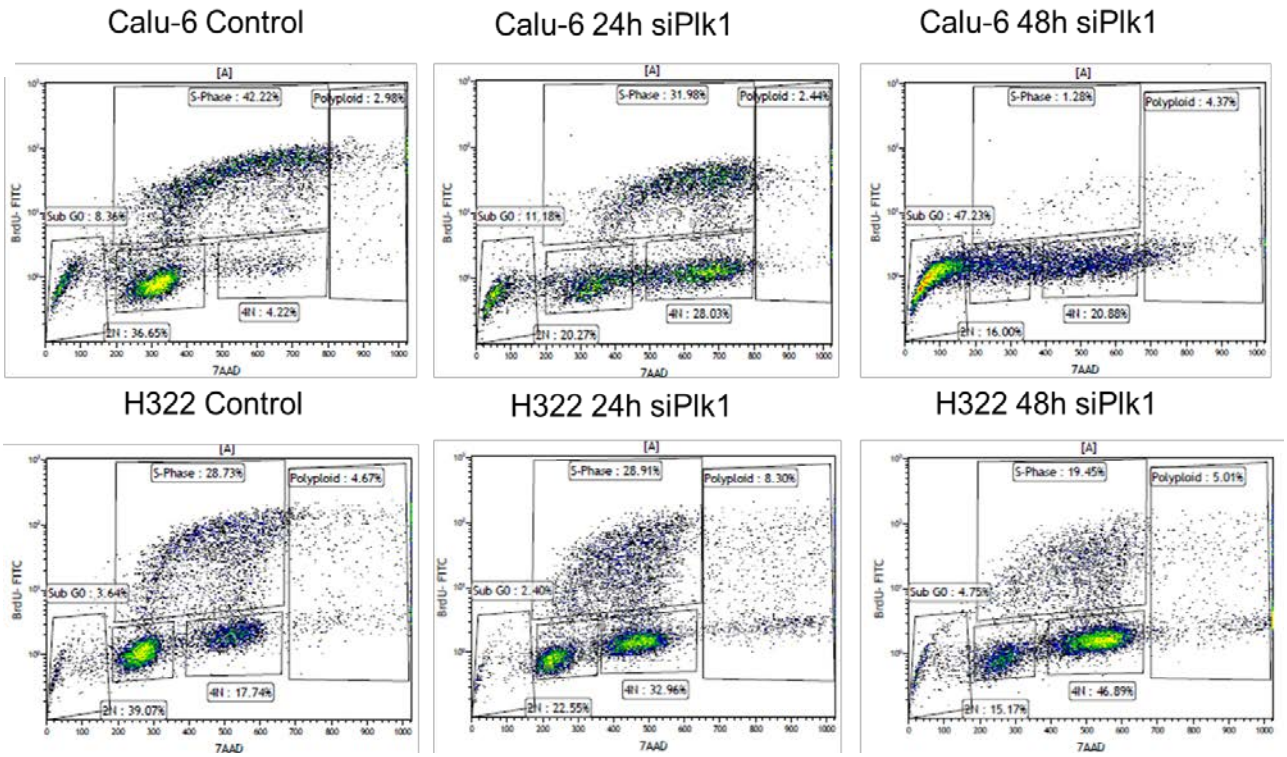

Figure 14. Plk1 knockdown using siRNA causes an increase in 4N cells. We observed an increase in sub-G0 cells in the sensitive cells while we observed an increase in polyploid cells in the resistant cells after Plk1 knockdown (A). Gated cell cycle profiles are given for a sensitive cell line Calu-6 and resistant cell line H322 after knockdown (B).

A

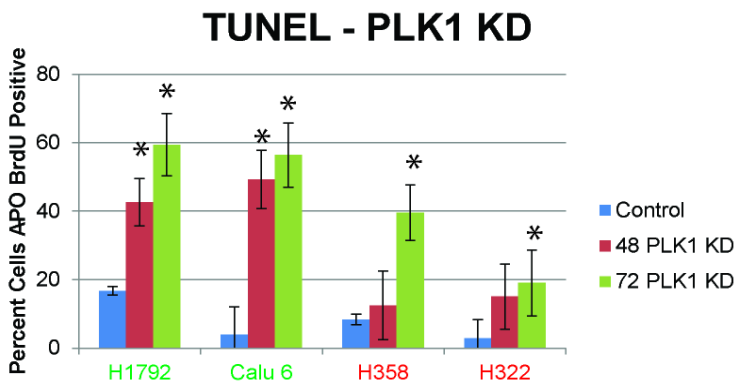

B

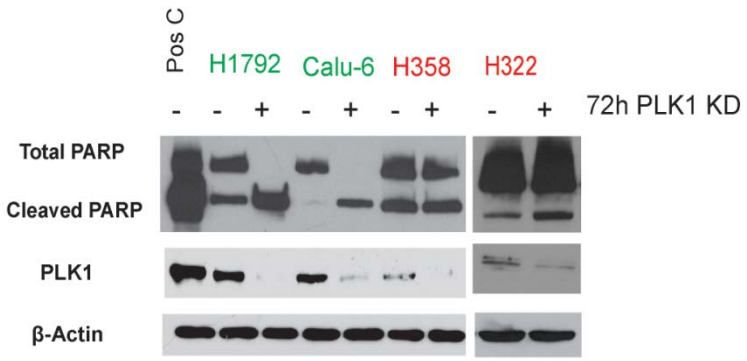

C

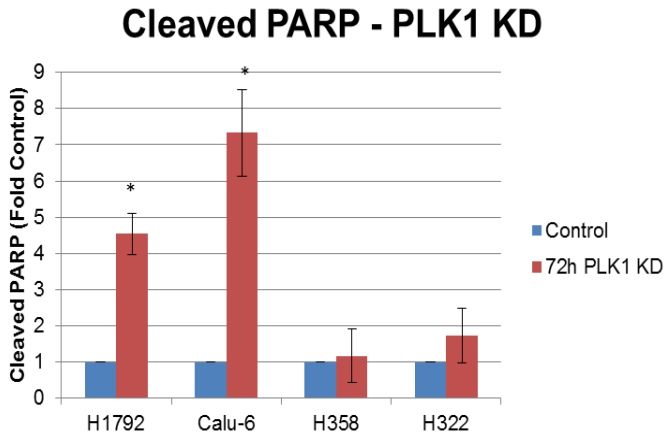

Figure 15. Plk1 knockdown causes significant apoptosis in NSCLC cell lines. Plk1 knockdown causes an increase in TUNEL positive cells (A) and cleaved PARP (B) in sensitive NSCLC cell lines. (C) Cleaved PARP bands were quantified using densitometry and adjusted for loading with β-actin. *, $P \leq 0.05$ compared to control or as indicated.

Doubling time does not correlate with Plk1 inhibition sensitivity

Theoretically, cells which cycle faster should go through G2 of the cell cycle more often and may be vulnerable to inhibition of Plk1. We studied if cell doubling time plays a role sensitivity because Plk1 affects the cell cycles and cells that divide faster will go through the cell cycle more times than slower growing cells during the assays. These cells with shorter doubling time would therefore be in G2 for an increased time period, causing them to be more vulnerable to Plk1 inhibition. We measured the doubling time of 9 (5 resistant, 4 sensitive) NSCLC cell lines. Using a two-sample t-test, there was no significant difference between the average doubling time and IC_{70} for the three Plk1 inhibitors tested (Fig. 16).

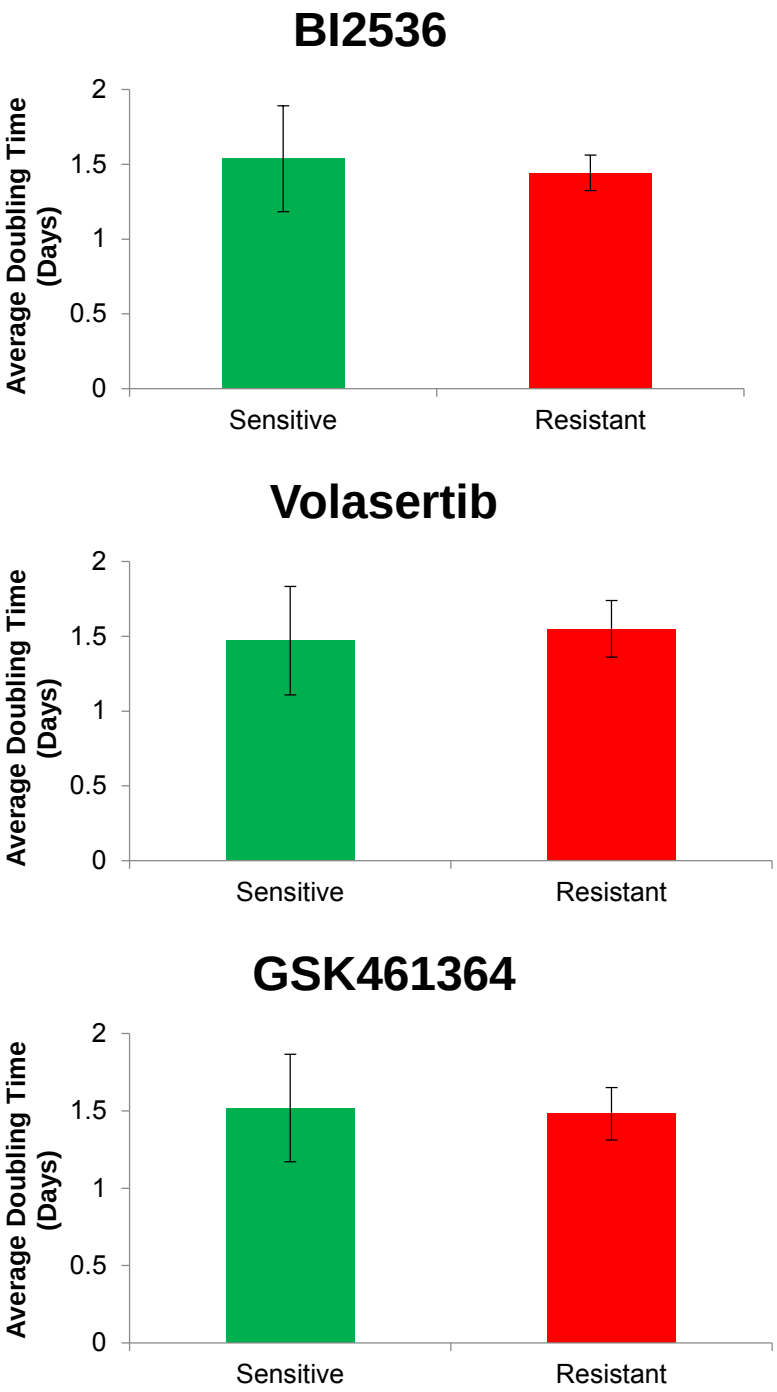

Figure 16. Doubling time did not correlate with sensitivity to Plk1 inhibition. Doubling time was measured based on growth curve assays done by Dr. Uma Giri from Dr. John Heymach's laboratory. Cell lines were grouped based on the definition of sensitive and resistant from the screening. There was no significant difference ($p > 0.05$) between the sensitive cell lines and resistant cell lines for each of the inhibitors tested.

NSCLC cell lines with RAS mutations are more sensitive to Plk1 inhibition than those with wild-type RAS

As *KRAS* mutations had been implicated with sensitivity to Plk1 inactivation (52, 64), we examined the correlation between gene mutations for 264 genes that are commonly associated with cancer and drug sensitivity for all cell lines treated with BI2536 and volasertib and for 63 cell lines treated with GSK461364. To be able to statistically analyze the *RAS* mutant cell lines, we grouped together the *KRAS* and *NRAS* mutant lines so as to have a larger sample size. More NSCLC cell lines with *RAS* mutations were sensitive to Plk1 inhibition than those with wild-type *RAS* (Table 3). No mutation other than *RAS* correlated with sensitivity for more than one drug. We examined co-occurrence of other mutations within the *RAS* mutant population because co-mutations may define subgroups with distinct clinical outcomes and drug sensitivities. We did not find any statistical correlation between Plk1 inhibitor sensitivity and the presence of *LKB* or *TP53* mutations within *RAS* mutant tumors possibly because the numbers of cell lines within these subgroups was small.

To further characterize the *KRAS* mutants, we applied an established KRAS dependency signature to *KRAS* mutant NSCLC cell lines (64). *KRAS*-dependent NSCLC cell lines, defined as those that undergo apoptosis when *KRAS* is knocked down, demonstrated classical epithelial morphology, whereas *KRAS*-independent cells demonstrated a mesenchymal phenotype (64). In an unsupervised analysis, *KRAS*-independent cell lines clustered in the sensitive group for GSK461364 (p of 0.0052) but not for the other 3 groups (Fig. 17).

Gene and drug sensitivity	No. of cell lines				P (Fisher test)
	Mutant		Wild type		
	Resistant	Sensitive	Resistant	Sensitive	
RAS					
Universal	5 (38%)	8 (62%)	9 (81%)	2 (19%)	**0.04718**
BI2536	9 (35%)	17 (65%)	18 (75%)	6 (25%)	**0.005402**
Volasertib	8 (31%)	18 (69%)	16 (67%)	8 (33%)	**0.02248**
GSK461364	20 (63%)	12 (37%)	22 (71%)	9 (29%)	0.595

Table 3. Cell lines with *RAS* mutations are more sensitive to Plk1 inhibition for BI2536 and volasertib, but not GSK461364. Cell lines with *KRAS and NRAS* mutations were grouped together to form a *RAS* mutant group. Cells with *RAS* mutations (*KRAS or NRAS)* were more sensitive ($p<0.05$) to Plk1 inhibition for BI2536 and volasertib, but not GSK461364 ($p>0.05$).

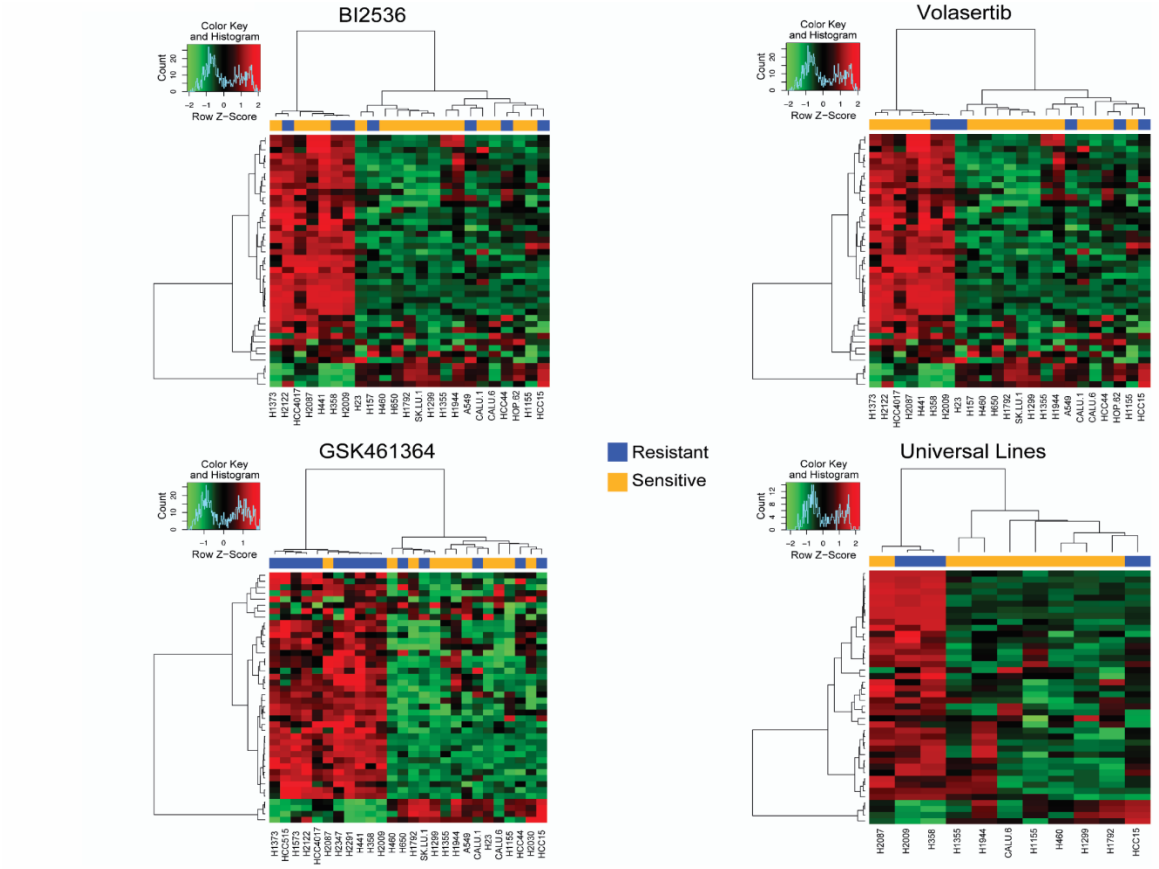

Figure 17. Genes associated with KRAS dependency correlate with sensitivity to GSK461364. In an unsupervised analysis, *KRAS* independent cells clustered in the sensitive region (p = 0.0052) for GSK461364, but not for the other two inhibitors or the universal lines. We generated heatmaps using an established *KRAS*-dependency signature (64) in *KRAS* mutant NSCLC cell lines with the help of the Bioinformatics department (Drs. Suk-Young Yoo, Pan Tong, Jing Wang) (64). Out of the 44 genes in the signature, we identified 31 genes with 42 probes in our gene expression data. The following numbers of cell lines were identified with expression data available for the genes of interest: for BI2536, 7 sensitive and 11 resistant cell lines; for volasertib, 11 sensitive and 5 resistant cell lines; for GSK461364, 12 sensitive and 17 resistant cell lines; and for all three drugs, 9 sensitive and 4 resistant cell lines.

***TP53* mutation and the expression of ABC transporters do not correlate with response to Plk1 inhibition in NSCLC cell lines.**

In order to validate candidate biomarkers of response according to the available literature, we tested correlation of TP53 mutational status (Fisher exact test), and gene expression of ABC transporters ABCB1 and ABCG2 (two-sample t test) with sensitivity to the three Plk1 inhibitors (Fig 18). No statistically significant correlation was found (P>0.05).

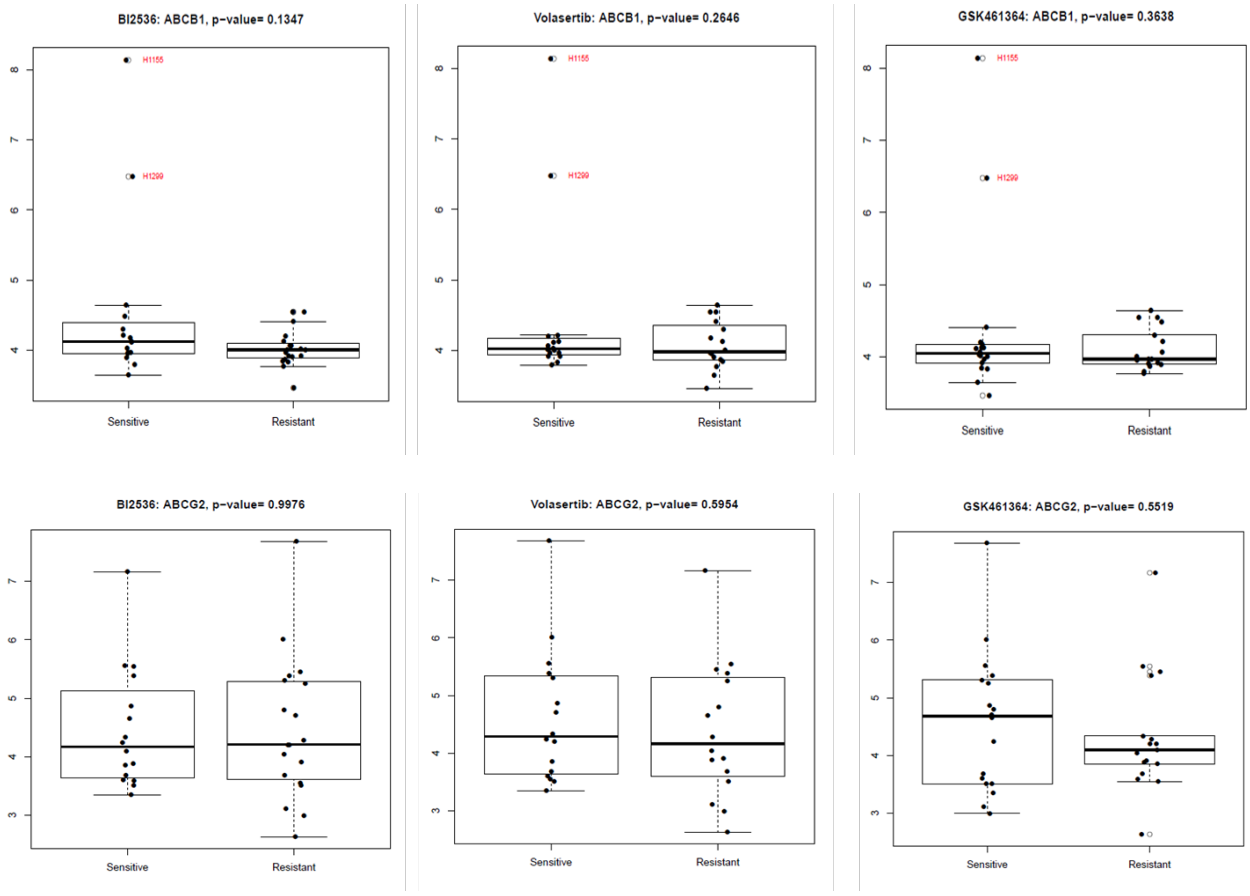

Figure 18. Expression of ABC transporter proteins did not correlate with sensitivity to Plk1 inhibitors. The gene expression of ABC transporter proteins ABCB1 and ABCG2 did not correlate with sensitivity to the Plk1 inhibitors tested (p>0.05).

Mesenchymal NSCLC cell lines are more sensitive to Plk1 inhibition than epithelial NSCLC cell lines

To determine why NSCLC cell lines had diverse sensitivities to Plk1 inhibition, we examined the relationship between drug sensitivity and basal gene/protein expression in four groups of cell lines: BI2536-sensitive/resistant, volasertib-sensitive/resistant, GSK461364-sensitive/resistant, and the universal cell lines. We found that the expression levels of several genes and proteins correlated with sensitivity to the Plk1 inhibitors (Fig. 19).

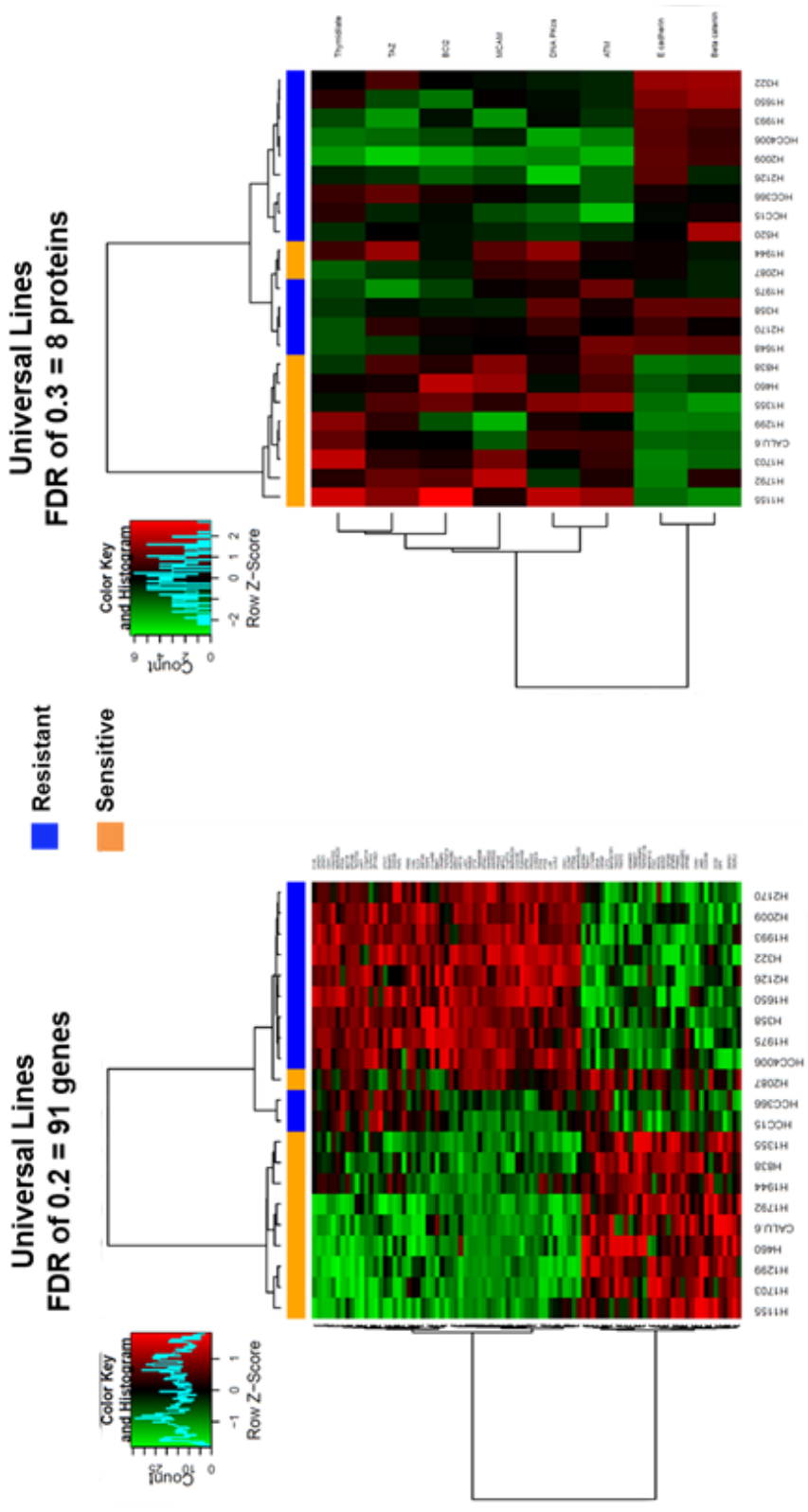
Universal Lines
FDR of 0.3 = 8 proteins
Thymidine
TAZ
BCI2
MCAM
Dick Price
ATM
E cadherin
Beta catenin
Color Key and Histogram
Count
Row Z-Score
Resistant
Sensitive
Universal Lines
FDR of 0.2 = 91 genes
Color Key and Histogram
Count
Row Z-Score

Figure 19. Baseline mRNA and protein expression correlates with sensitivity and resistance in universal cell lines. Shown are heatmaps of baseline gene expression after supervised clustering of the universal cell lines at FDR of 0.2 (n = 91 genes) and baseline protein expression after supervised clustering of the universal cell lines at FDR of 0.3 (n = 8 proteins).

We hypothesized that genes that were found in all four groups and that had the biggest differences in expression between resistant and sensitive cell lines would be the most likely to be involved in sensitivity specifically to Plk1 inhibition rather than to be involved in off-target drug effects. After correction for multiple comparisons, no gene expression levels correlated with sensitivity to BI2536 or volasertib. We discovered that the expression levels of several genes and proteins correlated with drug sensitivity (Table 4, 5).

Probe ID	Gene Symbol	Gene name	Function	Mean Expression (R/S)[1,2]
ILMN_1770940	CDH1	E-cadherin	adhesion, epithelial marker	59.95
ILMN_2412475	PRR5	proline rich 5	tumor supressor gene, component of mTORC2 signalling	58.17
ILMN_1791826	RAB25	member RAS oncogene family	membrane trafficking, member of the RAS family	33.86
ILMN_1782389	LAD1	ladinin 1	anchorin filament, epithelial marker	33.72
ILMN_2143685	CLDN7	claudin 7	tight junction, epithelial marker	27.42
ILMN_1752935	TMEM30B	transmembrane protein 30B	phospholipid translocator	25.59
ILMN_2160210	EPCAM	epithelial cell adhesion molecule	adhesion molecule, epithelial marker	24.24
ILMN_1680110	C10orf116 (ADIRF)	adipogenesis regulatory factor	function unknown, overexpressed in cancers/platin resistance	23.40
ILMN_1752932	MPZL2	myelin protein zero-like 2	cell adhesion/epithelial marker	21.60
ILMN_1796461	PRSS8	protease, serine, 8	membrane-anchored serine proteases/epithelial development	21.46
ILMN_1655261	ERP27	endoplasmic reticulum protein 27	endoplasmic reticulum protein	18.81
ILMN_1699887	ST14	suppression of tumorigenicity 14	epithelial-derived, integral membrane serine protease (HGF family)	12.61
ILMN_1710644	MARVELD3	MARVEL domain containing 3	tight junction	11.71
ILMN_1780255	KLK6	kallikrein-related peptidase 6	proliferation/epithelial marker	11.36
ILMN_1664265	EPHA1	EPH receptor A1	angiogenesis/invasion	10.11
ILMN_1801697	C19orf46 (SYNE4)	spectrin repeat containing, nuclear envelope family member 4	involved in changes in cellular organization	9.93
ILMN_1685709	TMEM125	transmembrane protein 125	transmembrane protein, function unknown	9.73
ILMN_1746801	CGN	cingulin	tight junction	8.97
ILMN_1688154	MST1R	macrophage stimulating 1 receptor (c-met-related tyrosine	cell migration	7.55

		kinase)		
ILMN_1751346	ERBB3	v-erb-b2 avian erythroblastic leukemia viral oncogene homolog 3	membrane protein from EGF receptor family - oncogenic	7.53
ILMN_1769201	ELF3	E74-like factor 3	epithelial-specific transcription factor, epithelial marker	7.44
ILMN_2132599	ANKRD22	ankyrin repeat domain 22	epithelial marker	7.01
ILMN_2064150	PRRG2	proline rich Gla (G-carboxyglutamic acid) 2	Hippo tumor suppressor pathway	6.85
ILMN_1723092	CRB3	crumbs family member 3	tight junction	6.78
ILMN_2111932	SERINC2 (TDE2)	serine incorporator 2	byossinthesis of membrane lipids, overexpressed in lung cancer	6.23
ILMN_2060145	GRHL2	grainyhead-like 2 (Drosophila)	regulates ERBB3, involved in EMT	6.13
ILMN_1713952	C1orf106	chromosome 1 open reading frame 106	function unknown	5.67
ILMN_1676322	C1orf172 (KDF1)	keratinocyte differentiation factor 1	proliferation/differentiation	5.61
ILMN_2405254	GRB7	growth factor receptor-bound protein 7	cell migration	5.49
ILMN_1717052	STARD10	StAR-related lipid transfer (START) domain containing 10	phospholipid transfer protein	4.97
ILMN_2352131	ERBB2	v-erb-b2 avian erythroblastic leukemia viral oncogene homolog 2	EGF receptor family - oncogenic/cell proliferation	4.40
ILMN_2043079	ILDR1	immunoglobulin-like domain containing receptor 1	involved in cancer development/progression	4.36
ILMN_2050790	C11orf52	chromosome 11 open reading frame 52	function unknown	4.24
ILMN_1724946	SPINT1 (HAI1)	serine peptidase inhibitor type 1	regulates membrane anchored serine proteases (HGF family)	3.94

ILMN_1734596	TC2N	tandem C2 domains, nuclear	involved in vesicular traffecking	3.87
ILMN_1692398	CNTNAP1	contactin associated protein 1	involved in Rho signalling	0.25
ILMN_2049536	TRPV2	transient receptor potential cation channel, subfamily V, member 2	cell migration/invasion	0.16
ILMN_1790778	PNMA2	paraneoplastic Ma antigen 2	paraneoplastic antigen	0.13
ILMN_2058251	VIM	vimentin	intermediate filament/cytoskeleton, mesenchymal marker	0.05

Table 4. Probe sets with expression that correlated with response to all three drugs.

[1]Fold change in mean gene expression for resistant (R) / sensitive (S) cell lines.
[2]P <0.015 for all values.

At the protein level, E-cadherin and β-catenin were consistently expressed at higher levels in the resistant lines, and DNA-dependent protein kinase catalytic subunit and thymidylate synthase were consistently overexpressed in the sensitive lines as seen in Table 5.

Sensitivity		Protein	Mean expression (R/S)	P
Universal	FDR = 0.1	E-cadherin	6.65	8.90E-07
		β-catenin	4.27	5.29E-05
	FDR = 0.2	ATM	0.44	0.0041
		TAZ	0.84	0.0043
	FDR = 0.3	Thymidylate synthase	0.62	0.0088
		DNA-PKcs	0.54	0.0104
		BCl2	0.62	0.0163
		MCAM	0.80	0.0179
GSK461364	FDR = 0.2	E-cadherin	3.78	0.0001
		β-catenin	2.46	0.0010
	FDR = 0.3	Thymidylate synthase	0.68	0.0041
		Rab25	1.23	0.0042
		P70s6k	1.35	0.0045
		MACC1	1.62	0.0064
BI2536	FDR = 0.1	E-cadherin	3.40	0.0008
	FDR = 0.2	DNA-PKcs	0.61	0.0040

Table 5. Proteins with expression that correlated with drug sensitivity
R, resistant. S, sensitive. FDR, false discovery rate. PKcs, protein kinase catalytic subunit.

As an exploratory analysis, we tested probe sets with at least a 2-fold difference in mean gene expression between sensitive and resistant lines and a corresponding P value of less than 0.05 for this difference. We performed pathway analysis of lines with genes whose expression correlated with sensitivity to the universal lines. Tight-junction, ErbB, and Rho signaling pathways were significantly altered in multiple gene sets (Table 6).

	Ingenuity canonical pathways	P	Genes
Universal FDR < 0.2	Tight junction signaling	3.5E-05	*F11R, JAM3, CGN, ARHGEF2, CLDN7, TNFRSF11B*
	RhoA signaling	0.001	*EPHA1, RTKN, BAIAP2, ARHGAP8/PRR5-ARHGAP8*
	Signaling by Rho family GTPases	0.002	*MAP3K12, CDH1, RHOQ, BAIAP2, ARHGEF2*
	RhoGDI signaling	0.004	*CDH1, RHOQ, ARHGEF2, ARHGAP8/PRR5-ARHGAP8*
	IL-15 production	0.004	*PTK6, MST1R*
	Production of nitric oxide and reactive oxygen species in macrophages	0.004	*MAP3K12,PTPN6,RHOQ,TNFRSF11B*
	Leukocyte extravasation signaling	0.006	*F11R,JAM3,CLDN7,ARHGAP8/PRR5-ARHGAP8*
	Diphthamide biosynthesis	0.011	*DPH5*
	Epithelial adherens junction signaling	0.017	*EPN3,CDH1,BAIAP2*
	Actin nucleation by ARP-WASP complex	0.018	*RHOQ,BAIAP2*
	Acute phase response signaling	0.025	*CRABP2,TAB,TNFRSF11B*
	Granulocyte adhesion and diapedesis	0.028	*JAM3,CLDN7,TNFRSF11B*
	STAT3 Pathway	0.030	*MAP3K12,PTPN6*
	Molecular Mechanisms of Cancer	0.047	*CDH1,RHOQ,ARHGEF2,TAB*
	SAPK/JNK Signaling	0.048	*MAP3K12,TAB*
	PPAR Signaling	0.048	*TAB,TNFRSF11B*

Table 6. Pathway analysis of genes that correlated with Plk1 inhibitor sensitivity in universal lines. Pathway analysis was performed using IPA from www.ingenuity.com.

Based on the differential expression of E-cadherin at mRNA and protein level (Fig. 20a-b) and several genes involved in EMT as well as our observations that NSCLC cells with a mesenchymal morphology were more sensitive to Plk1 inhibition than epithelial cells, we hypothesized that mesenchymal NSCLC cells are more sensitive to Plk1 inhibition. We applied a 76-gene EMT signature score developed by our department and the bioinformatics department and which had been validated in multiple datasets to distinguish sensitive and resistant cell lines (80). EMT scores correlated significantly with sensitivity to Plk1 inhibition in cell lines sensitive to any one of the three drugs and particularly in universal lines (Fig. 20c). Cell lines with higher EMT scores (mesenchymal) were more sensitive to Plk1 inhibitors. Protein expression as seen by Western blot also confirmed these correlations in the cell lines (Figure 20d).

A

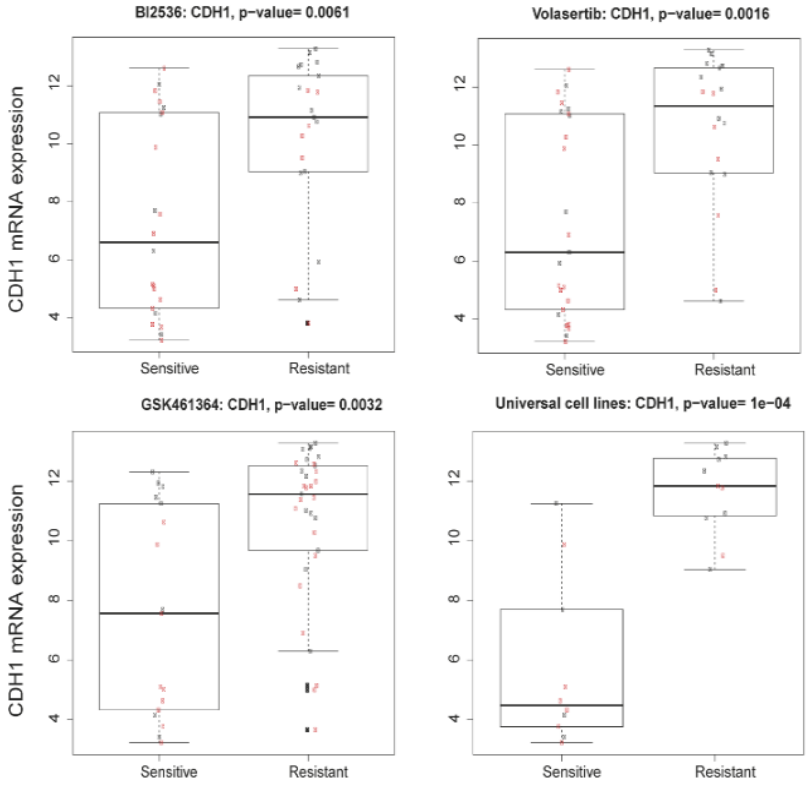
BI2536: CDH1, p−value= 0.0061
Volasertib: CDH1, p−value= 0.0016
GSK461364: CDH1, p−value= 0.0032
Universal cell lines: CDH1, p−value= 1e−04
CDH1 mRNA expression
Sensitive
Resistant

B

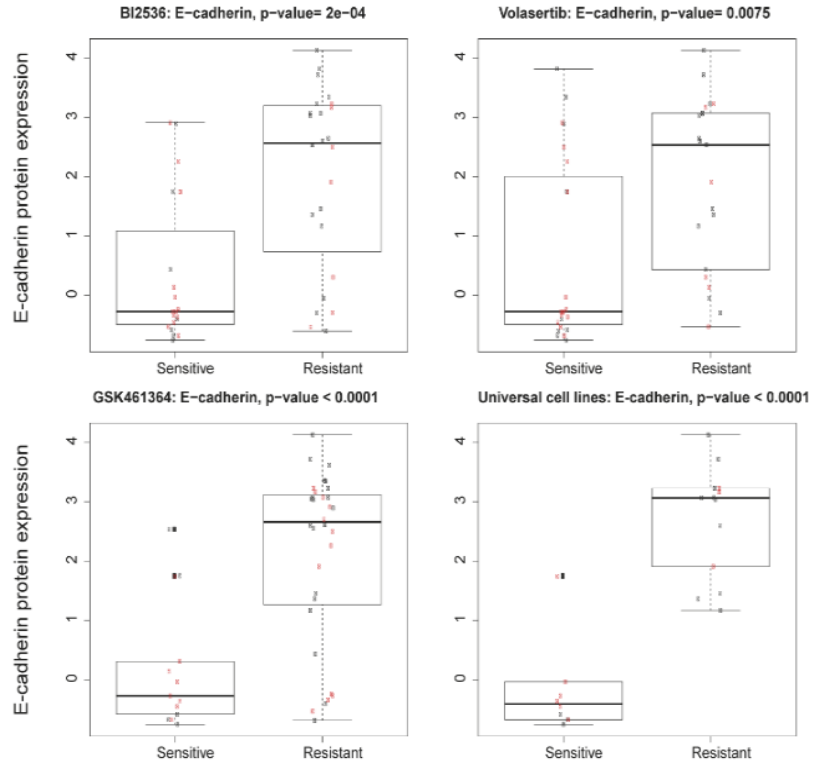
BI2536: E−cadherin, p−value= 2e−04
Volasertib: E−cadherin, p−value= 0.0075
GSK461364: E−cadherin, p−value < 0.0001
Universal cell lines: E−cadherin, p−value < 0.0001
E−cadherin protein expression
Sensitive
Resistant

C

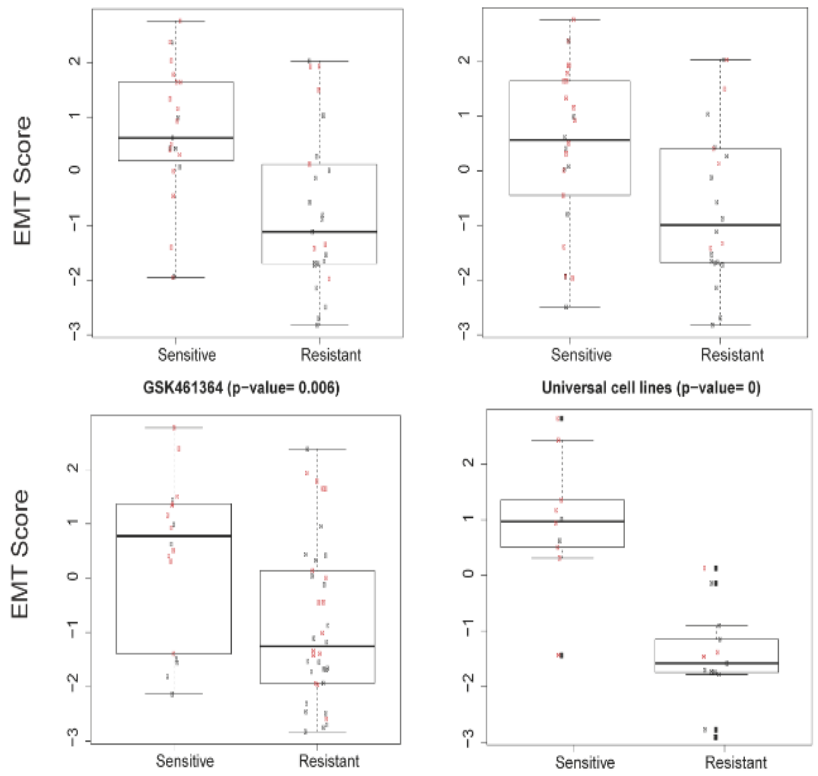

D

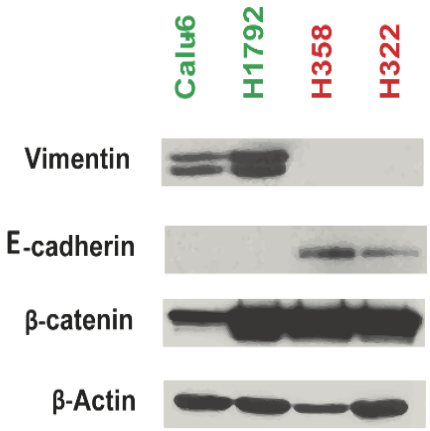

Figure 20. Mesenchymal phenotype correlates with sensitivity to Plk1 inhibition while epithelial phenotype correlates with resistance. E-cadherin gene and protein expression is significantly correlated with resistance to Plk1 inhibition. Cell lines with higher EMT scores are also more sensitive to Plk1 inhibition. Expression boxplots were created with the help of the Bioinformatics department: Drs. Suk Young Yoo, Pan Tong, Jing Wang.

As Plk1 inhibitor sensitivity correlated significantly to E-cadherin expression, we examined the effect of knocking down E-cadherin on volasertib sensitivity. Manipulation of E-cadherin alone was not sufficient to change the biological effects of Plk1 inhibition (Fig. 20).

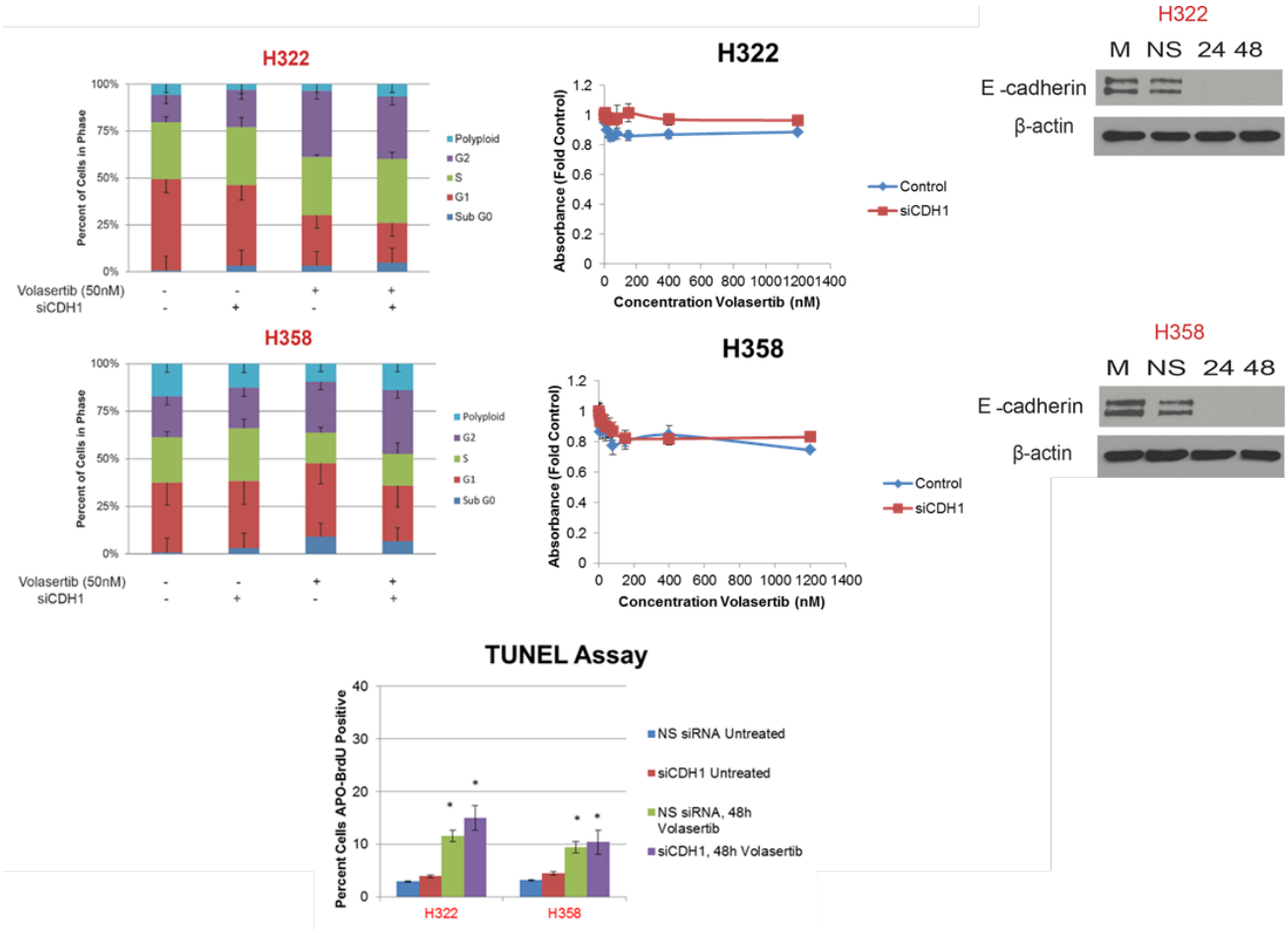

Figure 21. E-cadherin knockdown did not sensitize resistant NSCLC cell lines to Plk1 inhibition. E-cadherin knock down does not affect NSCLC cell lines' sensitivity to PLK1 inhibition. Two epithelial NSCLC cell lines were transfected with siRNA to E-cadherin and then incubated with volasertib 48 h later. The knock down of E-cadherin did not affect cell cycle (left panel), cell number as measured by MTT (right panel) or apoptosis as measured by TUNEL (bottom panel). *, $P \leq 0.05$ compared to control or as indicated.

Induction of epithelial or mesenchymal phenotype affects sensitivity to Plk inhibition in NSCLC cell lines

To determine if the correlation between EMT scores and drug sensitivity was biologically significant, we manipulated NSCLC cells and found that Plk1 inhibition led primarily to apoptosis in mesenchymal cells and cell cycle arrest in epithelial cells. We transfected NSCLC cell lines with miR-200b and miR-200ab, which have been shown to induce an epithelial protein expression pattern and phenotype (93). In the H1299 and H157 cell lines, miR-200b or miR-200ab, respectively, resulted in an increased expression of E-cadherin and a decreased expression of vimentin. Concurring with the finding that the epithelial NSCLC lines are more resistant, the induction of an epithelial phenotype increased the cell lines' resistance to volasertib, with IC70 values increasing from 374 nM to >1200 nM in H157 cells and from 321 nM to >1200 nM in H1299 cells (Fig. 21a). However, the quantity of TUNEL-positive cells did not significantly change between the uninduced cells and induced cells treated with volasertib. The induction of a mesenchymal phenotype using ZEB1 overexpression (Fig. 21b) increased the cell line's sensitivity to volasertib, with IC70 values decreasing from >1200 nM to 130 nM. The quantity of TUNEL-positive cells did not significantly change between the control and ZEB1 cells after treatment with volasertib. TGF-β (Fig. 21c) induced a mesenchymal phenotype and led to an increase in sensitivity to volasertib, with cell viability decreasing by over 40%, although the IC70 values could not be detected. Additionally, TGF- β treated cells underwent significantly more ($p < 0.05$) apoptosis in terms of TUNEL stained cells compared to the parental cells.

A

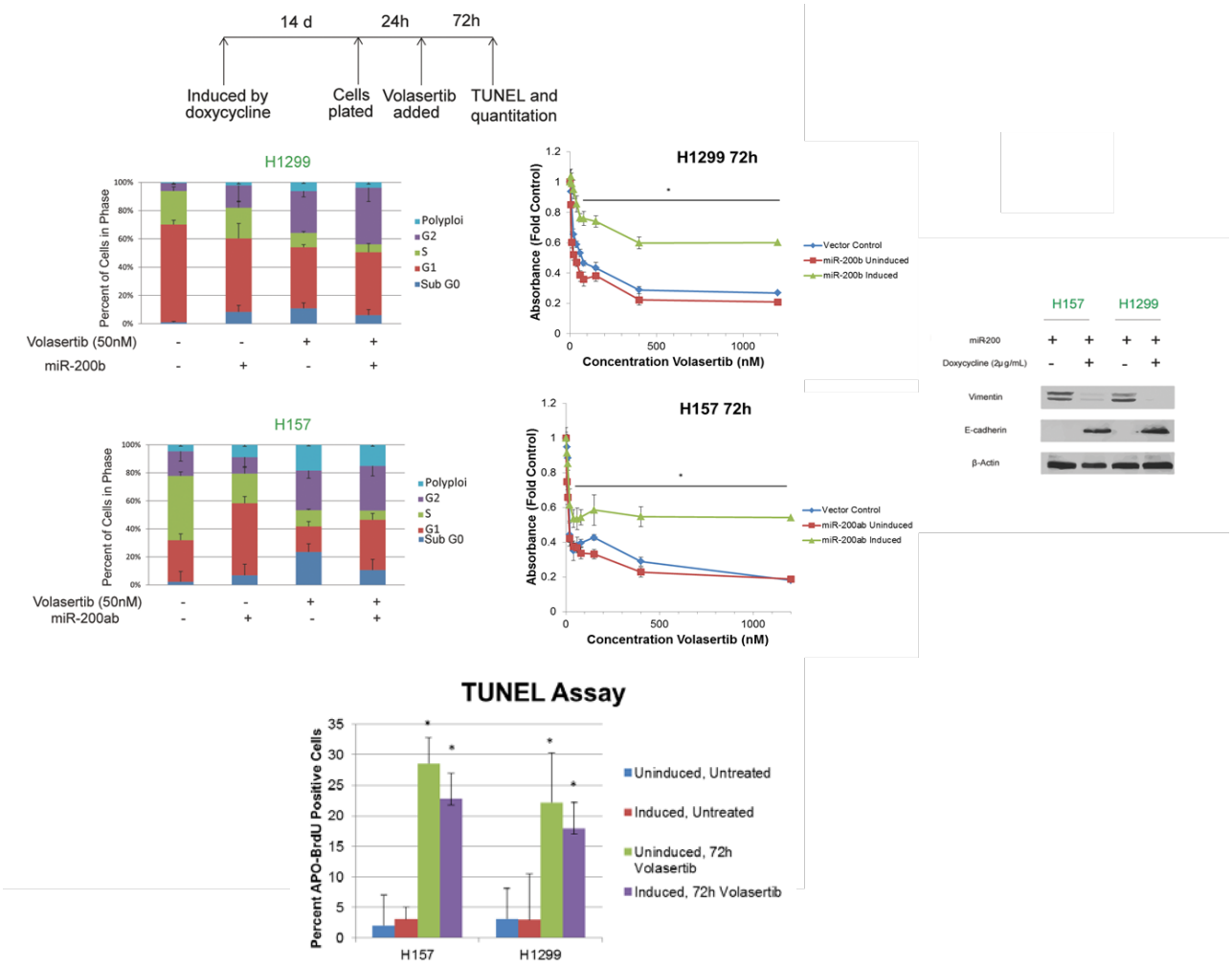
14 d
24h
72h
Induced by doxycycline
Cells plated
Volasertib added
TUNEL and quantitation
H1299
Percent of Cells in Phase
Polyploi
G2
S
G1
Sub G0
Volasertib (50nM)
miR-200b
H157
Volasertib (50nM)
miR-200ab
H1299 72h
Absorbance (Fold Control)
Concentration Volasertib (nM)
Vector Control
miR-200b Uninduced
miR-200b Induced
H157 72h
Concentration Volasertib (nM)
Vector Control
miR-200ab Uninduced
miR-200ab Induced
H157
H1299
miR200
Doxycycline (2µg/mL)
Vimentin
E-cadherin
β-Actin
TUNEL Assay
Percent APO-BrdU Positive Cells
Uninduced, Untreated
Induced, Untreated
Uninduced, 72h Volasertib
Induced, 72h Volasertib
H157
H1299

B

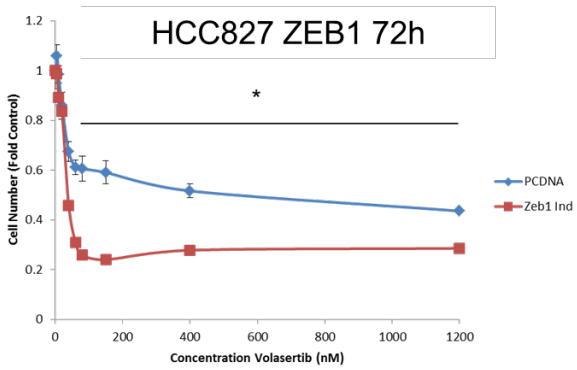
HCC827 ZEB1 72h
*
Cell Number (Fold Control)
Concentration Volasertib (nM)
PCDNA
Zeb1 Ind

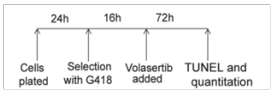
24h
16h
72h
Cells plated
Selection with G418
Volasertib added
TUNEL and quantitation

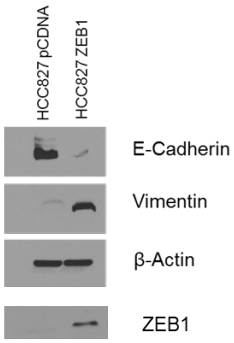
HCC827 pCDNA
HCC827 ZEB1
E-Cadherin
Vimentin
β-Actin
ZEB1

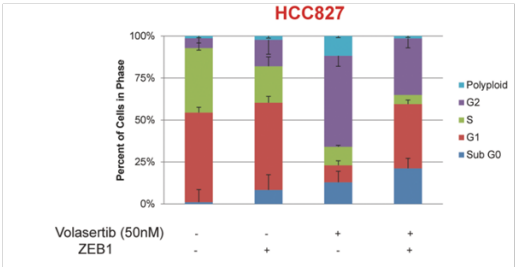
HCC827
Percent of Cells in Phase
Polyploid
G2
S
G1
Sub G0
Volasertib (50nM)
ZEB1

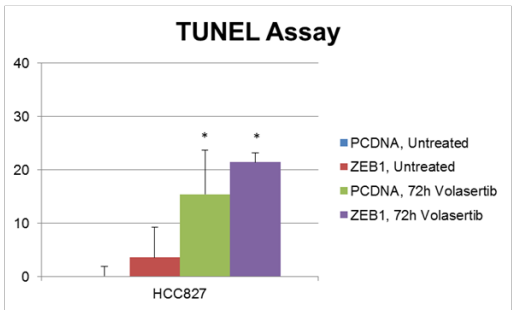
TUNEL Assay
PCDNA, Untreated
ZEB1, Untreated
PCDNA, 72h Volasertib
ZEB1, 72h Volasertib
HCC827

C

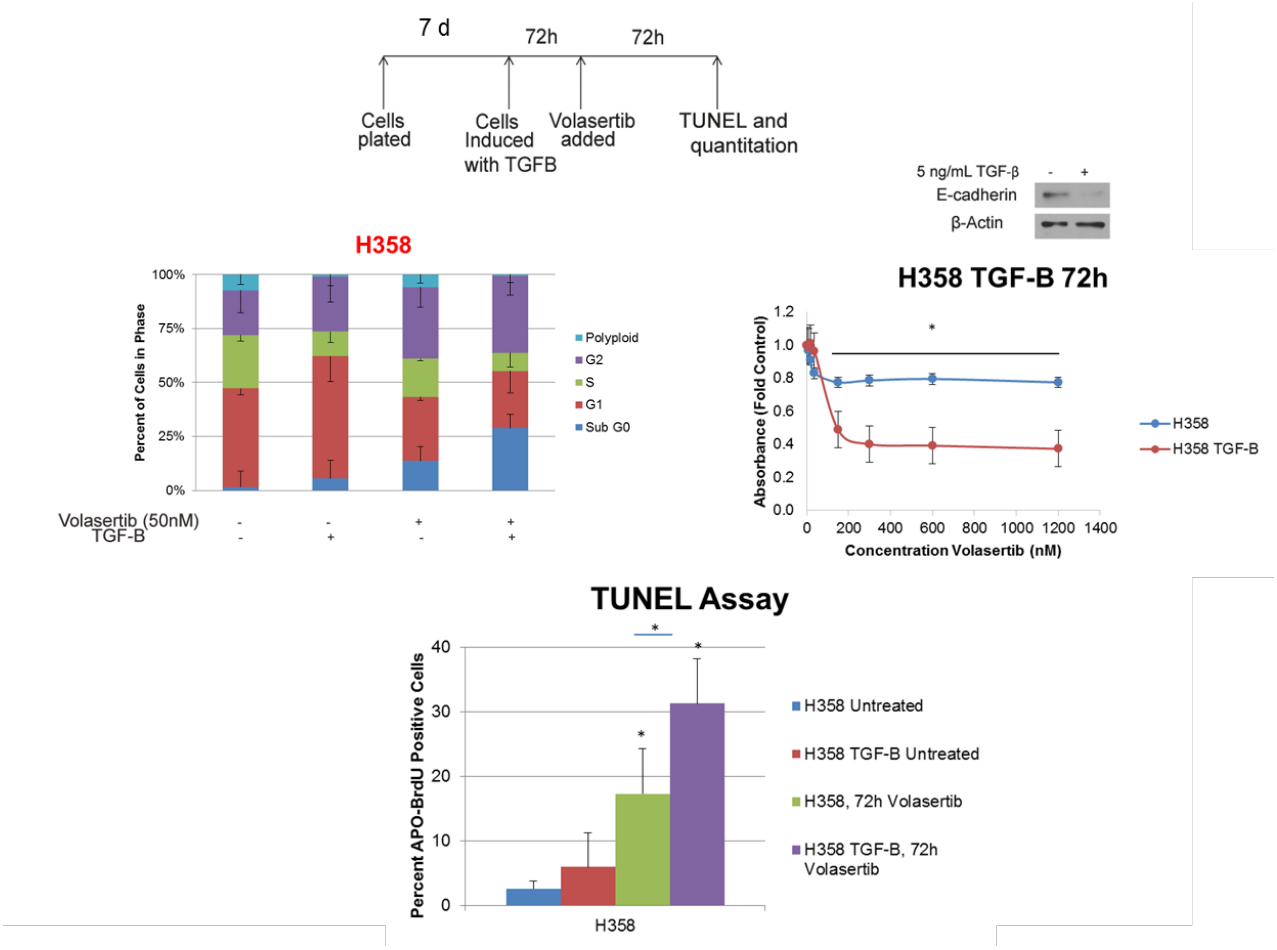

Figure 22. Induction of EMT sensitizes NSCLC cell lines to Plk1 inhibition whereas MET makes cell lines more resistant. Mesenchymal cells are more sensitive to PLK1 inhibition than epithelial cells using isogenic human NSCLC models. (A) Forced expression of miR-200 led to increased E-cadherin expression and decreased vimentin expression as determined by Western blotting and to resistance to volasertib as measured by MTT assay. Induction of a mesenchymal phenotype using ZEB1 expression (B) or 5 ng/mL TGF-β (C) led to volasertib sensitivity and increased volasertib-induced apoptosis. *, $P \leq 0.05$ compared to control or as indicated.

Chapter 4: Discussion

Large scale screen of NSCLC cell lines to Plk1 inhibitors

Previous studies have shown Plk1 inhibitors to have broad antitumor activity in diverse set of cancer cell lines (46, 58, 61, 94, 95) and mouse xenografts (49, 96). The GDSC (34) and CCLE (33) databases demonstrated that NSCLC cell lines responded to Plk1 inhibitors (Figure 6). However, it had not been shown in a large panel of NSCLC cell lines. In our study, we screened over 50 NSCLC cell lines with BI2536, volasertib, and GSK461364 by MTT and CellTiter-Glo. We observed that Plk1 inhibition led to decreased viability in all cell lines, but was substantially different in the sensitive cell lines compared to the resistant cell lines (Figure 6). We differentiated sensitive cell lines and resistant cell lines based on the inhibition of 70% of cell growth (IC70) being reached prior to the Cmax dose. After screening all the cell lines with the three Plk1 inhibitors, we found that a smaller subset of cell lines were either sensitive to all three inhibitors or resistant to all three inhibitors. This agrees with previous clinical studies that have shown low response rates to Plk1 inhibition in solid tumors (35, 46, 58, 61). We then proceeded to analyze correlations of Plk1 inhibitor sensitivity and potential candidate biomarkers from literature.

Plk1 inhibitors have been approved for use in acute myeloid leukemia (AML) (58, 95). One of the hallmarks of AML is that it has a high mitotic rate (97), meaning it has a short doubling time. Volasertib has been shown to be highly effective as single agent in AML (58). We studied if cell doubling time plays a role sensitivity because Plk1 affects the cell cycle, and cells that divide faster will go through the cell cycle more times than slower growing cells during the assays. Theoretically, the cells with shorter doubling

times would therefore be in G2 more frequently, causing them to be more vulnerable to Plk1 inhibition. This pattern is observed in regards to chemotherapy drugs targeting the S phase of the cell cycle, as seen by methotrexate (98).Based on the doubling time of 9 (5 resistant, 4 sensitive) NSCLC cell lines, it appears doubling time does not correlate with sensitivity to Plk1 inhibition. This may have been due to the low absolute number of NSCLC cell lines used in the analysis.

Previous studies had implicated *TP53* and *KRAS* mutations as predictive biomarkers of Plk1 inhibition sensitivity. In cancer cells with p53 mutations or low expression of the protein, depleting Plk1 led to apoptosis following cell cycle arrest and spindle checkpoint activation (31, 53, 60). Additionally, knockdown of Plk1 preferentially reduced the survival of p53 deficient, oncogenic transformed cells and tumor growth (54). In our study, we tested correlation of *TP53* mutational status with Plk1 inhibitor sensitivity, but found no significant correlation was found. This agrees with another study in which no significant different cytotoxic response between cancer cells with and without functional p53 was observed in colon, breast, lung, and cervical cancer cell lines after Plk1 depletion (99).

It has been suggested that *KRAS* mutant cells are sensitive to Plk1 inhibition, and it has been observed that *KRAS* G13D mutant colorectal cancer cell lines, increased cell death was observed after Plk1 depletion and inhibition (52). Due to the number of cell lines with only *KRAS* mutations being low, we put the *NRAS* and *KRAS* mutant cell lines in one group, the *RAS* mutant lines. The *RAS* mutant cell lines correlated with sensitivity for both BI2536 and volasertib (Table 3). To further characterize *KRAS* mutants, we applied an established KRAS dependency signature to

KRAS mutant NSCLC cell lines (64). KRAS-dependent NSCLC cell lines, defined as those that undergo apoptosis when KRAS is knocked down, exhibit classical epithelial morphology, whereas KRAS-independent cells display a mesenchymal phenotype (64). In unsupervised analysis, KRAS-independent cell lines clustered in the sensitive group for GSK461364 but not for the other 3 groups (Figure 17). Our data suggests that the response of *KRAS* mutant cell lines may depend on the inhibitors being used as they have different pharmacological properties. Additionally, the grouping the *NRAS* and *KRAS* mutant lines may have affected the correlations as they have different biological properties.

There have not been studies which examine correlation of basal gene and protein expression to a large panel of cell lines to Plk1 inhibition. As mentioned above, potential candidate biomarkers were not significantly correlated to response to Plk1 inhibition. To determine why NSCLC cell lines had diverse sensitivities to Plk1 inhibition, we examined the relationship between drug sensitivity and baseline gene and protein expression in four groups of cell lines: BI2536-sensitive/resistant, volasertib-sensitive/resistant, GSK461364-sensitive/resistant, and the universal cell lines. We found that the expression levels of several genes and proteins correlated with drug sensitivity (Table 4,5). E-cadherin and β-catenin were consistently expressed at higher levels in the resistant lines, while DNA-dependent protein kinase catalytic subunit (DNA-PKcs) and thymidylate synthase were consistently overexpressed in the sensitive lines. The correlation of high E-cadherin expression with resistance to Plk1 inhibition was true for all three inhibitors, as well as the universal cell lines (Figure 20). The correlation with E-cadherin had not been previously reported. One link which has been established was

in the *KRAS* dependent cell lines which demonstrated less sensitivity to Plk1 depletion and inhibition compared to *KRAS* independent colon cancer cell lines. These *KRAS* dependent cells exhibited classical epithelial morphology (52, 64). Additionally, DNA-PKcs synthase has been reported to associate with Plk1 to ensure proper chromosomal separation in preparation in anaphase (100). Additionally, β-catenin has been reported to be a substrate of Plk1 and is associated with signaling involved in chromosomal segregation, and is involved in cell-cell adhesion and EMT (101, 102).

Biological effects of Plk1 inhibition

Previous studies had used colony formation assays to assay for cell proliferation effects of Plk1 inhibition in glioma and medulloblastoma cells (99, 103). As another measure of proliferation, we analyzed colony formation, after pulse treating cells with volasertib and then continued culturing cells (Figure 10). This assay is distinct from the MTT as we are not exposing the drug to the cells for a prolonged period. Both total well area and average colony area decreased significantly in the sensitive cell lines compared to the resistant cell lines, indicating a greater decrease in proliferation in the sensitive cell lines. The result mirrored the results from the MTT assays, leading us to believe that the sensitive cells undergo an irreversible inhibition of proliferation compared to the resistant cells. The results agreed with previous findings in which diverse sensitivities were observed through the colony growth after Plk1 inhibitor treatment (94, 103).

We observed that some of the dose response curves increased upward at higher concentrations of the drug, representing increased cell number (Figure 6). This has also been previously by Raab, et al. at which they also saw increased cell number at very

high doses in HeLa cells (104). This may be resulting from the off-target effects of the inhibitors, which also target tumor suppressors Plk2 and 3 (30). A large scale proteomics screen done by the same group identified DAPK as a target which is targeted by Plk1 inhibition and allows for survival of cells with genetic aberrations (104). Thus, it is possible that in this study that the drugs are inhibiting tumor suppressors such as DAPK at high concentrations.

To determine whether the inhibitors were truly inhibiting Plk1 in cell lines, we looked at the expression of Plk1 targets in NSCLC cell lines. In our work, we demonstrated that mitotic substrates including Myt1 and indirectly CDK1 were inhibited by Plk1 inhibitors in both sensitive and resistant cells (Figure 7). Additionally, cyclin B levels increased following Plk1 inhibitor treatment. This was expected as the proteasomal degradation of cyclin B is Plk1 dependent. However, there was difference in the inhibition of phospho-TCTP at Ser46, which is a substrate involved in the spindle assembly checkpoint and chromosomal separation (42). This may suggest a possible resistance mechanism, suggesting the distinct biological differences we observe are occurring at the spindle checkpoint stage. Resistant cells appear to be able to bypass Plk1 spindle checkpoint signals and continue dividing with aberrant chromosomal separation. Previous studies have shown that Plk1 inhibition leads to polyploid cells and multipolar spindles (36, 41, 45, 49, 54, 58, 61). Additionally, assaying for Plk1 activity at longer timepoints (Figure 9) exhibited similar results. This may additionally suggest that the target may not be sufficiently inhibited in resistant cell lines at longer time points, allowing cells to start proliferating again. This is in agreement with what we observed in the colony formation assays.

Sensitive cell lines appeared to undergo cell cycle arrest, had increased sub-G0 population, and underwent apoptosis (Figure 11-13). In contrast, resistant cell lines had an increase in cells with 4N DNA content, increased number of polyploid cells, and underwent less apoptosis compared to the sensitive cell lines. We are unable to distinguish if the 4N cells were in G1 or G2 of different cell cycles as we also observe increased polyploid cells, especially with our resistant cells. Additionally, we observed an increase in polyploid cells in resistant cells using both through cell cycle analysis and microscopy. This may be a sign of cells undergoing a mitotic catastrophe. Here, cells would be able to bypass the spindle assembly checkpoint and divide. Cells which bypass this checkpoint would now be aneuploid due to improper chromosomal segregation. These cells are able to go into the next cell cycle and continue dividing (105). When comparing to Plk1 knockdown in the same cell lines, the same accumulation of 4N cells was seen after the Plk1 knockdown. There was significantly more apoptosis in the cells after knockdown compared to inhibition; however, the results mirrored those from the Plk1 inhibition where we see more apoptosis in that the sensitive cell lines compared to the resistant cell lines, confirming the effects of the inhibitors in NSCLC cell lines were mainly Plk1-driven.

One mechanism which may be leading to this resistance is the expression of ABC transporter proteins involved in multi-drug resistance. Plk1 inhibitor resistance has been implicated with the expression of ATP Binding Cassette transporter proteins which are involved in multi-drug resistance mechanisms (46, 90). We evaluated basal gene expression of ATP-binding cassette (ABC) transporters ABCB1 and ABCG2 with sensitivity to the three Plk1 inhibitors. No statistically significant correlation was found

(Figure 19). Although ABC transporter mRNA levels did not correlate, there is evidence to suggest that these proteins are highly regulated at the translational level (106, 107). In the case of the dose-dependent response Western blots, we saw substrate reactivation at high concentrations for GSK461364 (Figure 7). When we examined protein expression of different ABC transporters, we saw induction of expression of ABCB1 and ABCC10 (Figure 8). There have been previous reports of ABC transporters being involved in a possible resistance mechanism for this particular inhibitor (31, 90). Previous studies had demonstrated that treatment of GSK461364 in ABCB1 overexpressing ovarian cancer cell lines led to the efflux of transporter substrate dyes (90, 106, 107). Assaying for activity through dye efflux would help us understand if inhibitors are substrates of these proteins. Additionally, the combination of Plk1 inhibitors and MDR1 inhibitors may lead to sensitization of resistant cells if this is the major issue.

Plk1 inhibition and EMT

After analyzing gene and protein expression, it was evident that EMT related proteins are highly correlated with Plk1 inhibitor sensitivity in NSCLC cell lines. E-cadherin expression was highest in the resistant cell lines. In 2013, Byers et al published an EMT gene signature (80). The signature is based on a set of 76 genes related to EMT which were validated using gene expression from four platforms in NSCLC cell lines and tumor samples from the BATTLE study. The signature was able to predict resistance to EGFR inhibitors and PI3K/Akt inhibitors. We discovered that NSCLC lines with high EMT scores (more mesenchymal cell lines) are more sensitive to all three Plk1 inhibitors. In addition, forced induction of an epithelial phenotype resulted

in drug resistance, and forced induction of a mesenchymal phenotype increased drug sensitivity. Recent publications have demonstrated that the miR-200-ZEB1 axis is crucial in the regulation of the EMT phenotype (93, 108, 109). It was also seen that the manipulation of EMT related transcription factor ZEB1 and miR-200, which are repressors and activators of E-cadherin expression respectively, slightly reversed sensitivity or resistance. However, only knocking down E-cadherin using siRNA did not change sensitivity to the Plk1 inhibition. Treatment of cells with TGF- β is also known to induce EMT through the activation of Smad proteins and other EMT-related pathways (65, 66, 73, 74, 109). Inducing EMT through treatment with TGF- β resulted in a significant increase in apoptosis in a universal resistant cell line H358.

Tight-junction and Rho signaling pathways are also related to EMT, and these pathways were enriched, as seen by analyzing the pathways altered in our differential gene expression (Table 6). Tight junctions are an extremely important component of the signaling pathways that regulate epithelial proliferation and differentiation (110-112). Additionally, Rho family GTPases are essential for epithelial cell polarity, tight-junction assembly, and regulation of the actin cytoskeleton (113). It is also interesting to note that one of the ways TGF- β facilitates EMT in non Smad related processes is by regulating Rho GTPases (65).

No previous studies had linked mesenchymal phenotypes to Plk1 inhibitor sensitivity. However, previous studies had shown that breast cancer and glioblastoma cell lines were more susceptible to Plk1 inhibition; these cell lines are known to be more mesenchymal (50, 94). The change in morphology appears to dictate the sensitivity and resistance, as evidenced by our isogenic models, in which we were able to induce cells

to become either more epithelial or more mesenchymal. However, this may be a secondary effect of the alteration of several pathways rather than the primary mechanism. For example, when we manipulated the expression of E-cadherin through siRNA, we did not see significant changes in apoptosis. Additionally, ZEB1 and miR-200 primarily affect EMT status through modulation of E-cadherin expression (93). Although we saw changes in the MTT assays using these models, we did not observe significant differences in apoptosis after treatment compared to controls. However, TGF- β induced EMT resulted in cells undergoing significantly more apoptosis compared to the parental cell lines. TGF- β is known to affect several signaling pathways, not just EMT related, which may play a role in affecting sensitivity.

Conclusions

As we saw, the NSCLC cell lines demonstrated diverse sensitivities to Plk1 inhibition. Sensitive and resistant cell lines exhibited different biological responses to Plk1 inhibition. Sensitive NSCLC cell lines undergo significantly more apoptosis compared to resistant cell lines. Gene and protein expression profiles showed that expression of specific sets of genes and proteins, especially those related to EMT, significantly correlate with response to Plk1 inhibitors, which may be used as predictive biomarkers. Finally, modulation of EMT status in NSCLC cell lines leads to changes in sensitivity.

The major implications of this study are the potential for clinical benefits. As we chose the most clinically relevant Plk1 inhibitors, our findings have translational impact. Most mesenchymal type cancers are resistant to therapies (114, 115). Additionally, EMT is one of the mechanisms leading to loss of oncogene addiction (116). More

mesenchymal tumors usually have worse prognosis and represent an unmet need in terms of today's cancer therapy. If Plk1 inhibitors are effective in mesenchymal tumors in vivo, this may provide a possible therapeutic benefit for those patients who may suffer from this disease. Additionally, it would be interesting to see if the diverse biological responses we observed were distinguished based on EMT status.

One limitation of our study is the poor correlation of the effects of the two Boehringer Ingelheim compounds (BI2536 and volasertib) with the effects of GSK461364. The differences in the drugs' effects may be attributed to differences in the drugs' selectivities (GSK461364 is more selective against Plk1). Similar inconsistencies have been reported in two large-scale pharmacogenomic studies, where genomic data were well correlated between the studies, but responses of the drugs highly discordant (117). Additionally, we noted that in some cell lines, higher drug concentrations had less of an effect on cell viability than intermediate concentrations (Figure 6). Additionally, in our cell screening assays, the MTT and CellTiter-Glo assays do not distinguish if cells are in cell cycle arrest or are undergoing apoptosis (118). These assays may not completely reflect the cell growth of the cells following Plk1 inhbition.

Future Directions

Although we clearly demonstrated that mesenchymal NSCLC cell lines were more sensitive to Plk1 inhibition, future studies should focus on the mechanisms that lead to Plk1-inhibitor induced apoptosis in mesenchymal cells. To study this mechanism, we could use unbiased methods to identify potential mechanisms which are contributing to the link between EMT and the Plk1 inhibitor-induced apoptosis. As we have been able to establish isogenic models in which we are able to reverse sensitivity and resistance, we could run gene expression arrays and RPPA pre and post treatment to determine which signaling pathways are differentially regulated in the models. In this case, we are not focused to a singular pathway to study, but rather several different pathways which may contribute to the effects we are seeing. As we saw, induction of EMT through TGF-β sensitized the cells and MET through miR-200 made cells more resistant. We would be able to use these models and either use Plk1 inhibitors or siRNA against Plk1 to see which pathways are differentially regulated.

Additionally, we saw that tight junction signaling was enriched in our resistant cell lines based on our gene expression data. This may be an area of study in which we could manipulate the genes regulating this pathway in resistant cell lines to see if alteration may lead to a change in sensitivity. As we know, proteins related to tight junction signaling are related to epithelial cell polarity and adhesions, especially in the case of claudins and occluding, which were differentially expressed. The Rho-family of GTPases also is implicated in the regulation of these cell-cell junctions, and may be another area of study. Another major target we could study, in terms of mechanism is role of β-catenin. The expression of β-catenin, both at the mRNA and protein level

highly correlated with resistance. As has been reported, it is related to tight junction signaling, cell polarity, and cell-cell junctions. Additionally, it has been reported that β catenin and Wnt signaling play important regulatory roles in the nucleus where it is important in centrosomal separation (102), interacting with NEK2, which is a substrate of Plk1 (101).

Plk1 may synergize with DNA damaging agents such as chemotherapy and radiotherapy to kill cancer cells (95, 119). In this regard, in the differential gene expression patterns, sensitive cells lines had altered DNA damage-related proteins compared to resistant lines. This may open up new directions to study in terms of combinations. We may also be able to combine DNA damaging agents such as cisplatin or gemcitabine with Plk1 inhibitors. If the resistant cell lines are able to continue cycling and go into subsequent cell cycles with aneuploidy, we may be able to use drugs targeting the S phase to target cells which are resistant to Plk1 inhibition.

We observed that some EGFR tyrosine kinase inhibitor acquired resistant cell lines became more mesenchymal and more sensitive to Plk1 inhibition. Three different cell lines had been tested, and of these, two became more mesenchymal to acquire resistance to EGFR tyrosine kinase inhibitor erlotinib (preliminary data, not shown). HCC827 and HCC4006 parental cell lines were among those which were universally resistant in our screen of the Plk1 inhibitors. In these resistant clones, it has been seen that Axl kinase expression has been elevated. This has been reported as a potential mechanism leading to mitotic kinase inhibitor vulnerability in conjunction with Axl inhibitors by Dr. Jeff Settleman's group (120). Additionally, the isogenic model in which TGF-β was used to change the morphology of H358 cell line into a mesenchymal cell

line was shown to have significant increase in apoptosis in our study. It has been reported that TGF-β induced H358 is also resistant to erlotinib and had increased Axl (120). This may be another potential area of study in which we can determine if acquired resistance to erlotinib through EMT and increased Axl may contribute to Plk1 inhibitor sensitivity through the EGFR pathway. There also may be the potential for combination studies with erlotinib to sensitize cell lines which are resistant to erlotinib with a Plk1 inhibitor such as volasertib.

Our in vitro studies using Plk1 inhibitors have shown a strong correlation with EMT scores and E-cadherin alone. E-cadherin expression may present a simple biomarker for Plk1 inhibitor response. To test this hypothesis, the next logical step would be to move to in vivo models, using cell line xenografts with diverse EMT status. However, more telling in terms of translational relevance, it would be interesting to study the response in patient derived xenograft (PDX) or genetically engineered mouse models. The study of Plk1 inhibitor response in PDX models would be a stronger tool as these models are closer to human tumors. We may be able to establish PDX models to be able to treat tumors in mice and determine the EMT status of these tumors to see if the relationship of EMT status and Plk1 inhibitor sensitivity holds in this setting.

If the results from such in vivo studies would yield promising results, we may be able to test our conclusions in a clinical trial with FDA approved Plk1 inhibitors (volasertib). E-cadherin expression may serve as a simple biomarker to predict response to Plk1 inhibitors in NSCLC patients. Biopsies taken from patients may be analyzed for EMT biomarkers, such as E-cadherin, and patients can be randomized into different groups. In the clinical setting, mesenchymal tumors are typically more resistant

to standard therapeutic regimens. If our hypothesis holds, then Plk1 inhibitors will be a choice for patient treatment modalities.

Appendix

H358 Ungated Cell Cycle

Calu-6 Ungated Cell Cycle

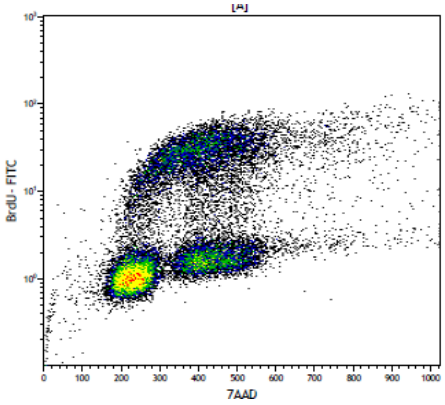

Control

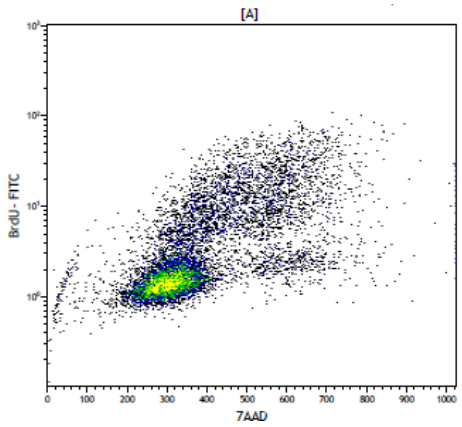

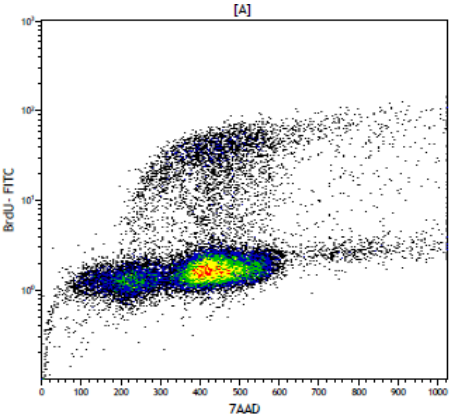

24h volasertib (50nM)

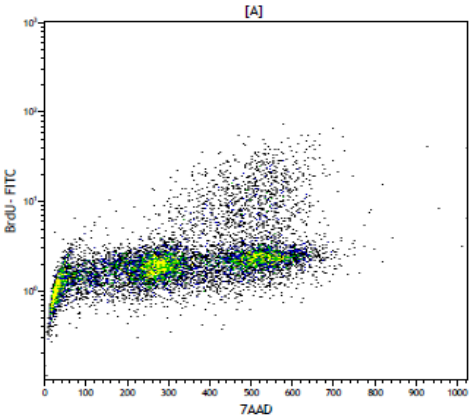

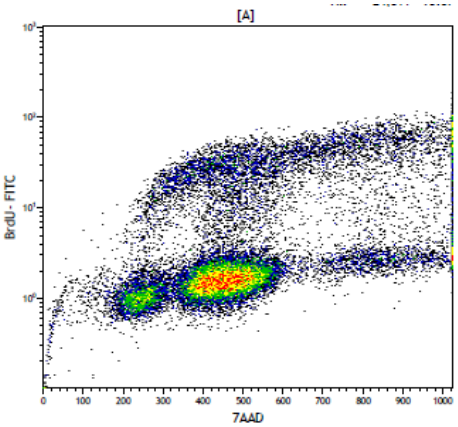

48h volasertib (50 nM)

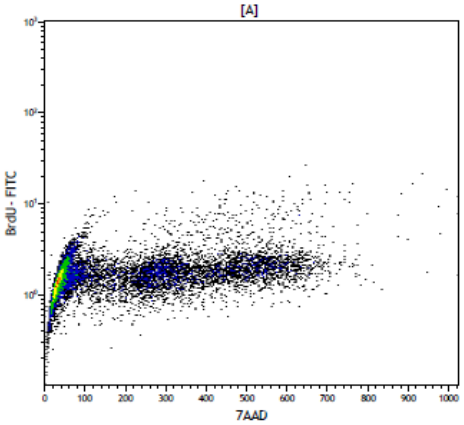

H322 si Plk1 Ungated Cell Cycle

Calu-6 siPlk1 Ungated Cell Cycle

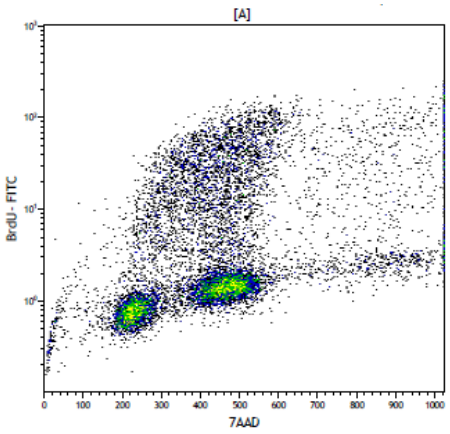

Control

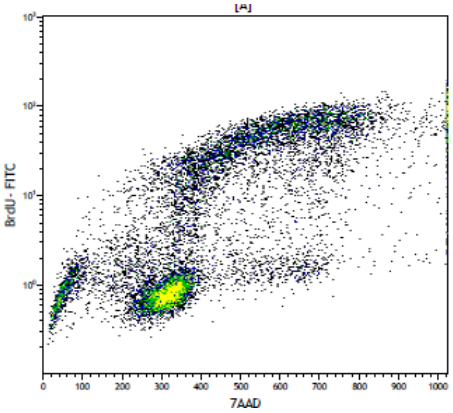

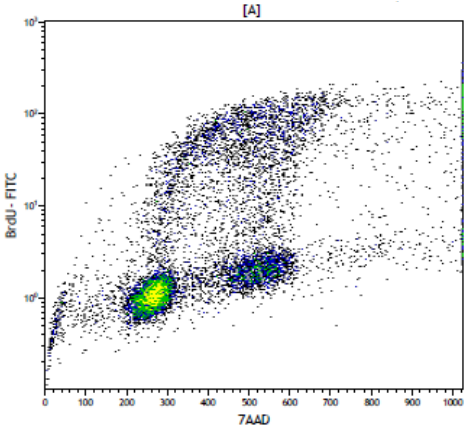

24h si Plk1

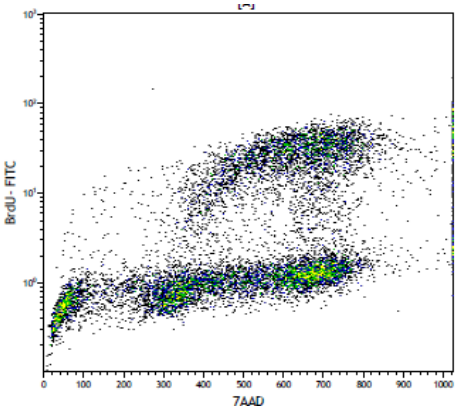

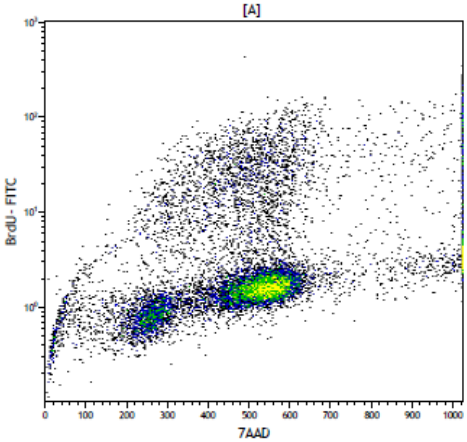

48h si Plk1

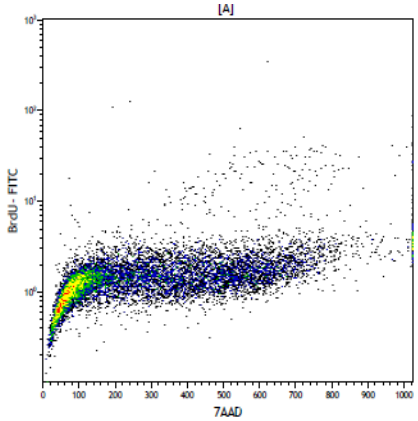

H358

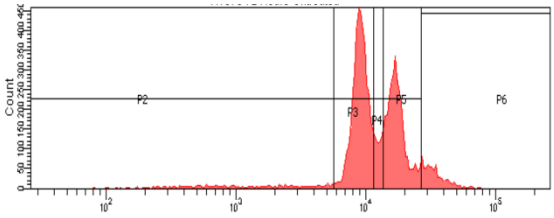

H358

TGF-B

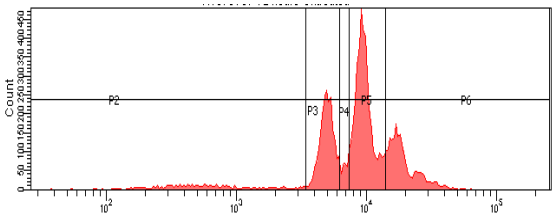

H358

+ Vol

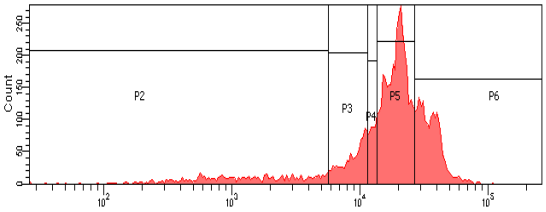

H358

TGF-B

+ Vol

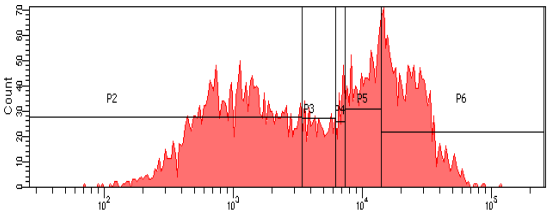

Cell Cycle for H358 parental cells (top panel) and H358 TGF-B cells (bottom panel)

Chapter 5: Bibliography

1. Siegel RL, Miller KD, Jemal A. Cancer statistics, 2015. CA: a cancer journal for clinicians. 2015;65(1):5-29.
2. Nawrot TS, Martens DS, Hara A, Plusquin M, Vangronsveld J, Roels HA, Staessen JA. Association of total cancer and lung cancer with environmental exposure to cadmium: the meta-analytical evidence. Cancer causes & control : CCC. 2015.
3. Devarakonda S, Morgensztern D, Govindan R. Genomic alterations in lung adenocarcinoma. The Lancet Oncology. 2015;16(7):e342-51.
4. Sardenberg RA, Mello ES, Younes RN. The lung adenocarcinoma guidelines: what to be considered by surgeons. Journal of thoracic disease. 2014;6(Suppl 5):S561-7.
5. Suh JH. Current readings: pathology, prognosis, and lung cancer. Seminars in thoracic and cardiovascular surgery. 2013;25(1):14-21.
6. Sangodkar J, Katz S, Melville H, Narla G. Lung adenocarcinoma: lessons in translation from bench to bedside. The Mount Sinai journal of medicine, New York. 2010;77(6):597-605.
7. Nakamura H, Saji H. Worldwide trend of increasing primary adenocarcinoma of the lung. Surgery today. 2014;44(6):1004-12.
8. Thomas A, Liu SV, Subramaniam DS, Giaccone G. Refining the treatment of NSCLC according to histological and molecular subtypes. Nature reviews Clinical oncology. 2015.
9. Couraud S, Zalcman G, Milleron B, Morin F, Souquet PJ. Lung cancer in never smokers--a review. European journal of cancer. 2012;48(9):1299-311.
10. Hanahan D, Weinberg RA. Hallmarks of cancer: the next generation. Cell. 2011;144(5):646-74.
11. The Cancer Genome Atlas Research N. Comprehensive molecular profiling of lung adenocarcinoma. Nature. 2014;511(7511):543-50.
12. Minuti G, D'Incecco A, Cappuzzo F. Targeted therapy for NSCLC with driver mutations. Expert opinion on biological therapy. 2013;13(10):1401-12.
13. D'Arcangelo M, D'Incecco A, Cappuzzo F. Rare mutations in non-small-cell lung cancer. Future oncology. 2013;9(5):699-711.
14. Mery B, Guy JB, Swalduz A, Vallard A, Guibert C, Almokhles H, Ben Mrad M, Rivoirard R, Falk AT, Fournel P, Magne N. The evolving locally-advanced non-small cell lung cancer landscape: Building on past evidence and experience. Critical reviews in oncology/hematology. 2015.
15. Rothschild SI. Targeted Therapies in Non-Small Cell Lung Cancer-Beyond EGFR and ALK. Cancers. 2015;7(2):930-49.
16. Ellis PM, Coakley N, Feld R, Kuruvilla S, Ung YC. Use of the epidermal growth factor receptor inhibitors gefitinib, erlotinib, afatinib, dacomitinib, and icotinib in the treatment of non-small-cell lung cancer: a systematic review. Current oncology. 2015;22(3):e183-215.
17. Malumbres M, Barbacid M. Cell cycle, CDKs and cancer: a changing paradigm. Nature reviews Cancer. 2009;9(3):153-66.
18. Reece JB, Campbell NA. Campbell biology / Jane B. Reece ... [et al.]. 9th ed. Boston: Benjamin Cummings / Pearson; 2011. xlvi, 1263 p. p.
19. Carnero A, Blanco-Aparicio C, Kondoh H, Lleonart ME, Martinez-Leal JF, Mondello C, Ivana Scovassi A, Bisson WH, Amedei A, Roy R, Woodrick J, Colacci A, Vaccari M, Raju J, Al-Mulla F, Al-Temaimi R, Salem HK, Memeo L, Forte S, Singh N, Hamid RA, Ryan EP, Brown DG, Wise JP, Sr., Wise SS, Yasaei H. Disruptive chemicals, senescence and immortality. Carcinogenesis. 2015;36 Suppl 1:S19-37.
20. Vermeulen K, Van Bockstaele DR, Berneman ZN. The cell cycle: a review of regulation, deregulation and therapeutic targets in cancer. Cell proliferation. 2003;36(3):131-49.
21. Lamond AI. Molecular biology of the cell, 4th edition. Nature. 2002;417(6887):383-.
22. Lindqvist A, Rodriguez-Bravo V, Medema RH. The decision to enter mitosis: feedback and redundancy in the mitotic entry network. The Journal of cell biology. 2009;185(2):193-202.

23. Aarts M, Sharpe R, Garcia-Murillas I, Gevensleben H, Hurd MS, Shumway SD, Toniatti C, Ashworth A, Turner NC. Forced mitotic entry of S-phase cells as a therapeutic strategy induced by inhibition of WEE1. Cancer discovery. 2012;2(6):524-39.
24. Chow JP, Poon RY. The CDK1 inhibitory kinase MYT1 in DNA damage checkpoint recovery. Oncogene. 2013;32(40):4778-88.
25. Barr FA, Sillje HH, Nigg EA. Polo-like kinases and the orchestration of cell division. Nature reviews Molecular cell biology. 2004;5(6):429-40.
26. Zitouni S, Nabais C, Jana SC, Guerrero A, Bettencourt-Dias M. Polo-like kinases: structural variations lead to multiple functions. Nat Rev Mol Cell Biol. 2014;15(7):433-52.
27. Xu J, Shen C, Wang T, Quan J. Structural basis for the inhibition of Polo-like kinase 1. Nature structural & molecular biology. 2013;20(9):1047-53.
28. Hyun SY, Hwang HI, Jang YJ. Polo-like kinase-1 in DNA damage response. BMB reports. 2014;47(5):249-55.
29. Kim JH, Ku B, Lee KS, Kim SJ. Structural analysis of the polo-box domain of human Polo-like kinase 2. Proteins. 2015.
30. Helmke C, Becker S, Strebhardt K. The role of Plk3 in oncogenesis. Oncogene. 2015.
31. Liu X. Targeting Polo-Like Kinases: A Promising Therapeutic Approach for Cancer Treatment. Translational oncology. 2015;8(3):185-95.
32. de Carcer G, Manning G, Malumbres M. From Plk1 to Plk5: functional evolution of polo-like kinases. Cell cycle. 2011;10(14):2255-62.
33. Barretina J, Caponigro G, Stransky N, Venkatesan K, Margolin AA, Kim S, Wilson CJ, Lehar J, Kryukov GV, Sonkin D, Reddy A, Liu M, Murray L, Berger MF, Monahan JE, Morais P, Meltzer J, Korejwa A, Jane-Valbuena J, Mapa FA, Thibault J, Bric-Furlong E, Raman P, Shipway A, Engels IH, Cheng J, Yu GK, Yu J, Aspesi P, Jr., de Silva M, Jagtap K, Jones MD, Wang L, Hatton C, Palescandolo E, Gupta S, Mahan S, Sougnez C, Onofrio RC, Liefeld T, MacConaill L, Winckler W, Reich M, Li N, Mesirov JP, Gabriel SB, Getz G, Ardlie K, Chan V, Myer VE, Weber BL, Porter J, Warmuth M, Finan P, Harris JL, Meyerson M, Golub TR, Morrissey MP, Sellers WR, Schlegel R, Garraway LA. The Cancer Cell Line Encyclopedia enables predictive modelling of anticancer drug sensitivity. Nature. 2012;483(7391):603-7.
34. Yang W, Soares J, Greninger P, Edelman EJ, Lightfoot H, Forbes S, Bindal N, Beare D, Smith JA, Thompson IR, Ramaswamy S, Futreal PA, Haber DA, Stratton MR, Benes C, McDermott U, Garnett MJ. Genomics of Drug Sensitivity in Cancer (GDSC): a resource for therapeutic biomarker discovery in cancer cells. Nucleic acids research. 2013;41(Database issue):D955-61.
35. Sebastian M, Reck M, Waller CF, Kortsik C, Frickhofen N, Schuler M, Fritsch H, Gaschler-Markefski B, Hanft G, Munzert G, von Pawel J. The efficacy and safety of BI 2536, a novel Plk-1 inhibitor, in patients with stage IIIB/IV non-small cell lung cancer who had relapsed after, or failed, chemotherapy: results from an open-label, randomized phase II clinical trial. Journal of thoracic oncology : official publication of the International Association for the Study of Lung Cancer. 2010;5(7):1060-7.
36. Liu D, Davydenko O, Lampson MA. Polo-like kinase-1 regulates kinetochore-microtubule dynamics and spindle checkpoint silencing. The Journal of cell biology. 2012;198(4):491-9.
37. Tavernier N, Panbianco C, Gotta M, Pintard L. Cdk1 plays matchmaker for the Polo-like kinase and its activator SPAT-1/Bora. Cell cycle. 2015:1-5.
38. Kishimoto T. Entry into mitosis: a solution to the decades-long enigma of MPF. Chromosoma. 2015.
39. van Vugt MA, Medema RH. Getting in and out of mitosis with Polo-like kinase-1. Oncogene. 2005;24(17):2844-59.
40. Ibrahim B. Toward a systems-level view of mitotic checkpoints. Progress in biophysics and molecular biology. 2015;117(2-3):217-24.

41. Eckerdt F, Strebhardt K. Polo-like kinase 1: target and regulator of anaphase-promoting complex/cyclosome-dependent proteolysis. Cancer research. 2006;66(14):6895-8.
42. Cucchi U, Gianellini LM, De Ponti A, Sola F, Alzani R, Patton V, Pezzoni A, Troiani S, Saccardo MB, Rizzi S, Giorgini ML, Cappella P, Beria I, Valsasina B. Phosphorylation of TCTP as a marker for polo-like kinase-1 activity in vivo. Anticancer research. 2010;30(12):4973-85.
43. Gachet Y, Tournier S, Lee M, Lazaris-Karatzas A, Poulton T, Bommer UA. The growth-related, translationally controlled protein P23 has properties of a tubulin binding protein and associates transiently with microtubules during the cell cycle. Journal of cell science. 1999;112 (Pt 8):1257-71.
44. Burgess A, Labbe JC, Vigneron S, Bonneaud N, Strub JM, Van Dorsselaer A, Lorca T, Castro A. Chfr interacts and colocalizes with TCTP to the mitotic spindle. Oncogene. 2008;27(42):5554-66.
45. Dai W, Huang X, Ruan Q. Polo-like kinases in cell cycle checkpoint control. Frontiers in bioscience : a journal and virtual library. 2003;8:d1128-33.
46. Degenhardt Y, Lampkin T. Targeting Polo-like kinase in cancer therapy. Clinical cancer research : an official journal of the American Association for Cancer Research. 2010;16(2):384-9.
47. Feng YB, Lin DC, Shi ZZ, Wang XC, Shen XM, Zhang Y, Du XL, Luo ML, Xu X, Han YL, Cai Y, Zhang ZQ, Zhan QM, Wang MR. Overexpression of PLK1 is associated with poor survival by inhibiting apoptosis via enhancement of survivin level in esophageal squamous cell carcinoma. International journal of cancer Journal international du cancer. 2009;124(3):578-88.
48. Craig SN, Wyatt MD, McInnes C. Current assessment of polo-like kinases as anti-tumor drug targets. Expert Opin Drug Discov. 2014;9(7):773-89.
49. Driscoll DL, Chakravarty A, Bowman D, Shinde V, Lasky K, Shi J, Vos T, Stringer B, Amidon B, D'Amore N, Hyer ML. Plk1 inhibition causes post-mitotic DNA damage and senescence in a range of human tumor cell lines. PloS one. 2014;9(11):e111060.
50. Tandle AT, Kramp T, Kil WJ, Halthore A, Gehlhaus K, Shankavaram U, Tofilon PJ, Caplen NJ, Camphausen K. Inhibition of polo-like kinase 1 in glioblastoma multiforme induces mitotic catastrophe and enhances radiosensitisation. European journal of cancer. 2013;49(14):3020-8.
51. Spankuch-Schmitt B, Bereiter-Hahn J, Kaufmann M, Strebhardt K. Effect of RNA silencing of polo-like kinase-1 (PLK1) on apoptosis and spindle formation in human cancer cells. J Natl Cancer Inst. 2002;94(24):1863-77.
52. Luo J, Emanuele MJ, Li D, Creighton CJ, Schlabach MR, Westbrook TF, Wong KK, Elledge SJ. A genome-wide RNAi screen identifies multiple synthetic lethal interactions with the Ras oncogene. Cell. 2009;137(5):835-48.
53. Liu X, Erikson RL. Polo-like kinase (Plk)1 depletion induces apoptosis in cancer cells. Proceedings of the National Academy of Sciences of the United States of America. 2003;100(10):5789-94.
54. Guan R, Tapang P, Leverson JD, Albert D, Giranda VL, Luo Y. Small interfering RNA-mediated Polo-like kinase 1 depletion preferentially reduces the survival of p53-defective, oncogenic transformed cells and inhibits tumor growth in animals. Cancer research. 2005;65(7):2698-704.
55. Stadler WM, Vaughn DJ, Sonpavde G, Vogelzang NJ, Tagawa ST, Petrylak DP, Rosen P, Lin CC, Mahoney J, Modi S, Lee P, Ernstoff MS, Su WC, Spira A, Pilz K, Vinisko R, Schloss C, Fritsch H, Zhao C, Carducci MA. An open-label, single-arm, phase 2 trial of the Polo-like kinase inhibitor volasertib (BI 6727) in patients with locally advanced or metastatic urothelial cancer. Cancer. 2014;120(7):976-82.
56. Schoffski P, Awada A, Dumez H, Gil T, Bartholomeus S, Wolter P, Taton M, Fritsch H, Glomb P, Munzert G. A phase I, dose-escalation study of the novel Polo-like kinase inhibitor volasertib (BI 6727) in patients with advanced solid tumours. Eur J Cancer. 2012;48(2):179-86.
57. Yang Y, Bai J, Shen R, Brown SA, Komissarova E, Huang Y, Jiang N, Alberts GF, Costa M, Lu L, Winkles JA, Dai W. Polo-like kinase 3 functions as a tumor suppressor and is a negative regulator of hypoxia-inducible factor-1 alpha under hypoxic conditions. Cancer research. 2008;68(11):4077-85.

58. Brandwein JM. Targeting polo-like kinase 1 in acute myeloid leukemia. Therapeutic advances in hematology. 2015;6(2):80-7.
59. Yim H. Current clinical trials with polo-like kinase 1 inhibitors in solid tumors. Anti-cancer drugs. 2013;24(10):999-1006.
60. Yim H, Erikson RL. Plk1-targeted therapies in TP53- or RAS-mutated cancer. Mutation research Reviews in mutation research. 2014.
61. Medema RH, Lin CC, Yang JC. Polo-like kinase 1 inhibitors and their potential role in anticancer therapy, with a focus on NSCLC. Clinical cancer research : an official journal of the American Association for Cancer Research. 2011;17(20):6459-66.
62. Choi M, Kim W, Cheon MG, Lee CW, Kim JE. Polo-like kinase 1 inhibitor BI2536 causes mitotic catastrophe following activation of the spindle assembly checkpoint in non-small cell lung cancer cells. Cancer Lett. 2015;357(2):591-601.
63. McCarroll JA, Dwarte T, Baigude H, Dang J, Yang L, Erlich RB, Kimpton K, Teo J, Sagnella SM, Akerfeldt MC, Liu J, Phillips PA, Rana TM, Kavallaris M. Therapeutic targeting of polo-like kinase 1 using RNA-interfering nanoparticles (iNOPs) for the treatment of non-small cell lung cancer. Oncotarget. 2014.
64. Singh A, Greninger P, Rhodes D, Koopman L, Violette S, Bardeesy N, Settleman J. A gene expression signature associated with "K-Ras addiction" reveals regulators of EMT and tumor cell survival. Cancer cell. 2009;15(6):489-500.
65. Papageorgis P. TGFbeta Signaling in Tumor Initiation, Epithelial-to-Mesenchymal Transition, and Metastasis. Journal of oncology. 2015;2015:587193.
66. Cichon MA, Radisky DC. Extracellular matrix as a contextual determinant of transforming growth factor-beta signaling in epithelial-mesenchymal transition and in cancer. Cell adhesion & migration. 2014;8(6):588-94.
67. Kalluri R, Weinberg RA. The basics of epithelial-mesenchymal transition. The Journal of clinical investigation. 2009;119(6):1420-8.
68. Dvorakova M, Nenutil R, Bouchal P. Transgelins, cytoskeletal proteins implicated in different aspects of cancer development. Expert review of proteomics. 2014;11(2):149-65.
69. Park SM, Gaur AB, Lengyel E, Peter ME. The miR-200 family determines the epithelial phenotype of cancer cells by targeting the E-cadherin repressors ZEB1 and ZEB2. Genes & development. 2008;22(7):894-907.
70. Tania M, Khan MA, Fu J. Epithelial to mesenchymal transition inducing transcription factors and metastatic cancer. Tumour biology : the journal of the International Society for Oncodevelopmental Biology and Medicine. 2014;35(8):7335-42.
71. Baulida J, Garcia de Herreros A. Snail1-driven plasticity of epithelial and mesenchymal cells sustains cancer malignancy. Biochimica et biophysica acta. 2015;1856(1):55-61.
72. Zhou L, Liu F, Wang X, Ouyang G. The roles of microRNAs in the regulation of tumor metastasis. Cell & bioscience. 2015;5:32.
73. Kim S, Lee J, Jeon M, Nam SJ, Lee JE. Elevated TGF-beta1 and -beta2 expression accelerates the epithelial to mesenchymal transition in triple-negative breast cancer cells. Cytokine. 2015.
74. Lamouille S, Xu J, Derynck R. Molecular mechanisms of epithelial-mesenchymal transition. Nature reviews Molecular cell biology. 2014;15(3):178-96.
75. Larue L, Bellacosa A. Epithelial-mesenchymal transition in development and cancer: role of phosphatidylinositol 3' kinase/AKT pathways. Oncogene. 2005;24(50):7443-54.
76. Talmadge JE, Fidler IJ. AACR centennial series: the biology of cancer metastasis: historical perspective. Cancer research. 2010;70(14):5649-69.
77. Gui P, Labrousse A, Van Goethem E, Besson A, Maridonneau-Parini I, Le Cabec V. Rho/ROCK pathway inhibition by the CDK inhibitor p27(kip1) participates in the onset of macrophage 3D-mesenchymal migration. Journal of cell science. 2014;127(Pt 18):4009-23.

78. Chu Y, Yao PY, Wang W, Wang D, Wang Z, Zhang L, Huang Y, Ke Y, Ding X, Yao X. Aurora B kinase activation requires survivin priming phosphorylation by PLK1. Journal of molecular cell biology. 2011;3(4):260-7.
79. Sen B, Peng S, Tang X, Erickson HS, Galindo H, Mazumdar T, Stewart DJ, Wistuba I, Johnson FM. Kinase-impaired BRAF mutations in lung cancer confer sensitivity to dasatinib. Science translational medicine. 2012;4(136):136ra70.
80. Byers LA, Diao L, Wang J, Saintigny P, Girard L, Peyton M, Shen L, Fan Y, Giri U, Tumula PK, Nilsson MB, Gudikote J, Tran H, Cardnell RJ, Bearss DJ, Warner SL, Foulks JM, Kanner SB, Gandhi V, Krett N, Rosen ST, Kim ES, Herbst RS, Blumenschein GR, Lee JJ, Lippman SM, Ang KK, Mills GB, Hong WK, Weinstein JN, Wistuba, II, Coombes KR, Minna JD, Heymach JV. An epithelial-mesenchymal transition gene signature predicts resistance to EGFR and PI3K inhibitors and identifies Axl as a therapeutic target for overcoming EGFR inhibitor resistance. Clinical cancer research : an official journal of the American Association for Cancer Research. 2013;19(1):279-90.
81. Byers LA, Wang J, Nilsson MB, Fujimoto J, Saintigny P, Yordy J, Giri U, Peyton M, Fan YH, Diao L, Masrorpour F, Shen L, Liu W, Duchemann B, Tumula P, Bhardwaj V, Welsh J, Weber S, Glisson BS, Kalhor N, Wistuba, II, Girard L, Lippman SM, Mills GB, Coombes KR, Weinstein JN, Minna JD, Heymach JV. Proteomic profiling identifies dysregulated pathways in small cell lung cancer and novel therapeutic targets including PARP1. Cancer discovery. 2012;2(9):798-811.
82. Sen B, Saigal B, Parikh N, Gallick G, Johnson FM. Sustained Src inhibition results in signal transducer and activator of transcription 3 (STAT3) activation and cancer cell survival via altered Janus-activated kinase-STAT3 binding. Cancer research. 2009;69(5):1958-65.
83. Brannan JM, Dong W, Prudkin L, Behrens C, Lotan R, Bekele BN, Wistuba I, Johnson FM. Expression of the receptor tyrosine kinase EphA2 is increased in smokers and predicts poor survival in non-small cell lung cancer. Clinical cancer research : an official journal of the American Association for Cancer Research. 2009;15(13):4423-30.
84. Tong P, Coombes KR, Johnson FM, Byers LA, Diao L, Liu DD, Lee JJ, Heymach JV, Wang J. drexplorer: A tool to explore dose-response relationships and drug-drug interactions. Bioinformatics. 2015;31(10):1692-4.
85. Pounds SB. Estimation and control of multiple testing error rates for microarray studies. Briefings in bioinformatics. 2006;7(1):25-36.
86. Carter SL, Eklund AC, Kohane IS, Harris LN, Szallasi Z. A signature of chromosomal instability inferred from gene expression profiles predicts clinical outcome in multiple human cancers. Nature genetics. 2006;38(9):1043-8.
87. Dean CB, Nielsen JD. Generalized linear mixed models: a review and some extensions. Lifetime data analysis. 2007;13(4):497-512.
88. Gyorffy B, Surowiak P, Budczies J, Lanczky A. Online survival analysis software to assess the prognostic value of biomarkers using transcriptomic data in non-small-cell lung cancer. PloS one. 2013;8(12):e82241.
89. Garnett MJ, Edelman EJ, Heidorn SJ, Greenman CD, Dastur A, Lau KW, Greninger P, Thompson IR, Luo X, Soares J, Liu Q, Iorio F, Surdez D, Chen L, Milano RJ, Bignell GR, Tam AT, Davies H, Stevenson JA, Barthorpe S, Lutz SR, Kogera F, Lawrence K, McLaren-Douglas A, Mitropoulos X, Mironenko T, Thi H, Richardson L, Zhou W, Jewitt F, Zhang T, O'Brien P, Boisvert JL, Price S, Hur W, Yang W, Deng X, Butler A, Choi HG, Chang JW, Baselga J, Stamenkovic I, Engelman JA, Sharma SV, Delattre O, Saez-Rodriguez J, Gray NS, Settleman J, Futreal PA, Haber DA, Stratton MR, Ramaswamy S, McDermott U, Benes CH. Systematic identification of genomic markers of drug sensitivity in cancer cells. Nature. 2012;483(7391):570-5.

90. Wu CP, Hsiao SH, Luo SY, Tuo WC, Su CY, Li YQ, Huang YH, Hsieh CH. Overexpression of human ABCB1 in cancer cells leads to reduced activity of GSK461364, a specific inhibitor of polo-like kinase 1. Molecular pharmaceutics. 2014;11(10):3727-36.
91. Gilmartin AG, Bleam MR, Richter MC, Erskine SG, Kruger RG, Madden L, Hassler DF, Smith GK, Gontarek RR, Courtney MP, Sutton D, Diamond MA, Jackson JR, Laquerre SG. Distinct concentration-dependent effects of the polo-like kinase 1-specific inhibitor GSK461364A, including differential effect on apoptosis. Cancer research. 2009;69(17):6969-77.
92. Tone S, Sugimoto K, Tanda K, Suda T, Uehira K, Kanouchi H, Samejima K, Minatogawa Y, Earnshaw WC. Three distinct stages of apoptotic nuclear condensation revealed by time-lapse imaging, biochemical and electron microscopy analysis of cell-free apoptosis. Experimental cell research. 2007;313(16):3635-44.
93. Chen L, Gibbons DL, Goswami S, Cortez MA, Ahn YH, Byers LA, Zhang X, Yi X, Dwyer D, Lin W, Diao L, Wang J, Roybal JD, Patel M, Ungewiss C, Peng D, Antonia S, Mediavilla-Varela M, Robertson G, Jones S, Suraokar M, Welsh JW, Erez B, Wistuba, II, Chen L, Peng D, Wang S, Ullrich SE, Heymach JV, Kurie JM, Qin FX. Metastasis is regulated via microRNA-200/ZEB1 axis control of tumour cell PD-L1 expression and intratumoral immunosuppression. Nature communications. 2014;5:5241.
94. Steegmaier M, Hoffmann M, Baum A, Lenart P, Petronczki M, Krssak M, Gurtler U, Garin-Chesa P, Lieb S, Quant J, Grauert M, Adolf GR, Kraut N, Peters JM, Rettig WJ. BI 2536, a potent and selective inhibitor of polo-like kinase 1, inhibits tumor growth in vivo. Current biology : CB. 2007;17(4):316-22.
95. Gleixner KV, Ferenc V, Peter B, Gruze A, Meyer RA, Hadzijusufovic E, Cerny-Reiterer S, Mayerhofer M, Pickl WF, Sillaber C, Valent P. Polo-like kinase 1 (Plk1) as a novel drug target in chronic myeloid leukemia: overriding imatinib resistance with the Plk1 inhibitor BI 2536. Cancer research. 2010;70(4):1513-23.
96. Shi JQ, Lasky K, Shinde V, Stringer B, Qian MG, Liao D, Liu R, Driscoll D, Nestor MT, Amidon BS, Rao Y, Duffey MO, Manfredi MG, Vos TJ, N DA, Hyer ML. MLN0905, a small-molecule plk1 inhibitor, induces antitumor responses in human models of diffuse large B-cell lymphoma. Molecular cancer therapeutics. 2012;11(9):2045-53.
97. Sun X, Medeiros LJ, Lu D, Rassidakis GZ, Bueso-Ramos C. Dysplasia and high proliferation rate are common in acute myeloid leukemia with inv(16)(p13q22). American journal of clinical pathology. 2003;120(2):236-45.
98. Martin DS. The scientific basis for adjuvant chemotherapy. Cancer treatment reviews. 1981;8(3):169-89.
99. Sanhaji M, Kreis NN, Zimmer B, Berg T, Louwen F, Yuan J. p53 is not directly relevant to the response of Polo-like kinase 1 inhibitors. Cell cycle. 2012;11(3):543-53.
100. Huang B, Shang ZF, Li B, Wang Y, Liu XD, Zhang SM, Guan H, Rang WQ, Hu JA, Zhou PK. DNA-PKcs associates with PLK1 and is involved in proper chromosome segregation and cytokinesis. Journal of cellular biochemistry. 2014;115(6):1077-88.
101. Mardin BR, Agircan FG, Lange C, Schiebel E. Plk1 controls the Nek2A-PP1gamma antagonism in centrosome disjunction. Current biology : CB. 2011;21(13):1145-51.
102. Mbom BC, Siemers KA, Ostrowski MA, Nelson WJ, Barth AI. Nek2 phosphorylates and stabilizes beta-catenin at mitotic centrosomes downstream of Plk1. Molecular biology of the cell. 2014;25(7):977-91.
103. Harris PS, Venkataraman S, Alimova I, Birks DK, Donson AM, Knipstein J, Dubuc A, Taylor MD, Handler MH, Foreman NK, Vibhakar R. Polo-like kinase 1 (PLK1) inhibition suppresses cell growth and enhances radiation sensitivity in medulloblastoma cells. BMC cancer. 2012;12:80.
104. Raab M, Kramer A, Hehlgans S, Sanhaji M, Kurunci-Csacsko E, Dotsch C, Bug G, Ottmann O, Becker S, Pachl F, Kuster B, Strebhardt K. Mitotic arrest and slippage induced by pharmacological inhibition of Polo-like kinase 1. Molecular oncology. 2015;9(1):140-54.

105. Vitale I, Galluzzi L, Castedo M, Kroemer G. Mitotic catastrophe: a mechanism for avoiding genomic instability. Nature reviews Molecular cell biology. 2011;12(6):385-92.
106. Balaguer TM, Gomez-Martinez A, Garcia-Morales P, Lacueva J, Calpena R, Reverte LR, Riquelme NL, Martinez-Lacaci I, Ferragut JA, Saceda M. Dual regulation of P-glycoprotein expression by trichostatin A in cancer cell lines. BMC molecular biology. 2012;13:25.
107. Stolarczyk EI, Reiling CJ, Paumi CM. Regulation of ABC transporter function via phosphorylation by protein kinases. Current pharmaceutical biotechnology. 2011;12(4):621-35.
108. Liu Y, Sanchez-Tillo E, Lu X, Huang L, Clem B, Telang S, Jenson AB, Cuatrecasas M, Chesney J, Postigo A, Dean DC. The ZEB1 transcription factor acts in a negative feedback loop with miR200 downstream of Ras and Rb1 to regulate Bmi1 expression. The Journal of biological chemistry. 2014;289(7):4116-25.
109. Pieraccioli M, Imbastari F, Antonov A, Melino G, Raschella G. Activation of miR200 by c-Myb depends on ZEB1 expression and miR200 promoter methylation. Cell cycle. 2013;12(14):2309-20.
110. Kyuno D, Yamaguchi H, Ito T, Kono T, Kimura Y, Imamura M, Konno T, Hirata K, Sawada N, Kojima T. Targeting tight junctions during epithelial to mesenchymal transition in human pancreatic cancer. World journal of gastroenterology : WJG. 2014;20(31):10813-24.
111. Kwon MJ. Emerging roles of claudins in human cancer. International journal of molecular sciences. 2013;14(9):18148-80.
112. Soini Y. Tight junctions in lung cancer and lung metastasis: a review. International journal of clinical and experimental pathology. 2012;5(2):126-36.
113. Van Aelst L, Symons M. Role of Rho family GTPases in epithelial morphogenesis. Genes & development. 2002;16(9):1032-54.
114. Roodhart JM, Daenen LG, Stigter EC, Prins HJ, Gerrits J, Houthuijzen JM, Gerritsen MG, Schipper HS, Backer MJ, van Amersfoort M, Vermaat JS, Moerer P, Ishihara K, Kalkhoven E, Beijnen JH, Derksen PW, Medema RH, Martens AC, Brenkman AB, Voest EE. Mesenchymal stem cells induce resistance to chemotherapy through the release of platinum-induced fatty acids. Cancer cell. 2011;20(3):370-83.
115. Mitra A, Mishra L, Li S. EMT, CTCs and CSCs in tumor relapse and drug-resistance. Oncotarget. 2015;6(13):10697-711.
116. Thomson S, Buck E, Petti F, Griffin G, Brown E, Ramnarine N, Iwata KK, Gibson N, Haley JD. Epithelial to mesenchymal transition is a determinant of sensitivity of non-small-cell lung carcinoma cell lines and xenografts to epidermal growth factor receptor inhibition. Cancer Res. 2005;65(20):9455-62.
117. Haibe-Kains B, El-Hachem N, Birkbak NJ, Jin AC, Beck AH, Aerts HJ, Quackenbush J. Inconsistency in large pharmacogenomic studies. Nature. 2013;504(7480):389-93.
118. Wang P, Henning SM, Heber D. Limitations of MTT and MTS-based assays for measurement of antiproliferative activity of green tea polyphenols. PloS one. 2010;5(4):e10202.
119. Hong M, Ren M, Silva J, Kennedy T, Choi J, Cowell JK, Hao Z. Sepantronium is a DNA damaging agent that synergizes with PLK1 inhibitor volasertib. American journal of cancer research. 2014;4(2):135-47.
120. Wilson C, Ye X, Pham T, Lin E, Chan S, McNamara E, Neve RM, Belmont L, Koeppen H, Yauch RL, Ashkenazi A, Settleman J. AXL inhibition sensitizes mesenchymal cancer cells to antimitotic drugs. Cancer research. 2014;74(20):5878-90.

VITA:

Ruchitha Goonatilake was born in Akron, Ohio on October, 27, 1991 to Rohitha and Chandrika Goonatilake. He attended high school in Laredo, Texas at Alexander High School. He received his Bachelor's degree in Chemistry from the University of Texas in 2013. In August of 2013, he entered the University of Texas- M.D Anderson Graduate School of Biomedical Sciences to obtain his Master's degree in biomedical sciences.